ALTERATIONS IN MITOCHONDRIAL METABOLISM AND DYNAMICS BY AUTOPHAGIC MODULATORS IN CARDIOMYOBLASTS

ASHOK S

PhD Thesis

2023

SREE CHITRA TIRUNAL INSTITUTE FOR MEDICAL SCIENCES AND TECHNOLOGY

TRIVANDRUM

Thiruvananthapuram

Alterations in Mitochondrial Metabolism and Dynamics by Autophagic Modulators in Cardiomyoblasts

A THESIS PRESENTED BY

ASHOK S

TO

THE SREE CHITRA TIRUNAL INSTITUTE
FOR MEDICAL SCIENCES AND TECHNOLOGY, TRIVANDRUM
THIRUVANANTHAPURAM

IN PARTIAL FULFILMENT OF THE REQUIREMENTS

FOR THE AWARD OF

DOCTOR OF PHILOSOPHY

2023

DECLARATION BY STUDENT

I, **Mr. ASHOK S** hereby certify that I had personally carried out the work depicted in the thesis entitled **"Alterations in Mitochondrial Metabolism and Dynamics by Autophagic Modulators in Cardiomyoblasts"** under the direct supervision of Dr. G Srinivas, Scientist G, Acting Head, Department of Biochemistry, SreeChitraTirunal Institute for Medical Sciences and Technology, Trivandrum, except where external help was sought and is acknowledged. No part of the thesis has been submitted for the award of any other degree or diploma prior to this date.

Date: 28/12/2021

CERTIFICATE BY THE RESEARCH GUIDE

This is to certify that **ASHOK S** has fulfilled the requirements prescribed for the PhD degree of the Sree Chitra Tirunal Institute for Medical Sciences and Technology, Trivandrum. The thesis entitled **"Alterations in Mitochondrial Metabolism and Dynamics by Autophagic Modulators in Cardiomyoblasts"** was carried out under my direct supervision. No part of the thesis has been submitted for the award of any other degree or diploma prior to this date.

Date: 28/12/2021

Dr. G. Srinivas (Guide)

Alterations in Mitochondrial Metabolism and Dynamics by Autophagic Modulators in Cardiomyoblasts

A THESIS PRESENTED BY

ASHOK S

TO

THE SREE CHITRA TIRUNAL INSTITUTE
FOR MEDICAL SCIENCES AND TECHNOLOGY, TRIVANDRUM
THIRUVANANTHAPURAM

IN PARTIAL FULFILMENT OF THE REQUIREMENTS

FOR THE AWARD OF

DOCTOR OF PHILOSOPHY

Suvro Chatterjee

Dr. Suvro Chatterjee

GUIDE

EXAMINER

Acknowledgements

First and foremost, I would like to pay high regards to my beloved parents and siblings for their encouragement, inspiration and support without which nothing would have been possible. I owe a great deal of gratitude to my mentor, Dr. G. Srinivas, Scientist G, for his guidance, advice, supervision and encouragement. I couldn't have imagined having a better advisor, mentor and companion, all through the course of my PhD tenure.

Besides my advisor I would also like to acknowledge all the faculties of SCTIMST including the current as well as the former Directors, Registrar and Deputy Registrar, SCTIMST for their support and encouragement with all the facilities which helped me to complete my work.

I wish to express my sincere gratitude to Retired Professors Dr. N. Jayakumari, and Dr. P. S. Appukuttan, Former HODs, Department of Biochemistry, SCTIMST, Dr, Shivkumar.K, Former HOD, Department of Cellular and Molecular Cardiology, SCTIMST, Retd Prof. Jayakumar. K, former HOD, Department of CardioVascular and Thoracic Surgery, SCTIMST, Dr.Vivek. V. Pillai, Professor, Department of CardioVascular and Thoracic Surgery, SCTIMST, Dr. Varghese T Panicker, Professor, Department of CardioVascular and Thoracic Surgery, Dr.HariKrisnan.V.S, Scientist E, Division of Laboratory Animal Sciences, SCTIMST.

Words are short to express deep sense of gratitude towards my friend and collaborator Ms.Mahalaxmi Ganjoo for always being willing to talk through experimental failures and successes and always reminding me to focus on the bigger picture. I acknowledge her help and companionship since the last 4 years without which designing and execution of the study would have been an onerous task. I am greatly indebted to my little sister, Aswathy S, without whom, most of the experiments would have been impossible. I take this opportunity to acknowledge the sharing and caring shown by my siblings which served as strength and support.

I owe a great deal of gratitude to Dr Manjunatha Shankarappa for all the discussion, advice and intellectual contributions, which helped in boosting scientific temper and aptitude towards research. I wish to express my sincere gratitude to Dr.Cibin T R, and Dr. Madhusoodhanan U K, for the encouragement and the patience all through the labmeets and discussions which helped me build confidence and beat the quandaries.

I am indebted to Dr.Raji S R and Dr.Nandhini R J, for sharing the experiences and the training that built my knowledge in research as well as life.

Also, I acknowledge my colleague Dr.Anand. C.R, who introduced me to the Department of Biochemistry, SCTIMST, for his help and training. I am greatly thankful to my seniors Dr.Dhanya Krishnan, and Dr.BhavyaBharathan for their kind gestures all through the course of my tenure in the

Department. I would take this opportunity to thank my juniors, Ms. Deepthi Chandran, Mrs. Ganga Anand, Ms. Jyothi Bose and Ms.Revathi G Nair for their support.

My sincere thanks to Dr.Geetha Syam, Scientific Assistant, Department of Biochemistry for her helping hand and advices which helped me a lot for successful completion of tasks assigned to me.

I would also like to extend warm thanks to Dr.Deepa, Technical Assistant, Department of Biochemistry for her care and concern. Also, I thank the Unit helper and cleaning attendant, Shaji and Shamnad, Department of Biochemistry, SCTIMST for helping me clear the mess and have a peaceful, clean working environment, all through the course of my PhD.

I appreciate and acknowledge the help, companionship and encouragement extended by my friends Dr. Jibin, Keerthi, Amalu, Dr. Vinu Rajentdran, Dr. Revathi R Nair, Dr. Gayathri and Dr. Amita which helped me strive through the hard times.

I gratefully acknowledge the financial support of CSIR for my fellowship which greatly motivated me complete the work.

Last but not least I wish to avail myself this opportunity to pay homage to all the Laboratory animals for their sacrifice towards enrichment of scientific knowledge, without which science would never add new insights.

TABLE OF CONTENTS

LIST OF FIGURES

List of Abbreviations

ADP	:	Adenosine di phosphate
AMP	:	Adenosine mono phosphate
AMPK	:	Adenosine monophosphate- activated protein kinase
APS	:	Ammonium persulphate
ATCC	:	American Type Culture Collection
Atg	:	Autophagy-related
ATP	:	Adenosine Triphosphate
BAF	:	Bafilomycin
Bcl-2	:	B cell lymphoma-2
BCA	:	Bicinchoninic acid
BIOPS	:	Biopsy Preservation solution
BNIP3	:	Bcl-2 interacting protein 3
BSA	:	Bovine Serum Albumin
CCCP	:	Carbonyl cyanide 3-chlorophenyl-hydrazone
cDNA	:	Complementary DNA
CQ	:	Chloroquine
DMEM	:	Dulbecco`s Modified Eagle Medium
DMSO	:	Dimethyl Sulfoxide
DNA	:	Deoxy ribonucleic acid
Drp	:	Dynamin-related protein
DTT	:	Dithiothreitol
EDTA	:	Ethylenediamine tetra acetic acid
EGTA	:	Ethylene glycol-bis (β-aminoethyl ether)-N, N, N', N'-tetraacetic acid
ETC	:	Electron transport chain
ETF	:	Electron transferring flavoprotein
FACS	:	Fluorescence-activated Cell Sorting
FBS	:	Fetal Bovine Serum
FDA	:	Food and Drug Administration
FIS1	:	Mitochondrial fission1
FUNDC1	:	FUN 14 domain-containing protein1

GTP	:	Guanosine triphosphate
HBSS	:	Hank's balanced salt solution
HCl	:	Hydrochloric acid
HCQ	:	Hydroxychloroquine
HRP	:	Horse Radish Peroxidase
HRR	:	High Resolution Respirometry
IEC	:	Institution Ethics Committee
LC3	:	Microtubule-associated protein1 light chain 3
LDH	:	Lactate Dehydrogenase
3- MA	:	3-Methyladenine
MID	:	Mitochondrial dynamics protein
MiR05	:	Mitochondrial respiration buffer
MFF	:	Mitochondrial fission factor
Mfn	:	Mitofusin
MMP	:	Matrix metalloproteinase
mM	:	Milli Molar
mRNA	:	messenger Ribonucleic acid
mtDNA	:	mitochondrial DNA
mTORC1	:	Mammalian target of rapamycin complex1
MTT	:	4,5- dimethylthiazol-2-yl
NaHCO3	:	Sodium Bicarbonate
NIX	:	Nip3-like protein
nmol	:	Nano Molar
NRF	:	Nuclear factor erythroid
OCR	:	Oxygen consumption rate
Opa	:	Optic atrophy protein
OXPHOS	:	Oxidative phosphorylation
Pal	:	Palmitoyl-L-carnitine
PBS	:	Phosphate buffered saline
P/O	:	Phosphate/Oxygen
PCR	:	Polymerase Chain Reaction
qPCR	:	Quantitative PCR
PGC-1α	:	Peroxisome proliferator-activated receptor-gamma coactivator 1α
PI	:	Propidium Iodide
PI3K	:	Phosphatidyl Inositol 3-Kinase

PINK1	:	Phosphatase and tensin homolog-induced putative kinase1
PKA	:	Protein kinase A
pmol	:	Pico Mole
PVDF	:	Polyvinylidene fluoride
qRT PCR	:	Quantitative Real Time Polymerase Chain Reaction
RES	:	Resveratrol
RIPA	:	Radio immuno Precipitation Assay
RNA	:	Ribonucleic acid
ROS	:	Reactive Oxygen Species
rpm	:	Revolutions per Minute
SDS-PAGE	:	Sodium dodecyl sulphate Polyacrylamide gel electrophoresis
SEM	:	Standard error of mean
Sirt1	:	Sirtuin 1
SQSTM	:	Sequestosome
SUIT	:	Substrate-Uncoupler-Inhibitor-Titration
T2DM	:	Type 2 Diabetes mellitus
TAC	:	Transverse aortic constriction
TBST	:	Tris Buffered Saline Tween 20
TBE	:	Tris/Borate/EDTA
TCA	:	Tri carboxylic acid
TEMED	:	Tetramethyl ethylene diamine
TFB	:	Transcription factorB
TFAM	:	Transcription factor A mitochondrial
TMPD	:	Tetramethyl-p-phenylenediamine
TMRM	:	Tetramethyl rhodamine methyl ester
TPVG	:	Trypsin-Phosphate-Versene-Glucose
w/v	:	Weight/Volume
µm	:	Micro Meter
µM	:	Micro Mol

SYNOPSIS

Alterations in Mitochondrial Metabolism and Dynamics by Autophagic Modulators in Cardiomyoblasts

Background

Autophagy, once thought as a bulk, nonselective degradative cellular process has proven to play critical role in cellular and tissue health especially in postmitotic tissues like Myocardium, where terminally differentiated cardiomyocytes are the functional players. Thus, any impairment could have an enormous impact on muscle function. Pharmacological inhibitors of autophagy are being increasingly used in clinical conditions as well as for research purposes; like chloroquine as an anti-malarial drug, recently as an effective anticancer agent, either alone or in combination with other drugs. However, the effect of these agents on the mitochondrial bioenergetics, particularly in Cardiac muscle cells remains elusive. As known already, myocytes rely heavily on mitochondrial OXPHOS for its function and survival; and its impairment can lead to muscle damage.

Here, we are trying to assess,

- To assess the role of autophagic modulators on mitochondrial metabolism
- To analyze the mitochondrial dynamics following autophagy inhibition and activation
- To assess the influence of autophagy modulators on mitochondrial function in an *in vivo* model system

Hypothesis

Autophagy modulation affects mitochondrial dynamics as well as function

Methodology

The study was carried out in H9c2 cells, embryonic cardiomyoblasts of rat origin and C57BL/6 mice model.

- High resolution respirometry was used for studying mitochondrial function by analyzing oxygen consumption rate following inhibition or activation of autophagy in cells as well as in isolated mitochondria from mice heart treated with Chloroquine and Resveratrol.

- Western blotting and Realtime qPCR assay were used for analyzing expression levels of proteins as well as mRNA related to mitochondrial dynamics
- Fluorescent probes were used to analyze mitochondrial network as well as mitochondrial and cellular ROS.

Principal findings:

- **Autophagy inhibition with Chloroquine and Bafilomycin**

- The reduction in formazan crystal formation indicates reduced cellular metabolic activity due to Chloroquine treatment.
- Intact cell bioenergetics falls significantly with Chloroquine treatment with a significant decline in coupling efficiency pointing towards damaged mitochondria.
- Substrate-linked respiration analysis done in the presence of exogenous substrates confirmed decreased mitochondrial efficiency.
- Bafilomycin, which have as similar effect to that of CQ on autophagy, showed similar results with mitochondrial function suggesting that the effects observed could be due to the autophagy inhibition.
- qPCR data revealed that Chloroquine induces mitochondrial biogenesis, and causes accumulation of mitochondria. The increase in mitochondrial content could be because of the reduction in mitophagy (mitochondrial degradation via Autophagy), due to Chloroquine treatment.
- TMRM staining showed decline in mitochondrial membrane potential while MitoSOX staining revealed increased mitochondrial ROS generation
- Thus, although higher in content, the mitochondrial population shows damage and inefficiency.
- Increased vacuolation and accumulation of acidic compartments with Chloroquine treatment suggests an increase in the lysosomes within the cell, due to the decline in the cellular degradation.
- The mitochondrial network analysis with Mitotracker staining showed disruption of mitochondrial network and increased fragmentation of mitochondria.

- The in vivo experiments shows that Chloroquine impairs the substrate-linked respiration of mitochondrial complexes in the cardiac tissue, substantiating the mitotoxic effects observed in the cell line study.
- Also, with the increase in the age of the animal, there could be a decline in the basal autophagy and when CQ was administered in that condition, the mtiotoxic effects were more pronounced.

- **Autophagy activation with Resveratrol**

- There was a decline in the intact cell respiration with Resveratrol treatment, this decline in the bioenergetics could be due to the changes in the cellular metabolite pool.
- The Substrate-linked respiration measurements done in the presence of exogenous substrates showed an improvement of mitochondrial efficiency.
- TMRM staining showed improvement in mitochondrial membrane potential suggesting highly efficient mitochondrial population.
- Although mitoctracker imaging showed fragmented mitochondrial network, this did not reflect in the overall mitochondrial performance.
- But the dose of Resveratrol could have a critical impact on the observable benefits with only a narrow optimal range proving beneficial for the improvement of mitochondrial efficiency.
- The *in vivo* studies showed that Resveratrol can help improve mitochondrial functional efficiency even under physiological conditions and this would be having more pronounced benefits under conditions with underlying cardiovascular challenges, like aging.

Conclusion and significance of the study

- Autophagy inhibition with CQ and associated autophagy inhibitors had detrimental effects on cardiac mitochondria.
- The autophagy induction by resveratrol had beneficial effects on cardiac mitochondrial efficiency in a dose dependent manner, and this could have greater significance in some cardiac challenges like age associated decline in cardiac mitochondrial health.
- The dose of the drugs which possess proven effects on the process of autophagy, like Chloroquine and Resveratrol could have critical impact on the beneficial effects and a narrow optimal dose must be determined before employing for any therapeutic targets.

I. INTRODUCTION

I.1. Autophagy

Autophagy is the process by which a cell digests macromolecules or even organelles, in part or as a whole, such that, it may either be removed from the cell altogether or recycled to retain its building blocks. Autophagy research marked its beginning when Christian de Duve discovered lysosomes biochemically as granules, with enclosed digestive enzymes, from tissue fractions of rat liver. De Duve proposed them to be involved in confined digestive pathways within the cells (de Duve et al., 1955). Later, the term 'Autophagy', which means 'self-eating' in Greek (Glick et al., 2010) was coined by De Duve himself to describe the process of cellular recycling. Now, the autophagic pathway can be described as a tightly regulated, intracellular recycling mechanism, with ~40 autophagy-related (ATG) genes identified so far, coding for a dedicated set of proteins that regulate the process regulating it at various levels, preserved from yeast to their mammalian counterparts (Nakatogawa et al., 2009).

Three different types of autophagy have been classified: Macroautophagy, Microautophagy and Chaperone-mediated autophagy.

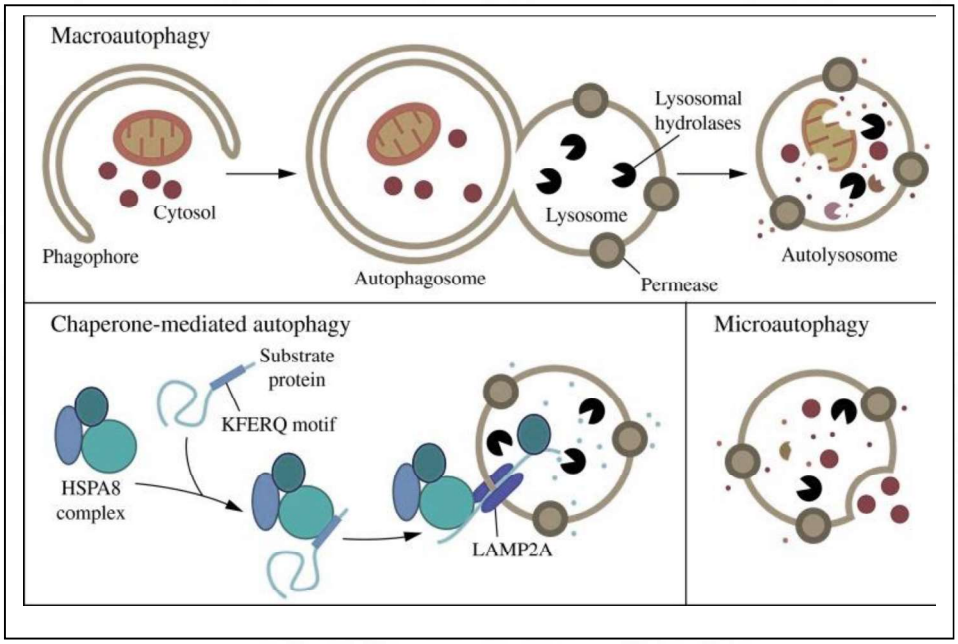

Figure I.1: Types of Autophagy - *A graphical representation of different types of autophagy.* (Parzych and Klionsky, 2014)

Macroautophagy is the key process, often referred to as Autophagy, which involves the formation and expansion of an isolation membrane structure, Phagophore, and its maturation in to a double membrane vesicle, autophagosome, which ultimately fuses with the lysosome to form Autophagolysosomes or Autolysosomes. Inside these autolysosomes, the cargo which could either be macromolecules, foreign bodies, a part of dysfunctional organelles or an organelle as a whole will be degraded in to its building blocks by the resident lysosomal enzymes, and the subsequently released molecules like amino acids, fatty acids and nucleotides would be utilized for various anabolic pathways and cellular functions. Thus, the process of autophagy is branded as the cellular 'recycling factory' that functions as an energy sensor and helps in efficient generation of cellular energy currencies (Parzych and Klionsky, 2014).

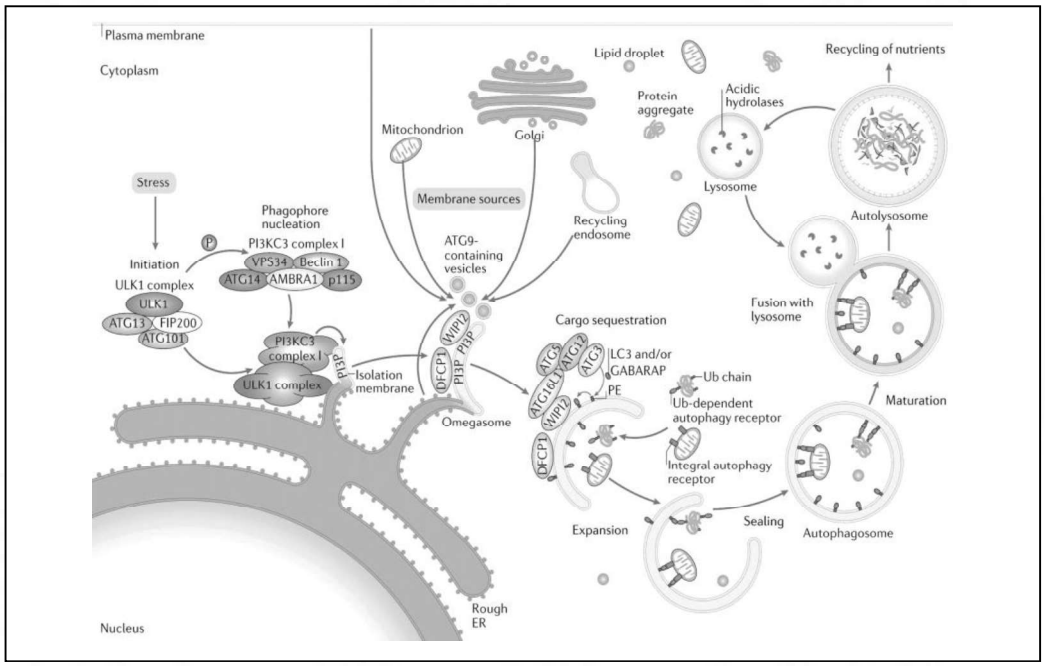

Figure I.2 : An overview of the autophagy process *(Dikic and Elazar, 2018)***,** *showing an overview of Autophagy machinery and shows the involvement of different ATG proteins at various levels.*

Basal level of autophagy is a ceaselessly on-going process in the cell, as it has a vital role in cellular quality control and homeostasis. However, depending up on the context and nature of the stress stimuli, the rate of autophagy can be altered and it could either be beneficial or lethal for cell survival. For example, starvation induced stress results

in the upregulation of bulk autophagy, and non-selectively degrades any protein or organelle (other than mitochondrial structures) to fuel the essential processes for cell survival. But prolonged starvation would have a negative impact on cell survival and can result in autophagic cell death. This demands the process be tightly regulated(Boya et al., 2013; Cecconi and Levine, 2008).

Myocardium is made mostly of terminally differentiated cardiomyocytes and, the renewal or replacement of these basic units of a functional heart is a slow and ineffective process. Evidences suggests that autophagy has a key role in the myocardium, maintaining the health of myocytes as well as in deterring their loss under pathological conditions, making it a subject of intense therapeutic interest. Mitochondrial dependence of myocardium is well established and, the cardiomyocytes, the contractile units of the heart, are tightly populated by mitochondria (~1/3 the cell volume) which ensures the preservation of the metabolic need of the heart muscles (Hom and Sheu, 2009).

Thickly populated mitochondrial reticulum in the myocytes forms a highly dynamic and complex structure, assuming varied distribution patterns, morphologies and functional roles in accord with the internal as well as external cues. This structural and functional plasticity of mitochondria is adeptly preserved by orchestration of a proper balance between mitochondrial fission and fusion processes as well as the biosynthesis of new mitochondrial masses and the programmed elimination of the mitochondrial fragments. These counteracting processes, together establish a quality control mechanism to ensure a healthy mitochondrial network. Mitochondrial dynamics thus involve the structural as well as functional remodelling of the organelle network by way of fission and fusion, the subcellular mitochondrial mobility (based on energy needs), mitochondrial biogenesis and mitophagy, the programmed clearance of mitochondria, either damaged or functional(Bereiter-Hahn, 1990; Glancy et al., 2017; Hoppel et al., 2009; Soubannier and McBride, 2009).

Mitochondrial morphology is intricately coupled to most of its functions, which include metabolism, calcium homeostasis, ROS generation and orchestration of programmed cell death (Ma et al., 2020). While proliferating cells are capable of

removing the ‘biological wastes’ by cell division, cardiac myocytes, being terminally differentiated, have to depend mainly on degradation pathways. Thus, any alterations in the autophagic status in-essence would contribute towards the accumulation of defective mitochondrial structures(Dutta et al., 2012a). In fact, the presence of giant mitochondria, oxidative stress and inefficient mitochondrial DNA repair and incompetent autophagy are the characteristics of aging or other related metabolic disorders. Evidences also suggests that mitochondrial DNA mutations can alter mitochondrial dynamics resulting I the accumulation of less energy efficient mitochondrial structures that are less susceptible to oxidative damage and less vulnerable to mitophagy(Druzhyna et al., 2008; Wang et al., 2019).

Autophagy has been linked to a number of cardiac ailments which includes ischemic cardiomyopathy, cardiac hypertrophy, diabetic cardiomyopathy, and hemochromatosis. Incompetent autophagy plays a serious role in the development of these myocardial abnormalities, and any therapeutic intervention that improves the process of autophagy may contribute towards increased cardiac health. This proposition is substantiated by the improvement of myocardial health under calorie restriction or fasting (Cao et al., 2009; Dutta et al., 2012a; Goswami and Das, 2006; Rifki and Hill, 2012).

Thus, the intention of our study was to analyse the beneficial/detrimental alterations in mitochondrial function and dynamics in cardiac cells inflicted by modulation of autophagic status.

II. REVIEW OF LITERATURE

II.1. Autophagy in Myocardium

Autophagy plays an important role in the heart as this fist sized organ is made predominantly of muscle fibres, formed from a functional syncytium of cardiomyocytes widely connected via gap junctions. The renewal or replacement of these terminally differentiated cells is a slow and ineffective process.

Under physiological as well as pathological conditions, the self-cannibalistic progress of autophagy plays a crucial role in the degradation and recycling of cytoplasmic components. In physiological conditions, the process of autophagy helps in the degradation of cytoplasmic materials such as long-lived proteins and organelles. While, pathological insults like ischemia/reperfusion (I/R), heart failure, etc., would induce the process of autophagy as an essential cytoprotective mechanism (Rifki and Hill, 2012).

The most effective physiological autophagy induction observed so far, is via nutrient depletion. Scarceness in the availability of various nutrients like, amino acids, growth factors, and oxygen, can upregulate autophagy; amino acid starvation is the most widely used and effective method for the activation of autophagy in mammalian cell culture. Robust induction of autophagy is observed in all tissues in the early neonatal period, and it is essential for survival as well as development; with neonatal lethality observed in animal models with mutations in autophagy related genes (Kuma et al., 2004).

The terminally differentiated cells, like the cardiomyocytes in heart, are reliant on autophagy pathway, not just to evade physiological cues like starvation, but more notably it helps in the protein quality control and removal of damaged organelles (Singh and Cuervo, 2011). Any derangements in this recycling process can have adverse effects. Conditional knockdown of autophagy-related genes in myocardium is shown to result in rapid cardiac abnormalities (Nakai et al., 2007; Nishino et al., 2000). Inhibition of autophagic flux by targeting Atg7 has shown to affect the viability of neonatal rat cardiomyocytes (NRCMs). The lack of Atg5 in the adult heart resulted in contractile dysfunction as well as contributed towards the accumulation of disorganized sarcomeric structures, aggregation of mitochondria, and aberrant

concentric membranous structures which were evident in ultra-structural analysis (Nakai et al., 2007; Nishida et al., 2009). Furthermore, Atg5 deficiency is shown to promote ER stress and affect cell viability (Nishida et al., 2009; Song et al., 2017). Knockdown of proteins like LAMP-2 and anti-apoptotic protein BCL-2, both having an important role in autophagy, is shown to culminate into heart failure as well as impaired stress responses (Mayorga et al., 2004, p. 2; Thomas et al., 2013). These studies offer a strong credibility to the conception that constitutive autophagy is a critical housekeeping function in the myocardial cells and is fundamentally required for the maintenance of homeostasis.

II.2. Autophagy and Metabolism in Heart

The cardiac tissue is entrusted with an enormous task of continuously pumping the blood which necessitates the myocardial cells to be metabolically efficient enough to meet the incessant demand for energy. This imposes the requirement of an effectual coordination between the quality control and fuel generation, making the two processes heavily entwined. Evidences suggest that the process of autophagy is activated within 30 min post-delivery in neonatal heart, probably as a mechanism to rapidly restore the nutrient supply once the placental source is terminated (Kuma et al., 2004). When nutrient supply is restricted, autophagy plays a crucial role in adult heart too, replenishing the fuel supply via protein breakdown, lysosomal digestion of sugars and lipids as well as nucleic acid degradation, (Ren and Xu, 2015). As autophagy plays a significant role in the orchestration of heart metabolism, inhibition of autophagic process can hamper cardiac performances and accelerates cell death coupled with diminution in concentration of energy currencies within the myocardial cells (Troncoso et al., 2012), while enhancement of autophagic process is reported to have protective role under conditions like starvation, by preventing ATP loss as well as ER stress (Sciarretta et al., 2015).

II.3. Autophagy in Cardiovascular Disorders

While autophagy is usually deciphered as an adaptive response to pathological stimuli and act as a rescue mechanism to promotes cell survival, excessive autophagy activation beyond a certain threshold as well as an inappropriate inhibition is often

detrimental, as illustrated in the Fig. Perturbations in autophagy status is observed in almost all cardiovascular diseases, while modulation of autophagy plays a critical role in these disease triggers as well as cure (Ren and Xu, 2015; Shirakabe et al., 2016).

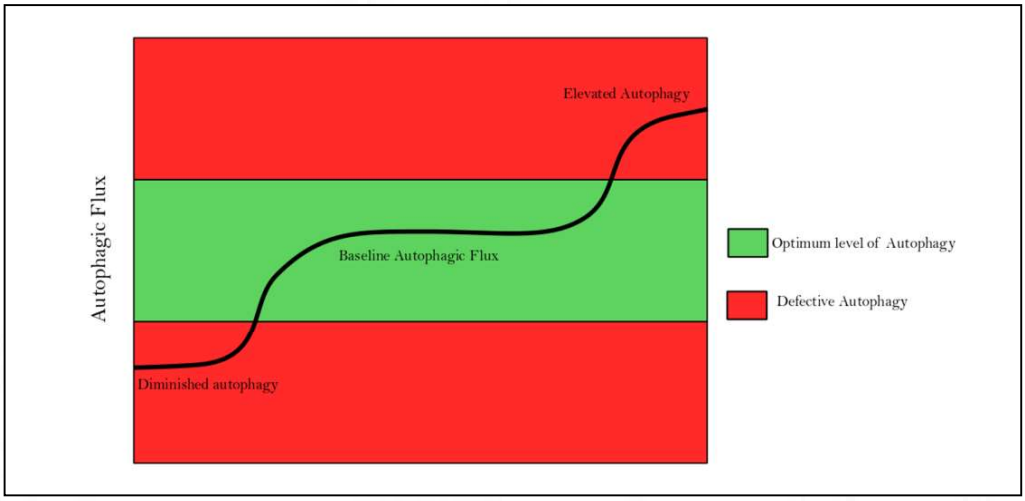

Figure II.1: Autophagic flux*: Maintenance of Optimal levels of Autophagy flux as it helps in keeping the essential resources in dynamic homeostasis. When the autophagy becomes dysregulated, either more than or less than what is required for that tissue type in the given physiological setting, the proper functioning of the tissue gets hindered (Sivasailam et al., 2019).*

Studies on animal models of Transverse aortic constriction (TAC) induced cardiac hypertrophy shows that the adaptive inhibition of autophagy in the myocardium via Akt axis, aids the improvement of cardiac function (Lin et al., 2015). While, deficiency in mTORC1 activity by depletion of raptor, results in the inhibition of adaptive hypertrophy in the heart and this results in rapid progression in to dilated cardiomyopathy (Shende et al., 2011). Cardiac-specific deletion of Atg5 and SQSTM1 in mice resulted in premature aging as well as cardiovascular complications with reduced fractional shortening and left ventricular hypertrophy (Taneike et al., 2010). This provides evidences for the compensating effect of the process of autophagy and enforces that modulation of the process of autophagy has to be done carefully as it can have grave negative impacts on the Myocardium.

As the myocardium is mainly built of post mitotic cells, the cardiomyocytes, aging is one among the major factors that contributes obvious impairments in heart functions.

This could be a consequence of the unavoidable loss in the efficiency of the quality control mechanisms, resulting in an array of molecular changes affecting the normal functioning of the cardiomyocytes (Nakou et al., 2016; Rubinsztein et al., 2011). Elevated expression of autophagy related genes like Atg5 and Atg7 are shown to induce anti- senescence properties, with increased insulin sensitivity, resistance towards obesity, enhanced motor function as well as extended survival; these protective effects could be attributed to the enhancement of autophagy (Pyo et al., 2013, Bhuiyan et al., 2013). Rapamycin, a well-established inducer of autophagy, is also reported to have an anthesis effect on cardiac aging and associated inflammation as well as cardiac hypertrophy (Flynn et al., 1 2013, Dai et al., 2014).

Most metabolic disorders involving cardiovascular complications like diabetes, obesity, hypertension and hyperlipidaemia are experimentally proven to alter autophagic status in the myocardium; this would ultimately result either in the accumulation of dysfunctional organelles and proteins, or involves the chronic hyperactivation of autophagy, culminating in the loss of cardiac health especially in conditions like reperfusion after an ischaemic insult (Sciarretta et al., 2011; Xianmin Xu et al., 2013; Xihui Xu et al., 2013).

II.4. Mitochondria in the heart:

Cardiomyocytes, the contractile units of the heart are thickly populated by mitochondria and this constitutes for ~1/3 the cell volume. The dense population of mitochondria forms a continuous network within the myotubes, but continue to preserve their identity as individual entities coupled through inter-mitochondrial junctions(Hom and Sheu, 2009). This segmentation of mitochondrial units within the network ensures the rapid separation and removal of dysfunctional mitochondrial units from the functional syncytium(Glancy et al., 2017; Hoppel et al., 2009).

Being a metabolic omnivore by nature, the adult myocardium is competent enough to exploit any available energy source like fatty acids, carbohydrates or ketone bodies, for the contraction-relaxation cycle. But under normal physiology, ~70% of the energy requirement is met through fatty acid oxidation. Alterations in the selection of substrates occur at the level of mitochondria, influencing the nature of the

mitochondrial reticulum that wires the cell. Thus, it is not startling that the heart diseases are associated with changes in the mitochondria.

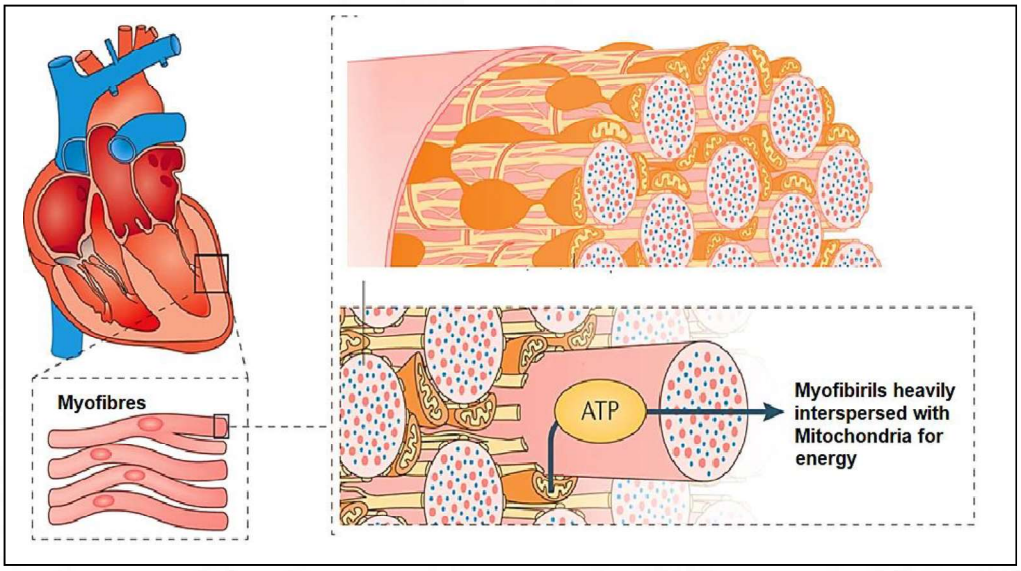

Figure II.2: **Mitochondria in heart**: A schematic representation showing the densely populated mitochondria in the myofibrils of the cardiac tissue**.**

II.5. Mitochondrial dynamics:

Mitochondria in the cardiac myofibrils, form a highly dynamic and intricate network, which adopts diverse morphologies and distribution patterns with altered functional roles in accordance with the cellular signals, either internal or external. Thus, mitochondrial network possesses a very high structural as well as functional plasticity, preserved by the proficient orchestration of a proper balance between the counteracting processes like fission and fusion as well as the biogenesis of new mitochondrial masses and the programmed elimination of the mitochondrial fragments.

Mitochondria are highly dynamic organelles that have to change their function and architecture as per the internal and external cues received by the cells. The term, Mitochondrial dynamics encompasses mitochondrial biogenesis, mitochondrial fragmentation/ fission, mitochondrial fusion, the subcellular localization of the mitochondria as well as the programmed clearance of mitochondrial units.

.

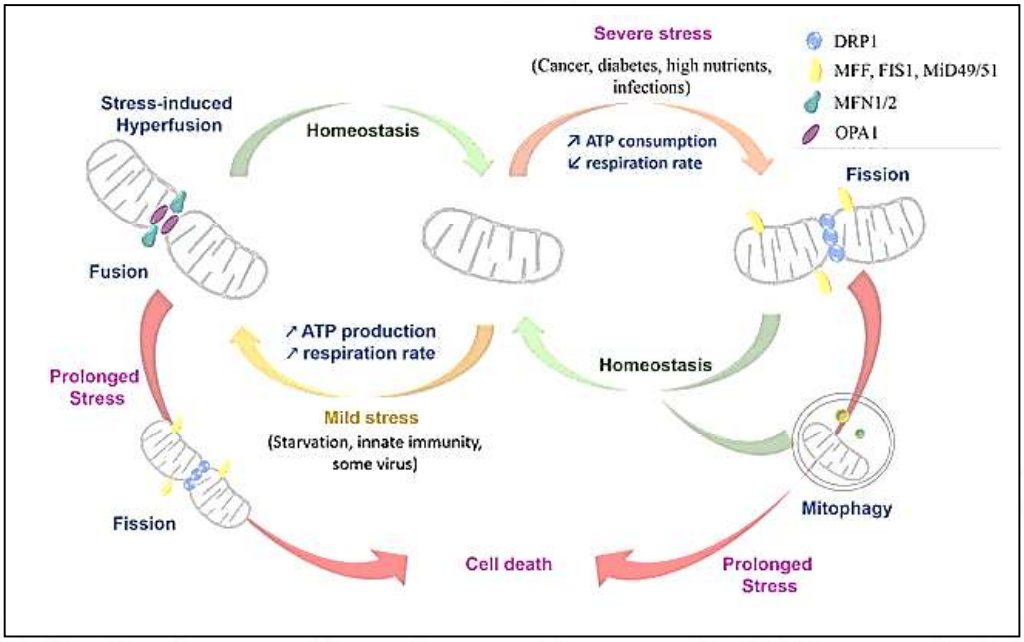

Figure II.3: **Mitochondrial dynamics** (Zemirli et al., 2018). *Mitochondrial network continuously undergoes the counteracting processes: fission and fusion. The equilibrium between these processes could be altered and the balance can lean towards one side according to environment. For example, under starvation, individual mitochondrial units could fuse together to form an elongated and interconnected network that resists mitophagy and increase ATP production. Conversely, under severe stresses, the mitochondrial network could fragment to smaller units. Failure of these pathways could affect the maintenance of homeostasis*

Mitochondrial dynamics is the most critical component ensuring its quality control. When certain components of the mitochondria get damaged, that part of the mitochondria can be truncated off from the mitochondrial network to be then given off for degradation while the healthy mitochondria can get fused for better coordination of the mitochondrial matrix components and electron transport chain enzymes between the mitochondrial fragments(Ichishita et al., 2008; Ingerman et al., 2005). The fission and fusion are mediated in the mammalian systems by the specific proteins like Mitofusin 1, Mitofusin 2 (Mfn1 and 2) and Optic atrophy protein 1 (Opa1) that mediate the fusion of the outer and the inner mitochondrial membranes between two

mitochondrial units. While the fission is mediated by Dynamin related protein 1, a GTPase that upon activation through the phosphorylation of its serine 616 subunit, localizes onto the damaged part of the mitochondrial unit and recruits other activated Drp1 moieties thus constricting the mitochondrial unit until it is broken off from the mitochondrial network. Drp1 also works in association with other mitochondrial fission proteins like Mitochondrial fission factor (Mff), mitochondrial dynamics protein of 49 KDa and 51 KDa (MID 49 and MID51) and Fission 1 (Fis1) (Hansen et al., 2008; Jia et al., 2004; Kuroyanagi et al., 1998). It is observed in studies that mitochondria with high membrane potential which is the hallmark of healthy population have activated fusion proteins and proceed to fusion while those with diminished membrane potential which are the damaged mitochondrial fragments have activated fission proteins to trigger them for degradation by trimming them off from the network.

Mitochondrial dynamics have a critical impact on the mitochondrial metabolism(Gomes et al., 2011a; Westermann, 2012). Mitochondrial units with minimal damage which can be reversed, undergo fusion as this can have a favourable repair in the function of the damaged unit. Fusion of mitochondrial subunits also reduces the formation of new mitochondrial DNA and reduce the mitochondrial ROS production, thereby reducing the ROS mediated damage upon the mtDNA(Seo et al., 2010; Youle and van der Bliek, 2012). With networked mitochondria, there is sharing of the intermediates of the TCA cycle which in turn makes the fused mitochondria more adept. The fragments that are siphoned off from the network have shown to have lowered mitochondrial membrane potential and are thus dysfunctional having poor capacity for ATP generation (Twig et al., 2008a).

II.6. Autophagy and mitochondrial dynamics:

The clearance of mitochondria through autophagy is reported to depend on various molecular mediators that includes, PTEN-induced putative protein kinase 1 (PINK1), Parkin, Bnip3 (Bcl2/adenovirus E1B 19 kDa protein-interacting protein 3), NIX/Bnip3L (Nip3-like protein X), FUNDC1 (Fun14 domain containing 1) as well as Cardiolipin, a critical component of mitochondrial membrane

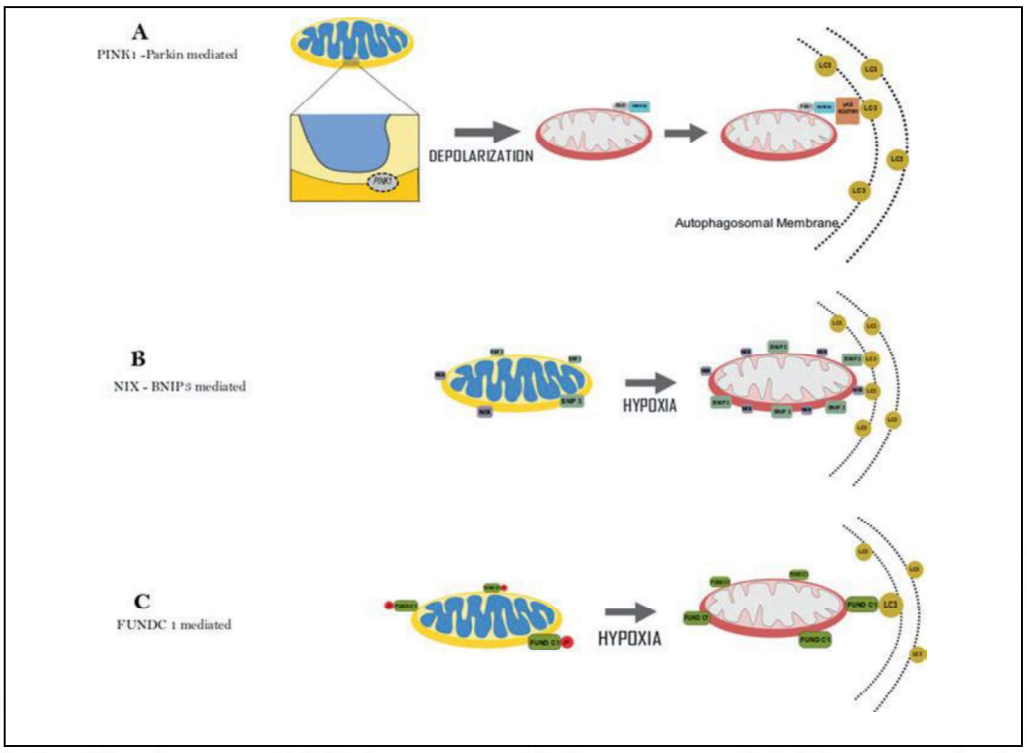

Figure II.4: **Mitophagy -** ***(a)*** *In a depolarized mitochondrion, PINK1 accumulates on the outer mitochondrial membrane and results in Parkin translocation and ubiquitination of outer mitochondrial membrane, targeting it for autophagic degradation. (**b**, **c**) BNIP3/NIX and FUNDC1 are alternate pathways where they serve as receptors that tether mitochondria to LC3 in the autophagosomal membrane* (Sivasailam et al., 2019)

The mediators that recruit mitochondria for autophagy often varies with the nature of the stress that serves as the induction; PINK1/Parkin is reported to be associated with the targeting of depolarized/damaged mitochondria while the involvement of Bnip3, NIX and FUNDC1 are reported mainly in the hypoxic-stress induced mitochondrial clearance.

Mitochondrial architecture is acutely affected by the cellular state including those that govern the autophagic state in the cell, like nutrient and growth factor starvation, etc. mitochondrial morphology has been shown to impact the cellular response to the macroautophagic process. The process that trigger autophagy causes increased fusion of the mitochondria in both in vitro and in vivo model systems. Starvation induced increase in the cellular AMPK levels promotes the activation of PKA which in turn

increases the inactivation phosphorylation of Drp1. This results in the inactivation of fission signals and elongation of the mitochondria. Elongated mitochondria show better cristae structure thus having better ATP production capacity and are also prevented from autophagic degradation as the networked mitochondria escapes the engulfment by the autophagosome membranes (Gomes et al., 2011a; Strauss et al., 2008). Any irregularities in the autophagy causes there to be abnormalities in the mitochondrial dynamics as well, resulting in considerable cellular stress and also considered a means of senescence (Rubinsztein et al., 2011; Seo et al., 2010; Youle and van der Bliek, 2012).

II.7. Autophagy modulators used in Research

Autophagy modulation is regarded as a promising programmed cell death mechanism which could contribute immensely towards the prevention and cure of great number of diseases. Thus, it is crucial to understand the specific mechanism by which this process can be targeted either by pharmacological modulation or genetic manipulation. Pharmacological modulation offers a better scope as site directed genetic manipulation could be a cumbersome process. Chloroquine is one such pharmacological inhibitor which has an established and widely understood influence on the process of autophagy and is an FDA approved drug.

II.7.1. Chloroquine and cardiac function:

Chloroquine (CQ) has been in medical use as an anti-malarial agent along with the potential use as a broad spectrum anti-viral (Al-Bari, 2017; Seo et al., 2010). Nonetheless, there are numerous reports that have shown cardiac complications attributed to the use of CQ or its functional analogue hydroxychloroquine (HCQ). An important meta-analysis that analysed the data from 86 reports that included cohort studies and case reports showed that many patients developed adverse cardiac events with the use of CQ and HCQ for management of inflammatory conditions with the average daily dose for CQ as 250 mg while that of HCQ as 400 mg (Chatre et al., 2018). Another recent study analysed data from various data sets and had 702274 participant data assessed. They observed that the use of both the drugs was significantly linked with adverse cardiac events with CQ showing more cardiotoxicity

than HCQ (Kifle et al., 2021). Many animal model experiments have been carried out to assess the mechanisms and the functional implications of CQ on cardiac function and output. It was shown that acute treatment with 10- 30 μM CQ in animals had a significant decline in the cardiac function as well as in the heart rate. While low dose given chronically had similar effect on the cardiac function with decreased aortic output (Blignaut et al., 2019).

II.7.2. Effects of Chloroquine on mitochondria:

Chloroquine has been used in multiple in vitro and in vivo studies as an autophagy inhibitor, but as it is an already used FDA approved drug, there are many cellular toxicity studies done. Most studies focused on the role of CQ in mediating cancer cell toxicity and have revealed CQ to have mitochondrial effects. To determine the mechanisms of the antitumour effects seen with the use of CQ, the cellular bioenergetics and mitochondrial role in apoptosis have been elucidated (Liu et al., 2018; Qu et al., 2017). It has been shown that CQ decreased the human lung cancer cell growth by activating PI3K/Akt pathway and mediating mitochondrial dysregulation causing apoptosis. The study also showed that CQ supplementation caused decline in the mitochondrial membrane potential and release of cytochrome c thus substantiating mitotoxic effects of CQ. Autophagy also has a significant role in hypoxic insult mediated tissue injury and with the administration of CQ in neuronal hypoxic models in rats, CQ although reduced the autophagy and autophagy mediated apoptosis, increased mitochondrial ROS production and decreased mitochondrial membrane potential and caused higher mitochondrial dysfunction mediated apoptosis(Li et al., 2018). These and other studies have pointed out that CQ might have strong mitotoxic effect may not be tissue specific.

II.7.3. Resveratrol and cardiac function:

Resveratrol, a potent autophagy inducer, is polyphenolic compound which is non-flavonoid and a derivative of stilbene, a plant product and most notable found in grapes, chocolates etc. It has been considered to be the cause behind the ‘French Paradox’ wherein the French population due to their high wine intake have been noted to have reduced risk of cardiovascular diseases despite the high intake of saturated

fatty acids, carbohydrate, etc (Renaud and de Lorgeril, 1992). One of the most notable mechanisms of the beneficial effects of resveratrol is through its property of scavenging of free radicals (Camont et al., 2012; Shiea et al., 2005). In cardiac hypertrophy models' resveratrol has been shown to restore the levels of antioxidants and help in the recovery of the heart. With its pre-treatment the infract size and the necrotic tissue formation showed significant reduction (Mohiuddin, 20190122). In other models which induce cardiac complications as well resveratrol has shown to be cardioprotective. In streptozotocin induced diabetic rats and mice resveratrol improved diastolic function (Gu et al., 2014; Huang et al., 2010; Zhang et al., 2010).

II.7.4. Effects of Resveratrol on mitochondria:

As cardiac contractility and function is critically dependent upon the cardiac mitochondrial capacity to generate ATP; it is hypothesised by various research groups that the cardioprotective effects of resveratrol could have an underlying impact on the cardiac mitochondria. This prompted many studies looking into the molecular pathways that are impacted by resveratrol and how it may impact the mitochondria. Resveratrol has many molecular targets that are directly related with the mitochondrial efficiency and function. In studies with how it mediates glucose homeostasis, a means to reduce diabetic complications; it was observed that resveratrol caused deacetylation of PGC1-alpha via SIRT1 thus inducing mitochondrial biogenesis (Barger et al., 2008; Csiszar et al., 2009). In rat model of T2DM, resveratrol supplementation showed improved function of the cardiac mitochondria as compared with the mitochondria of diabetic animals (Beaudoin et al., 2014).

II.8. Gaps in the literature:

Autophagy is critical in maintaining a pool of healthy and efficient mitochondria and any dysregulation in the basal autophagy results in an observable dysfunction in mitochondria. Mitochondrial function is associated with the mitochondrial quality control within the cells and any derangement of mitochondrial homeostasis causes mitochondrial inefficiency. The cardiac cells are heavily reliant on mitochondria for their contractile function, and it logically follows that with compromised mitochondrial function, there would be a proportional compromise in the cardiac

output. As described earlier, the commonly used autophagy modulators, CQ and RES are shown to have vital impact on the cardiac efficiency. In case of CQ, an autophagic inhibitor, there is known cardiotoxicity and inefficiency reported while RES, an autophagy inducer, there are reported cardioprotective effects. But if these effects are due to their effects on the cardiac mitochondrial function and dynamics has not been studied. We hypothesize that the underlying mechanisms of the cardiotoxic and cardioprotective aspects are governed by their effects on the cardiac mitochondria.

II.9. Hypothesis:

Autophagy modulation influence mitochondrial dynamics as well as function

II.10. Objectives of the study:

- To assess the role of autophagic modulators on mitochondrial metabolism.
- To analyze the mitochondrial dynamics following autophagy inhibition and activation.
- To assess the influence of autophagy modulators on mitochondrial function in an *in vivo* model system.

III.MATERIALS AND METHODS

III. 1. Reagents

High-Glucose DMEM (#D5648), Chloroquine-diphosphate (#C6628), Hydroxychloroquine sulfate (#H0915), Bafilomycin, 3Methyladenine, Resveratrol, the reagents required for the isolation of mitochondria, various Substrates, Uncouplers and Inhibitors for the Mitochondrial oxygen consumption studies (SUIT protocols), and all other chemicals if not mentioned otherwise were purchased from Sigma Aldrich (MO, USA). Fetal Bovine Serum (South American origin) was sourced from Invitrogen. For Realtime PCR gene expression assays qPCR master mix was purchased from Applied Biosystems, NJ, USA. RNA isolation reagent, Tri-Xtract and the specific primers targeting the Genes of Interest were sourced from G-Biosciences, MO, USA). Rapamycin was purchased from Cayman Chemical Company, Michigan, USA.

Antibodies against LC3 #12741, TOM20 #42406, vinculin #13901, OPA-1, DRP-1 and Horse Raddish Peroxidase conjugated anti-rabbit IgG- #7074 were obtained from Cell Signaling Technology, Inc. (MA, USA). Clarity ECL kit #1705061, ClarityMax ECL Kit #1705062, and 29:1 Acrylamide: Bisacrylamide (40%) solution were procured from Bio-Rad Laboratories (CA, USA). TMRM #T5428 was obtained from Sigma Aldrich (MO, USA).

III. 2. Cell culture and maintenance

H9c2, rat embryonic cardiac myoblast (adherent) cells, obtained from ATCC, was generous gift from DIVISION OF TISSUE CULTURE, SCTIMST. In a humidified atmosphere of 5% CO_2 at 37^{o}C, the cells were grown in 25 mm cell culture flask as monolayer culture in DMEM (25mM glucose) containing 10% FBS and antibiotic antimycotic solution (penicillin, streptomycin and amphotericin B). Based on the growth rate, the medium was changed every 2 days for maintaining the culture. For detaching the adherent cells from the plate/flask Trypsin-Phosphate-Versene-Glucose (TPVG) was used. The cells were centrifuged and the supernatant was removed. Then the cells were in a density of ~1x10^6 cells per mL freezing medium (65% medium, 30% FBS, 5% DMSO) and stored at -80^0C freezer or Liquid nitrogen storage facility.

Upon reaching a confluence of 70-80%, the cells were given specific treatments in growth medium with 5% FBS.

Fig. III.1: Study design for cell culture experiments

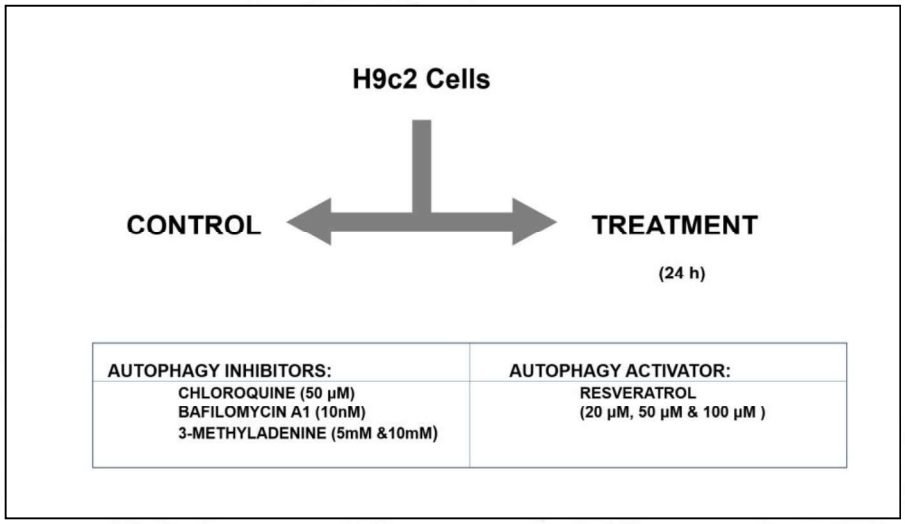

Flow chart representing the study design taken for cell culture experiments

III. 2. 1. Reagents used

III. 2. 1. 1. DMEM preparation (1 litre) (pH 7.4)

25 mM DMEM (16 g), Sodium bicarbonate (2.7 g), Sodium pyruvate (0.11 g), 100 U/ml Penicillin/ Streptomycin, Amphoterixcin B in sterile MilliQ water, filtered and stored in autoclaved bottles.

III. 2. 1. 2. Phosphate-buffered saline (PBS) (pH 7.4)

Sodium chloride 137 mM, potassium chloride 2.7 mM, disodium hydrogen phosphate 10.14 mM, potassium dihydrogen phosphate 1.76 mM in sterile MilliQ water.

III. 2. 1. 3. Trypsin EDTA solution (pH 7.4)

0.25% trypsin, 0.53mM EDTA in PBS.

III. 2. 1. 4. Chloroquine

For cell culture treatments, Chloroquine (10mM stock) was freshly prepared in PBS and diluted to desired concentrations in cell culture media.

III. 2. 1. 5. Bafilomycin

Bafilomycin (1mM stock) was prepared in ethanol and diluted to desired concentrations in cell culture media.

III. 2. 1. 6. Methyladenine

3Methyladenine (1M stock) was freshly prepared in PBS and diluted to desired concentrations in cell culture media.

III. 2. 1. 7. Resveratrol

Resveratrol (100mM stock) was prepared in ethanol and diluted to desired concentrations in cell culture media.

III. 2. 1. 8. Rapamycin

Rapamycin (1mM stock) was prepared in ethanol and diluted to desired concentrations in cell culture media.

III.3. Cell viability assays

III.3.1. LDH cytotoxicity assay

LDH assay is a colorimetric assay that measures release of the stable, cytosolic, lactate dehydrogenase (LDH) enzyme, from damaged cells which is an extensively used biomarker for cellular cytotoxicity. The LDH released in to the extracellular space/ cell culture medium is measured with a coupled enzymatic reaction, the conversion of a tetrazolium salt (iodonitrotetrazolium (INT)) into a red color formazan by diaphorase. The resulting formazan absorbs maximally at 492nm and thus provides colorimetric at 490nm which is a direct indication of cell death.

To analyse the cell viability after the preferred treatments,

Optimal number of cells were seeded on to a 96well cell culture plate in 100µL of Phenol red free High glucose DMEM.

Assay was included with the following controls as per manufacturer's protocol,

a. A complete media control, with the serum concentration used in the experiment, without cells to determine LDH background activity present in the sera used.

b. A serum-free media control, to determine the amount of LDH activity in the sera.

c. LDH Activity Controls: Cells with control conditions.

d. Maximum LDH Activity Controls: Cells with maximum cell lysis, done with the lysis buffer provided along with the LDH assay kit.

Cells with desired treatments and the aforementioned controls were prepared and incubated for 24h time point in a incubator at 37°C, 5% CO2. Following the incubation period, the maximum lysis control was treated with lysis buffer and placed in the incubator at 37°C, 5% CO2 for 45 minutes, after which, 50µl media from each sample was transferred to a 96-well flat-bottomed plate in triplicate wells. The media collected was mixed with the Reaction Mixture, as mentioned in the manufacturer's protocol. The reaction setup was then incubated at room temperature for 30 minutes in dark. 50µl Stop Solution was then added to each sample and mixed by gentle tapping. The absorbance was then measured at 490nm.

Percentage cytotoxicity was then calculated as,

$$\%Cytotoxicity = \frac{\text{Compound Treated} - \text{LDH activity control}}{\text{Maximum LDH release} - \text{LDH activity control}} X100$$

III. 3.2. Hoechst –PI staining procedure

Cell death analysis was performed by means of Hoechst/PI double staining method. Optimal number of cells were seed on to 8 well chamber slides, and after the desired treatments were done for 24h, the cells were incubated with 1µg/mL Hoechst (Sigma-Aldrich, Gillingham, UK) at 37˚C for 15 min, washed with PBS and incubated with 1µg/mL Propidium Iodide (PI) (Sigma-Aldrich, Gillingham, UK) for 3-5 min. The fluorescent images (Hoechst- Ex/Em:350/460 nm; PI- Ex/Em:530/640 nm) were obtained from five different fields for each group, and at least 200 cells were counted using ImageJ version 1.49a (NIH, USA).

Cell death after CQ treatment was analyzed by fluorescence microscopy (Carl Zeiss: AxioVision) after staining with Hoechst/PI.

The cell death percentage was then calculated as,

$$\%Cell\ death = \frac{\text{No. of PI (T)/No. of Hoechst (T)}}{\text{No. of PI (C)/No. of Hoechst (C)}} X100$$

III. 3. 2. 1. Reagents Used

Hoechst 33342 stock (10 mM)

2 mg in 1 mL DMSO

Propidium iodide stock (10 mg/mL)

5 mg in 500 µL DMSO

III. 4. MitoSOX Red staining for Mitochondrial ROS measurement

MitoSOX Red (Molecular Probes [Invitrogen] Eugene, OR, USA), a mitochondrion targeted fluorogenic probe was used for the determination of Mitochondrial ROS generation. The stain is selectively targeted to the mitochondria where it is oxidized by superoxide and becomes fluorescent on binding to nucleic acids.

MitoSOX Red stock (5mM) was prepared by dissolving 50 µg of probe in 13 µL anhydrous DMSO and the working solution was prepared in Phenol red free High glucose DMEM.

Post treatments, the cells were probed with MitoSox and analyzed either microscopically or using a Fluorescence-activated Cell Sorter.

For FACs based analysis, the cells were detached with Trypsin-EDTA, post treatments, washed with HBSS and loaded with MitoSox (5 µM) for 10 minutes in HBSS and directly subjected to flow cytometry analysis using BD FACSJazz™ (BD Biosciences, CA, USA). MitoSox was excited by laser at 488 nm and the data collected

at 585/29 nm. Cell debris were gated out by distinct forward and side scatter and the data were collected by recording 10,000 fluorescence events.

For fluorescence microscopy-based analysis, optimal number of cells were seeded on 8-well chambered coverslips and post treatments, the cells were washed and were incubated with 5 µM of MitoSOX Red probe for 10 min at 37 °C. After two washes with warm HBSS/PBS, the cells were counterstained with Hoechst following which the Fluorescent (Ex-500nm/Em-590nm) emission was imaged using an Zeiss AxioObserver 7 with Apotome 3.0 fluorescence microscope with 63X oil immersion objective.

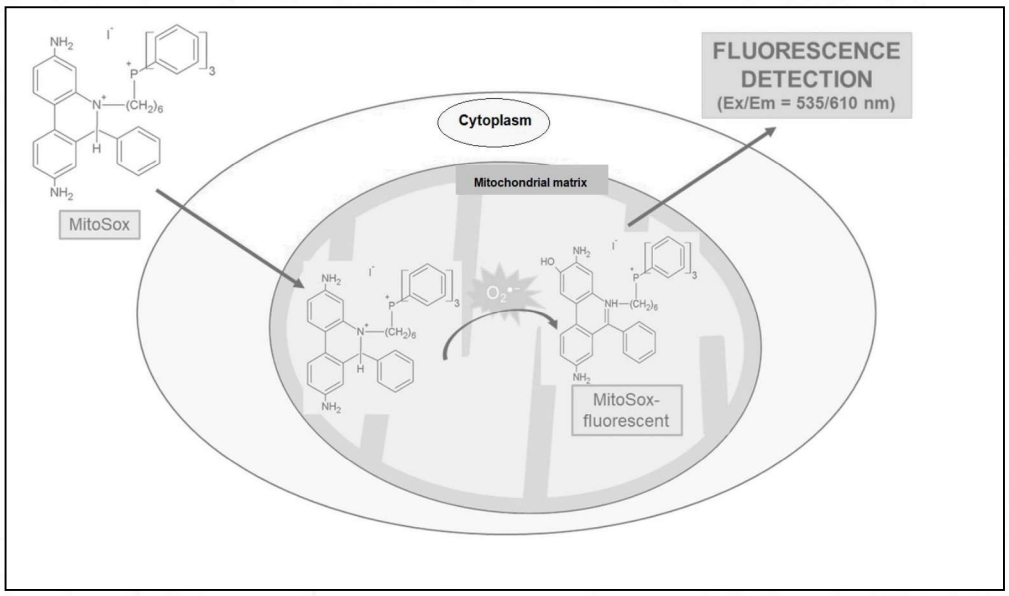

Fig. III.2. Mechanism of MitoSOX Red - *MitoSOX is an Ethidium Bromide derivative which upon entering the cell is readily targeted specifically to the mitochondria where the superoxide radicals oxidise it forming a red fluorescence emitting moiety.*

III. 5. Real-Time qR T-PCR for Gene Expression Assays

III. 5.1. Agarose Gel electrophoresis

TBE Buffer (5X)

1.1M Tris, 900 mM Borate & 25 mM EDTA, pH 8.3.

Agarose gel

Low EEO Agarose (1%) molten in 1X TBE and casted in a gel cast

EtBr (Ethidium Bromide)

EtBr dissolved at 3% concentration in distilled water.

III. 5.2. RNA extraction and cDNA synthesis

Cells after treatments were washed with HBSS; lysed and total RNA was extracted using were isolated using Tri-Xtract (G-Biosciences, MO, USA) with slight modifications in the manufacturer's protocol. Here, after the aqueous phase was separated out from the Tri-Xtract-Chloroform mix, it was mixed with equal volume of ethanol and loaded on to the spin-columns of **RNeasy Mini Kit** (**Qiagen**, Germany). Rest of the steps were followed as per the instructions from the kit insert. Briefly, the mixture was transferred in to spin cartridges, centrifuged and the flow-through was discarded. The columns were then washed with wash buffer I followed by wash buffer II. The RNA elution from the spin columns were done in 30 µL RNase free water. The concentration, purity of the RNA was assessed using BioPhotometer Plus (Eppendorf AG, Hamburg, Germany) by measuring A260, A260/A230 and A260/A280 absorbance, following which the RNA samples were aliquoted and stored at -80ºC till use. Repeated freeze-thaws were avoided preserve RNA integrity.

Using 1 µg RNA for each sample, cDNA was synthesized for the whole transcriptome in Mastercycler Pro PCR system (Eppendorf, Hamburg, Germany), with iScript cDNA Synthesis Kit (Bio-Rad, CA, USA) as per manufacturer's protocol.

III. 5.3. Analysis of mRNA levels of Mitochondrial related transcription factors

For the analysis of the gene expression pattern of Transcription Factors related to mitochondrial biogenesis – NRF1, NRF2A, NRF2B, TFB1, TFB2 and TFAM, as well as mitochondrial fusion and fission proteins, OPA-1 and Mitochondrial Fission Protein (FIS1), specific primers were designed using NCBI Primer Blast online tool and were custom synthesized from G-Biosciences (MO, USA). The qPCR assay protocol was optimized and primer efficiency for individual pairs were calculated. The qPCR aasays

were performed either in QuantStudio 5 Real-Time PCR System or CFX96 Touch Real-Time PCR System using TB Green Premix Ex Taq II (Takara, Japan). Briefly, 2 min hold at 50 °C followed by 10 min hold at 95 °C and then 40 cycles of Denaturation: 15 sec at 95 °C and Annealing/Extension: 30 sec at 60 °C. PCR efficiency for each reaction was calculated by LinRegPCR version 2021.1 (Ruijter et al., 2009) and Paffl method was employed to calculate relative gene expression data while accounting for differences in primer efficiencies (Pfaffl, 2001).

III. 6. Immunoblot analysis

III. 6. 1. Whole cell lysate preparation

H9c2 cardiomyoblasts were seeded on to 100 mm culture plates and treatments were given for respective time course described. After the treatment periods, the cells were washed with ice-cold PBS and scrapped in ice cold RIPA (Radio Immuno Precipitation Assay) buffer containing proteinase inhibitor and phosphatase inhibitor cocktail. The lysate is then gently vortexed at 4^0C for 30 minutes followed by centrifugation at 13,000 rpm for 20 min at 4^0C. The supernatants were then aliquoted in to equal volumes and stored at -80^0C for use.

III. 6. 2. Protein quantification

Protein quantifications were performed using BCA-assay kit (Pierce Biotechnology, MA, USA). Pre-diluted BSA protein standards in range of 125 to 2000 µg/mL were used to generate a standard curve of Absorbance versus Micrograms of protein, and the concentration of proteins in the cell lysates were determined.

III. 6. 3. SDS PAGE

Whole cell lysates were quantified and (20-40µg) proteins were heat denatured with β- Mercaptoethanol, for 5 minutes, and resolved on Sodium Dodecyl Sulphate- Poly Acrylamide Gel Electrophoresis (SDS-PAGE) at 100V. Resolved proteins were transferred on to PVDF membrane at 10V for 40 minutes in a semi dry transfer apparatus or 100V for 20-30 minutes in a wet transfer apparatus. The membrane was blocked for overnight at 4ºC with blocking buffer (5 % Milk in TBST). The membrane was then probed with antibodies against LC3 B, DRP1, OPA-1, MFF, vinculin, β-

Actin (1:1000) at 4ºC overnight. HRP conjugated anti rabbit (1:5000) secondary antibody used for the study.

III. 6. 4. Chemiluminescent detection

FemtoLUCENT™ PLUS-HRP chemiluminescence Detection Kit (GBiosciences, MO, USA) was used for visualizing protein bands. Equal volumes of luminol and peroxide solutions were mixed and added on to the membranes. An X-ray film was used to capture light emitting bands. The film was then developed and documented in Gel Doc™ XR Imaging System (Bio-Rad Laboratories, Hercules, CA, USA) and quantified using Image J Analysis Software (NIH).

III. 6. 5. Reagents used

Acrylamide 30%

Acrylamide- 29 % (w/v) and N, N'-methylene bisacrylamide- 1% (w/v) in 100 mL in deionized water.

Blocking solution

BSA- 1 % (w/v) in 1X TBST.

10 X Electrode buffer (Running Buffer)(pH 8.3)

Trizma base – 25 mM, Glycine –192 mM, SDS –1% in deionised water.

Ponceau S stain

1% Ponceau in 5% glacial acetic acid.

8 X Resolving gel buffer (pH 8.8)

SDS - 0.2%, Tris – 3 M in deionized water.

SDS gel loading buffer (2X)(pH 6.8)

SDS – 4%, 2- mercaptoethanol – 10%, Glycerol – 20%, Bromophenol blue – 0.004%, Tris-, HCl - 0.125 M in deionized water.

4 X Stacking gel buffer (pH 6.8)

SDS – 0.1%, Trizma base 0.5 M in deionised water.

10 X Transfer buffer, pH 8.3

Trizma base – 25 mM, Glycine –192 mM, 20% methanol in deionised water.

Tris-buffered saline (10 X, pH 7.6)

Tris base- 24.2 g, sodium chloride- 80 g in 1L deionized water.

Tris-buffered saline with Tween-20 (TBST) [1 X]

1X TBS containing 0.5% Tween-20.

III. 7. Animal models

Animal experiments were conducted with the approval of the Committee for the Purpose of Control and Supervision of Experiments on Animals (CPCSEA), Government of India, and Institutional Animal Ethics Committee of SCTIMST, Trivandrum. Male C57BL/6 mice were selected for the study and were bred at division of laboratory animal science, Biomedical Technology Wing, SCTIMST. All Animals were housed in specific pathogen-free, individually ventilated cage facility with recommended temperature and humidity, on a 12:12h light-dark cycle, with free access to standard diet and water with proper bedding. After completing their corresponding period of treatments, the animals were sacrificed by cervical dislocation and the whole heart was extracted and immersed in ice cold BIOPS (Biopsy Preservation solution) solution and immediately taken for mitochondrial isolation.

III. 7.1. Grouping of Animals

The animals at the age of 12 weeks and 22 weeks as Mature-adults (Group A) and Elderly (Group B) respectively("The Mouse in Biomedical Research - 2nd Edition," n.d.), were included in the study. Both groups were further sub-grouped into Control and Drug-treated (with at least four animals per sub group).

III. 7.2. Drug treatment for mice

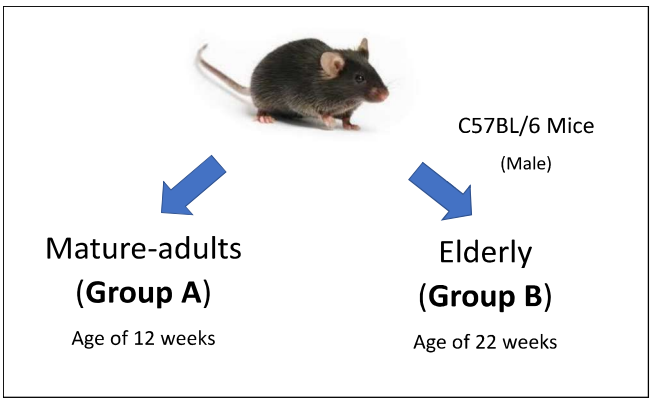

Figure III.3: Selection of animals for *in-vivo* study - *A schematic representation*

For studying the impact of Autophagy modulation on the cardiac mitochondrial respiration in mice, an autophagic activator, Resveratrol (5 mg/kg body weight, single dose per day, dissolved in normal saline) and an autophagy inhibitor, Chloroquine (10 mg/kg body weight, single dose per day, dissolved in normal saline) were administered intraperitoneally for 14 days, whereas the control group received normal saline. On completion of the treatment, the animals were euthanized and the whole heart was extracted to evaluate the mitochondrial metabolism.

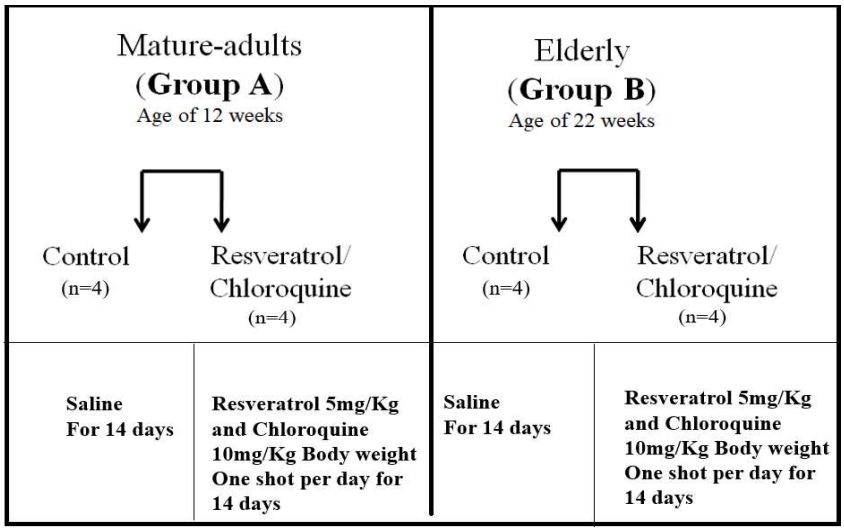

Fig. III.4: **Strategy for *in-vivo* study**

III. 7. 3. Reagents used

Saline preparation (1 litre)

Sodium chloride (0.9 %) in sterile autoclaved distilled water.

Resveratrol solution

Resveratrol (5 mg/kg) in 100 % ethanol.

Chloroquine solution

Chloroquine (10 mg/kg) in saline solution.

III.8. High Resolution Respirometry

Mitochondrial functional analyzes were performed in Oxygraph-O2k, High-Resolution Respirometry (Oroboros Instruments, Innsbruck, Austria) at 37°C with a stirring speed of 750 rpm. Amplified signals from the oxygen sensor were recorded at sampling intervals of 2 s using DatLab-6.1 Software (Oroboros). Air-calibration of the respirometer at specific media was performed at air saturation, 37°C before the commencement of each experiment. Addition of substrates, uncoupler, and specific inhibitors of mitochondrial electron transport chain (ETC) complexes was performed using Hamilton syringes manually.

III.8.1. Analysis of Mitochondrial bioenergetics in cardiomyoblasts

H9c2 cells cultured with or without CQ treatment for 24 h were harvested using 0.1% Trypsin-EDTA, washed, and resuspended in respiration media, and added to the 2 ml glass chambers (1.5–2 million cells/ml) of O2k-Respirometer.

III.8.1.1. *Intact Cell respiration measurements*

Intact cell respiration was measured using serum free cell-culture media. In accordance with Oroboros guidelines ("MiPNet08.09 CellRespiration - Bioblast," n.d.), coupling control protocol for intact cells with oligomycin was used and respiration in different coupling control states, ROUTINE (R), LEAK (L), and Maximal electron transfer capacity (E) was derived from the O_2 flux values. 'R' corresponds to the physiological

respiration of intact cells with endogenous substrates and is measured after adding cells to the chambers. 'L' respiration means the residual respiration independent of ATP synthase and corresponds to the proton leak, proton slip, and cation cycling across the inner mitochondrial membrane; Oligomycin (2.5 µM), complex-V inhibitor, was used to induce leak-state. Here, the Oligomycin sensitive respiration, i.e., the difference between 'R' and 'L', represents the ATP-linked respiration (R-L). Hereafter, the maximal respiration, 'E' was established experimentally by stepwise titration of CCCP (Carbonyl cyanide 3-chlorophenylhydrazone), 0.5 µM each time. The Spare-capacity of mitochondria was calculated as a difference between the Maximal-capacity and the Routine respiration (E-R). Residual oxygen consumption, ROX is the respiration connected to non-mitochondrial oxygen-consuming processes and instrument background; Rotenone (5 nM), an inhibitor of Complex-I and Antimycin A (2.5 mM), an inhibitor of Complex-III, were added to the system to inhibit mitochondrial oxygen consumption, giving ROX.

III.8.1.2. *Analysis mitochondrial complex linked respiration*

Analysis of the mitochondrial activity following exogenously given substrates in permeabilized cells was carried out in mitochondrial respiration buffer (MiRO5) consisting of 110 mM sucrose, 60 mM potassium-lactobionate, 20 mM taurine, 10 mM monobasic potassium phosphate, 3 mM magnesium chloride, 20 mM HEPES, 1 mM EGTA, and 0.1% (w/v) BSA at pH 7.1. Either, the SUIT (Substrate-Uncoupler-Inhibitor-Titration) protocol mentioned by Pesta et al., was followed with slight modification (Pesta and Gnaiger, 2012) i.e., in the presence of Palmitoyl Carnitine (25 µM), Malate (2 mM), Pyruvate (5 mM), Glutamate (5mM) and Succinate (10 mM) at saturating concentration of ADP (5 mM), or the specific substrates and the inhibitors for each complex were used in a sequential manner. In the first method, after the addition of the substrates to measure State 3 respiration (i.e., respiration in the presence of exogenous substrates at saturating concentration of ADP), mitochondrial uncoupling was achieved by stepwise titration of CCCP, followed by Rotenone (0.1 µM) and Antimycin A (2.5 µM) to measure ROX, where as in the second method, after the addition of the specific substrates to measure the respiration, specific inhibitors

like Rotenone for Complex I, Malonate for Complex II and Sodium Azide for complex IV were used, while no uncouplers are used.

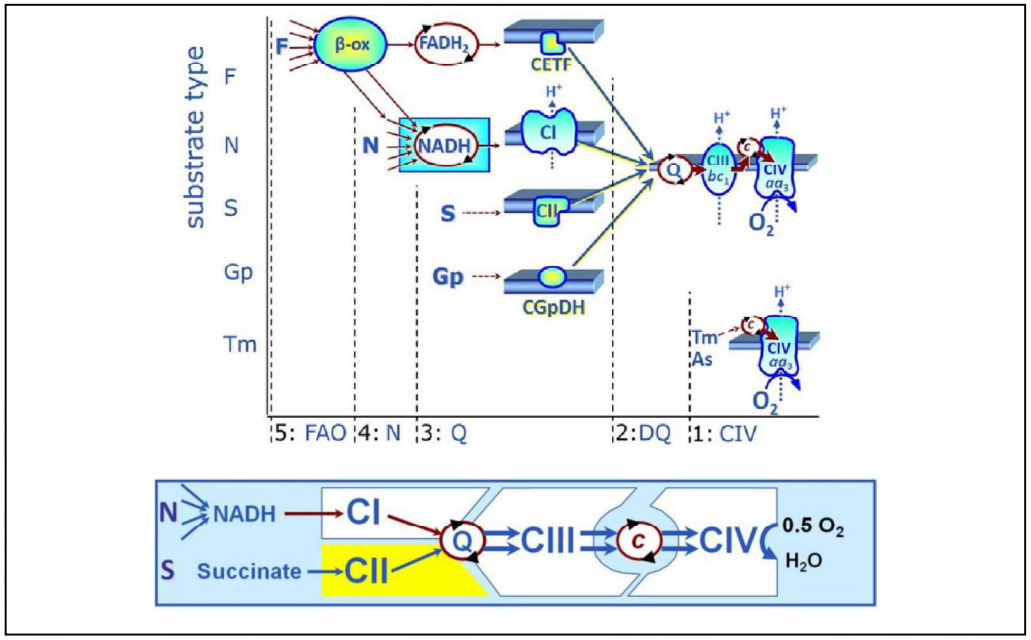

Fig. III.5: Respiratory complexes and the path of electrons - *A schematic representation showing the in the mitochondrial electron transport chain.*

III. 8. 2. Mitochondrial function studies using isolated mitochondria

Isolated cardiac mitochondria for functional studies were added to each 2-mL chamber containing mitochondrial respiration buffer (MiR05). Data acquisition and analysis of oxygen consumption rate (OCR) were done with Datlab 5 software (Oroboros, Innsbruck, Austria). Using micro syringes, supraphysiological concentrations of various substrates/inhibitors/uncouplers for respiratory experiments were carefully added to the respiration medium in the chambers in a step-by-step manner.

III. 8. 2. 1. Isolation of mitochondria from freshly extracted whole heart

After sacrificing mice, the whole heart was immediately immersed in ice-cold BIOPS buffer for mitochondrial isolation. As described by Fontana *et al* published in Mitochondrial Physiology Network Oroboros O2k protocols (2015), mitochondria were isolated from the heart tissue by differential centrifugation protocol. The freshly isolated mitochondria were immediately used for oxygen consumption studies.

The protocol is as follows:

- The animals were sacrificed and dissected the heart without blood vessels and fat.
- Immediately transferred the tissue into ice cold BIOPS and washed.
- The weight of heart tissue was recorded.
- Transferred heart to a cooling petridish containing BIOPS, excised ventricle (rat experiments) or taken whole heart (mice experiments) and carefully eliminated blood clots.
- Transferred heart into 1.5 mL microfuge tube on ice with 0.5 mL of ice cold BIOPS and cut the heart tissue into small pieces with cooled scissors.
- Transferred the tissue paste into 5 mL motor glass and added 4 mL isolation buffer and dounced slowly 6-8 times (maximum 1 min at 150 rpm).
- Transferred tissue homogenate to 50 mL falcon tube and added 2 mL isolation buffer.
- Centrifuged homogenate at 800 x g for 6 minutes at 4^{o}C.
- Transferred supernatant to new 50 mL falcon tube.
- Centrifuged the supernatant at 10,000 x g for 10 min at 4^{o}C.
- Removed the supernatant and carefully re-suspend the mitochondrial pellet in 500 µL isolation buffer and then made the volume up to 2 mL of isolation buffer. (Pipette was not used to re-suspend, but by gentle tapping)
- Centrifuged at 10,000 x g for 10 min at 4^{o}C.
- Removed the supernatant and carefully re-suspended the mitochondrial pellet in suspension buffer and the mitochondria was ready for using in oxygen consumption measurements.
- The protein content of mitochondria was analyzed using pierce 660 nm method.

III. 8. 2. 2. Buffers for mitochondrial isolation

BIOPS

	Final Conc.	FW	Stock Solution	Addition to 1 litre final Vol:
CaK_2EGTA	2.77 mM		100 mM	27.7 mL
K_2EGTA	7.23 mM		100 mM	72.3 mL
Na_2ATP	5.77 mM	551.1		3.180 g
$MgCl_2.6H_2O$	6.56 mM	203.3		1.334 g
Taurine	20 mM	125.1		2.502 g
Na_2Phosphocreatine	15 mM	255.1		3.827 g
Imidazole	20 mM	68.1		1.362 g
Dithiothreitol (DTT)	0.5 mM	154.2		0.077 g
MES hydrate	50 mM	195.2		9.76 g

BIOPS contain the following ion concentrations:

Ca^{2+} free	0.1µM
Mg^{2+} free	1mM
MgATP	5mM
Ionic strength	160mM

- Adjusted the pH to 7.1 (with 5 M KOH) at 0^{o} C. Store BIOPS and K_2EGTA/CaK_2EGTA solutions at -20^{o} C in plastic vials.

Mitochondrial respiration medium (MiR05)

	FW	Final Conc (mM)	Addition to 1 litre final Vol:
EGTA	380.4	0.5	0.190 g
$MgCl_2.6H_2O$	203.3	3	0.610 g
K-lactobionate	358.3	60	120 mL of 0.5 M stock
Taurine	125.1	20	2.502 g
KH_2PO_4	136.1	10	1.361 g
HEPES	238.3	20	4.77 g
Sucrose	342.3	110	37.65 g
BSA (FA free)		1 g/L	1 g

Preparation of MiR05 stock solution

- Weighed given amounts of the listed chemicals (expect BSA and lactobionic acid) and transferred to a 1000 mL glass beaker.
- The big lumps were mechanically disrupted. (It was recommended to do this before adding water, because during dissolution these lumps do not disintegrate easily).
- Added ~ 800 mL H_2O and dissolved using a magnetic stirrer at ~30ºC.
- Added 120 mL of K-lactobionate stock solution.
- Adjusted the pH to 7.1 with 5 N KOH at 30ºC.
- Dissolved the BSA in a subsample of the MiR05 stock solution and added to the final MiR05 (Separate preparation of the BSA solution is recommended, since BSA produces foams that do not dissolve easily).

- Added H_2O to a final volume of 1000 mL and checked the pH and finally MiR05 was prepared.
- Divided into 40 mL portions in plastic vials and stored at -20ºC.
- Each vial was warmed to 37^0C before use and foam formation was avoided by gentle shaking. (It was recommended to use the stock solution on a single day only, to avoid microbial contamination of the respiration medium).

Preparation of K-lactobionate stock solution

Dissolved 35.83 g lactobionic acid in 100 mL H_2O, adjust pH to 7.0 with KOH, and adjusted volume to 200 mL with H_2O. pH - 7.1 (5 N KOH), divided and frozen at -20º C in falcon tube.

Isolation buffer

Stock solution	Final Conc.	Addition to 200 ml final volume
D-Mannitol	225 mM	90 mL
Sucrose	75 mM	30 mL
EGTA	1 mM	2 mL
BSA	1 g/L	0.2 g

Suspension buffer

Stock Solution	Conc.	FW	Addition to 1 litre final volume
D-Mannitol	0.5 M	182.17	91.085 g
Sucrose	0.5 M	342.3	171.15 g

EGTA	0.1 M	380.35	38.35 g

For the oxygen consumption study of cardiac mitochondria, following mitochondrial substrate/inhibitor protocols was adopted:

III. 8. 2. 3. Fatty acid + Carbohydrate protocol

State 1, the first respiratory state in an oxygraphic protocol is achieved when isolated mitochondria are added to mitochondrial respiration medium containing oxygen and inorganic phosphate, but no ADP and no reduced respiratory substrates. State 2, substrate limited state of residual oxygen consumption was measured with palmitoyl-L-carnitine (Pal) (25 μmol/L) and malate (M) (2 mmol/L) ($PalM_0$), give oxygen consumption rate through β oxidation. After addition of ADP (5 mmol/L) to the medium, state 3 respiration ($PalM_{ADP}$) is achieved which will provide electrons to electron transferring flavoprotein (ETF) and complex I. The outer mitochondrial membrane integrity was evaluated by stimulation of respiration by exogenously added cytochrome *c* (2 μmol/L). The normalized *c* effect was expressed as flux control factor. Then the carbohydrate substrates like pyruvate ($PalMP_{ADP}$) (5 mmol/L), glutamate ($PalMPG_{ADP}$) (10 mmol/L) and succinate ($PalMPGS_{ADP}$) (10 mmol/L) are sequentially added. Adding pyruvate or glutamate as substrates, display capacity of complex I and succinate give that of complex II by being donors of electrons to specific molecules in electron transport system.

Fig. III.6: Fatty acid + Carbohydrate protocol

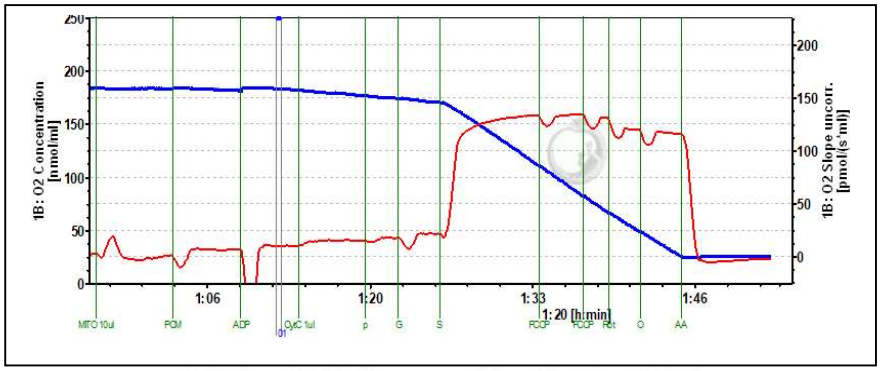

Dat-file representation of the SUIT protocol adopted for the isolated cardiac mitochondria

SUIT Protocol			
S/ U/ I	**Event**	**Volume (µL)**	**State**
Mitochondria	MITO	10	State 1
Palmitoyl- Carnitine Malate	PCM	5 5	State 2
Adenosine 5' diphosphate	ADP	20	State 3 ETF
Cytochrome *c*	C	1	
Pyruvate	P	5	State 3 ETF + CI
Glutamate	G	10	State 3 ETF + Cl
Succinate	S	20	State 3 ETF + Cl + Cll
Rotenone	Rot	1	State 3 Cll
Oligomycin	O	1	State 4
Carbonyl cyanide p-trifluoro-methoxy phenyl-hydrazone	FCCP	1+1	ETS
Antimycin A	AA	1	ROX

III. 8. 2. 4. Chemicals for mitochondrial substrate-uncoupler-inhibitor titration (SUIT) protocols with isolated mitochondria

Substrates

Substrate	FW	Stock solution Conc. (mM)	Stock solution Amount	Final concentration in 2ml Volume within the Chambers(A&B)
G: L- Glutamic acid	169.1	2000	3.382 g/ 10 mL H_2O	10 mM
M: L-Malic acid	134.1	400	536 mg/10 mL H_2O	2 mM
P: Pyruvic acid sodium salt	110	2000	44 mg/ 0.2 mL H_2O	5 mM
S: Succinate disodium salt, hexahydrate	270.1	1000	2.701 g/ 10 mL H_2O	10 mM
Pal: Palmitoyl-DL-carnitine-HCl	436.1	10	8.72 mg/ 2 mL H_2O	25 μM
***c*:** Cytochrome *c*	12500	4	50 mg/ mL H_2O	2 μM
D: ADP (Adenosine 5' diphosphate, potassium salt)	501.3	500	0.501 g/ 2 mL H_2O	5 mM

As: Ascorbate sodium salt,	198.1	800	1.584 g/ 10 mL H_2O	
Tm: TMPD N,N,N',N'-Tetramethyl-pphenylenediamine dihydrochloride	237.2	200	47.4 mg/ mL H2O	

Uncouplers

Uncouplers	FW	Stock solution Conc (mM)	Stock solution Amount	Final concentration in 2ml Volume within the Chambers(A&B)
F(FCCP): Carbonyl cyanide p-(trifluoro-methoxy) phenyl-hydrazone	254.2	1	2.54 mg/ 10mL ethanol	0.5+0.5 µM

Inhibitors

Inhibitors	FW	Stock solution Conc. (mM)	Stock solution Amount	Final concentration in 2ml Volume within the Chambers(A&B)
AA: Antimycin A	540	5	11 mg/ 4mL ethanol	2.5 µM
Omy: Oligomycin	800	5	4 mg/ 1mL ethanol	2.5 µM

Rot: Rotenone	394.4	1	3.94 mg/10mL ethanol	0.05 µM
Azd: Sodium azide,	65.01	4000	260 mg/1 mL H_2O	

III. 9. Statistical analysis

All statistical calculations and preparation of graphs were carried out in Microsoft EXCEL 2020 software. Values are expressed as the mean ± standard deviation (SD) with n≥3 for all the experiments. The significance of the difference from the respective control for each experimental test conditions was assayed by Student's *t*-test as the distributions were normal. For all statistical analysis, differences between means were considered statistically significant at a *p*- value of less than 0.05.

IV. Results

IV.A. Autophagy inhibition

To study the effect of autophagy inhibition on cardiac cells in the *in-vitro* settings H9c2 cells were treated with autophagy inhibitors, Chloroquine (CQ), Bafilomycin (BAF) and 3-Methyladenine (3-MA) for 24h. Chloroquine was the primary choice for autophagy inhibition as it is an FDA approved drug in use, with a well-established and documented autophagy inhibitory effect in a variety of cells.

IV.A.1. Effects of CQ on mitochondria in cardiac cells

IV.A.1.1. Determination of CQ concentration for *in vitro* assays In order to find out a non-toxic concentration of CQ that would yet significantly inhibit autophagy, an assessment of cell death and cytotoxicity was performed in H9c2 cells.

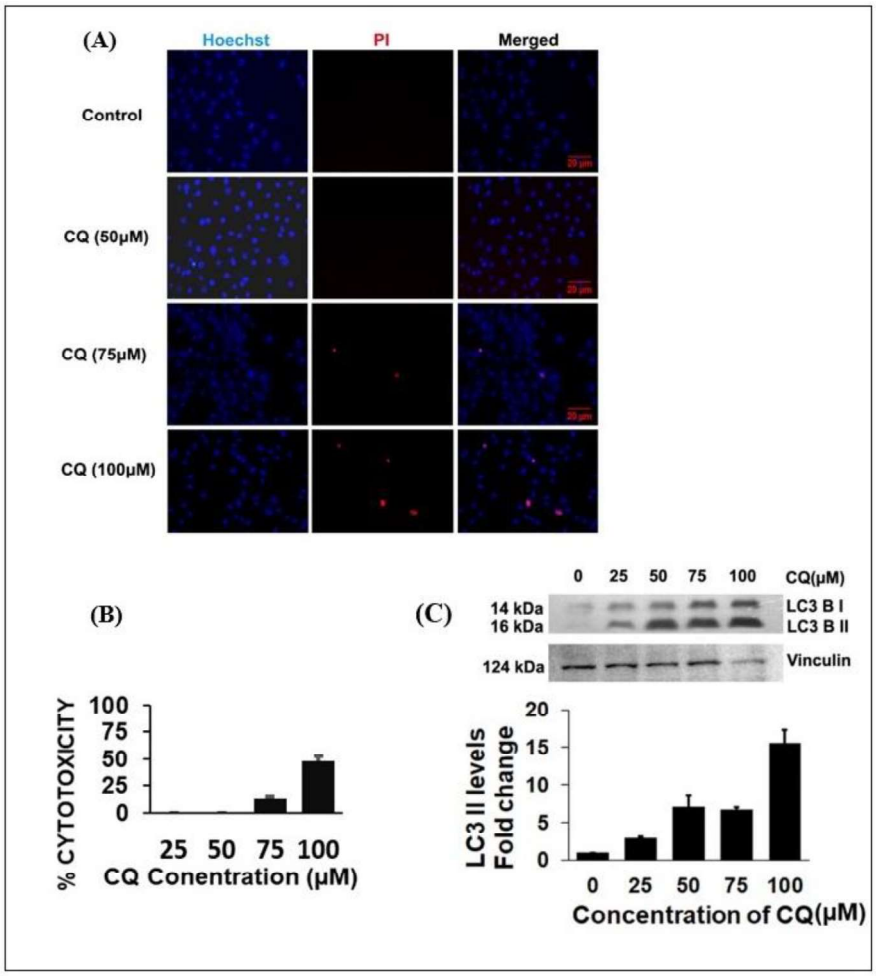

Figure IV. 1: Determination of CQ concentration for *in vitro* assays: A- *Hoechst Propidium Iodide imaging shows no cell death at 50 µM concentration while with increasing concentrations the cellular toxicity increases.* **B –** *Cytotoxicity assessment of different concentrations of CQ by LDH assay, which shows that as the concentration of CQ increases beyond 50 µM for 24 h, the cytotoxicity also increases.* **C –** *Western Blot analysis for assessment of LC3 II accumulation (which gives a measure of the autophagic arrest) showed that 50 µM CQ caused significant autophagic cessation.*

CQ inhibits the fusion of autophagosome with lysosome and would induce cell death at higher concentrations, thus the optimal concentration of CQ for *in-vitro* experiments was determined by assessing the cell viability (Fig. 1**A)** as well as cytotoxicity (Fig. 1**B)** in cardiomyoblasts exposed to different concentrations of CQ (25-100 µM).

Assessment of the accumulation of autophagic vacuoles (with LC3II, as a readout for autophagosome accumulation) showed that 50 µM of CQ for 24 h caused similar LC3-II accumulation to that of higher concentrations with minimal cell death (Fig. 1**C**). Therefore, 50 µM of CQ for 24h was used for all *in-vitro* experiments.

IV.A.1.2. Assessment of cellular metabolic activity

Metabolic activity post CQ treatment was assessed by MTT assay, which relies on the enzymatic reduction of MTT to MTT-formazan, catalysed by cellular oxido-reductases, thus providing a direct indication of the metabolic activity. With CQ treatment, we observed a significant decline in the metabolic activity of cardiomyoblasts (Fig. 2).

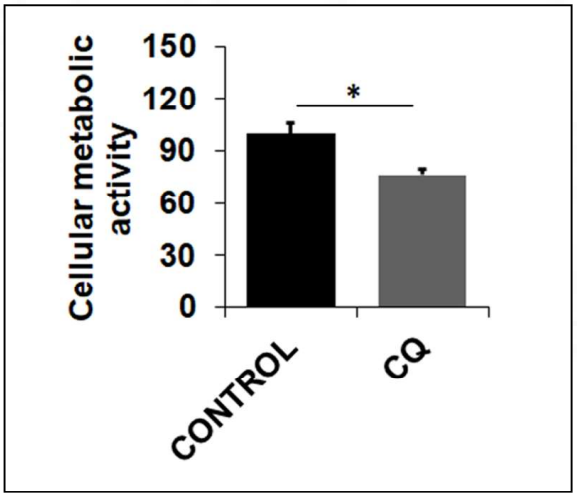

Figure IV. 2: **Cellular metabolic activity-** *The bar graph shows the* % Cellular metabolic activity *which suggests that 50 µM CQ significantly reduces the action of cellular dehydrogenases and thus impedes metabolism.*

IV.A.1.3. CQ causes decline in the intact-cell bioenergetics

Cellular respiration and mitochondrial efficiency assessed with standard coupling control protocol for intact cells show that, exposure to CQ resulted in significant decline of overall respiratory parameters which includes Routine (**R**), Maximal (**E**), ATP-linked (**R-L**) and Spare capacity (**E-R**) of mitochondria, implying a decline in the cellular bioenergetics (Fig. 3**A**-3**D**).

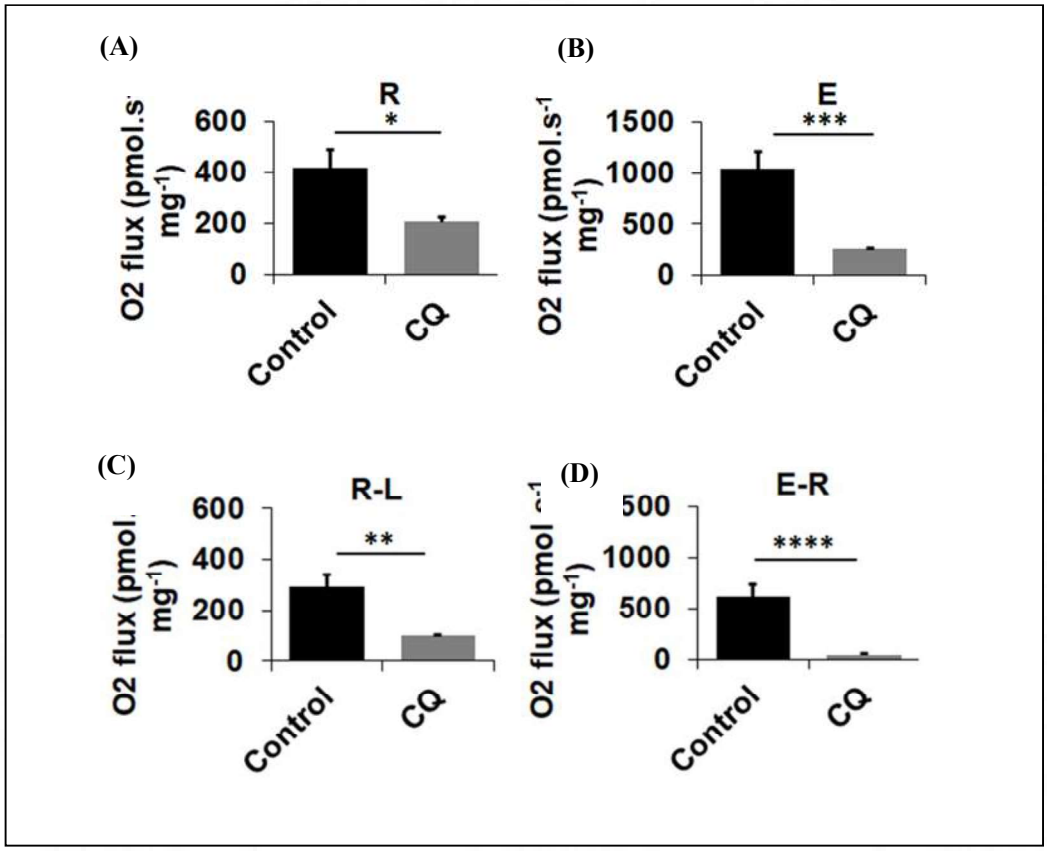

Figure IV. 3: CQ treatment diminished cellular bioenergetics. ***A –*** *Intact cell respiration of CQ treated cells along with respective controls were measured following resuspension of cells in serum free DMEM in Oroboros Oxygraph O2K. In accordance with Oroboros guidelines different respiratory parameters were recorded as Routine respiration (R)* ***B –*** *Maximal respiration (E) following uncoupling with CCCP* ***C –*** *ATP turnover (R-L)* ***D –*** *Spare respiratory capacity (E-R)*

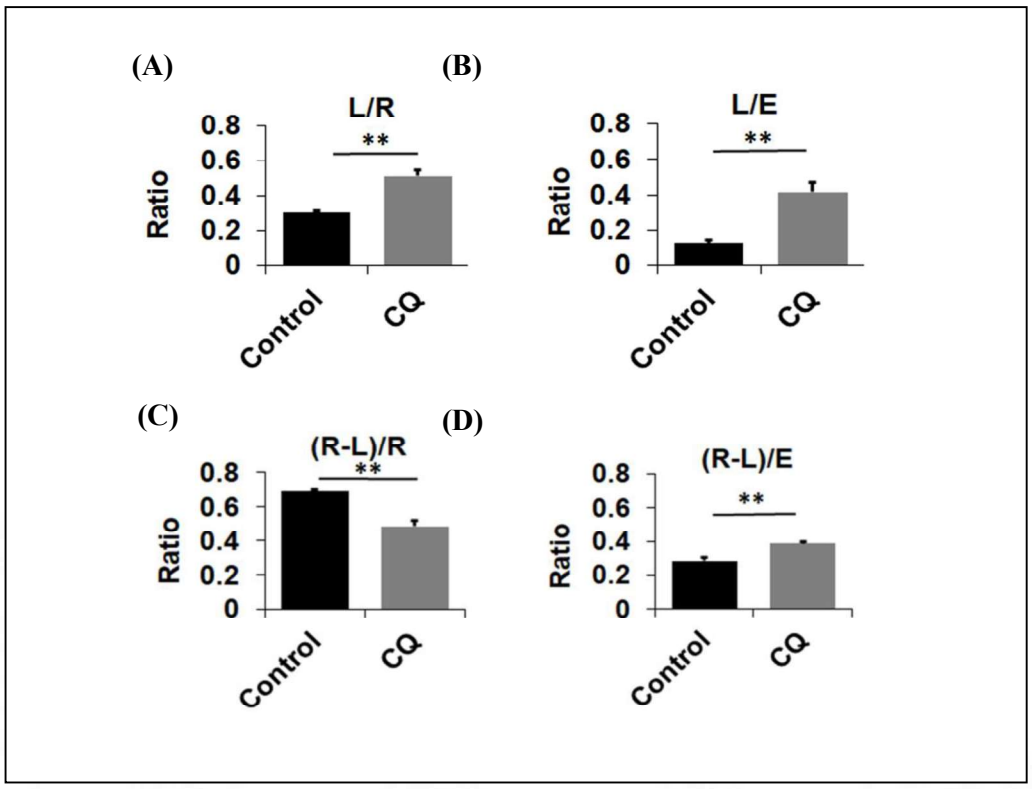

Figure IV. 4: Respiratory control ratios *derived from the respiratory parameters measured in the intact cell respiration*. **A–** (L/R), **B –** (L/E), **C –** (R-L)/R, **D –** (R-L)/E

The coupling control states measured were used to derive Coupling Control Ratios (with a theoretical lower and upper limits of 0 and 1.0), which provides a comprehensive analysis of mitochondrial efficiency (Gnaiger, 2009; Pesta and Gnaiger, 2012). The ratio of Leak to Routine (L/R) and Leak to ETS capacity (L/E) showed an increase in CQ treated group compared to the control group (Fig. 4**A** & 4**B**). The coupling efficiency, (R-L)/R, showed a significant decline with CQ treatment (Fig. 4**C**) while the fraction of net-Routine to ETS capacity i.e., (R-L)/E shows an increase (Fig. 4D).

IV.A.1.4. Substrate linked respiration

To confirm if the mitochondrial functional decline observed was due to a fall in the efficiency of the ETC complexes, the substrate-linked respiration of mitochondrial electron transport chain complexes like, Complex-I/N-linked respiration, Complex-II

linked respiration and Complex-IV linked respiration were assessed in the presence of exogenously supplied substrates as well as inhibitors specific for each complex. Cells were permeabilized and mitochondrial functional measurements were made in the presence of Pyruvate, Glutamate and Malate for Complex-I/N-junction followed by the addition of Rotenone, a Complex I inhibitor. Succinate was used as Complex-II substrate followed by Malonate addition, which is a competitive inhibitor of Complex-II. Complex-IV assessment was done in the presence of TMPD, an electron donor for Complex IV and ascorbate, followed by the addition of azide, a Complex IV inhibitor, to negate the rise in oxygen consumption induced by the auto-oxidation of TMPD. CQ treatment resulted in significant reduction in the substrate-linked respiration of Complex-I (Fig. 5**A**)., II (Fig. 5**B**), and IV (Fig. 5**C**).

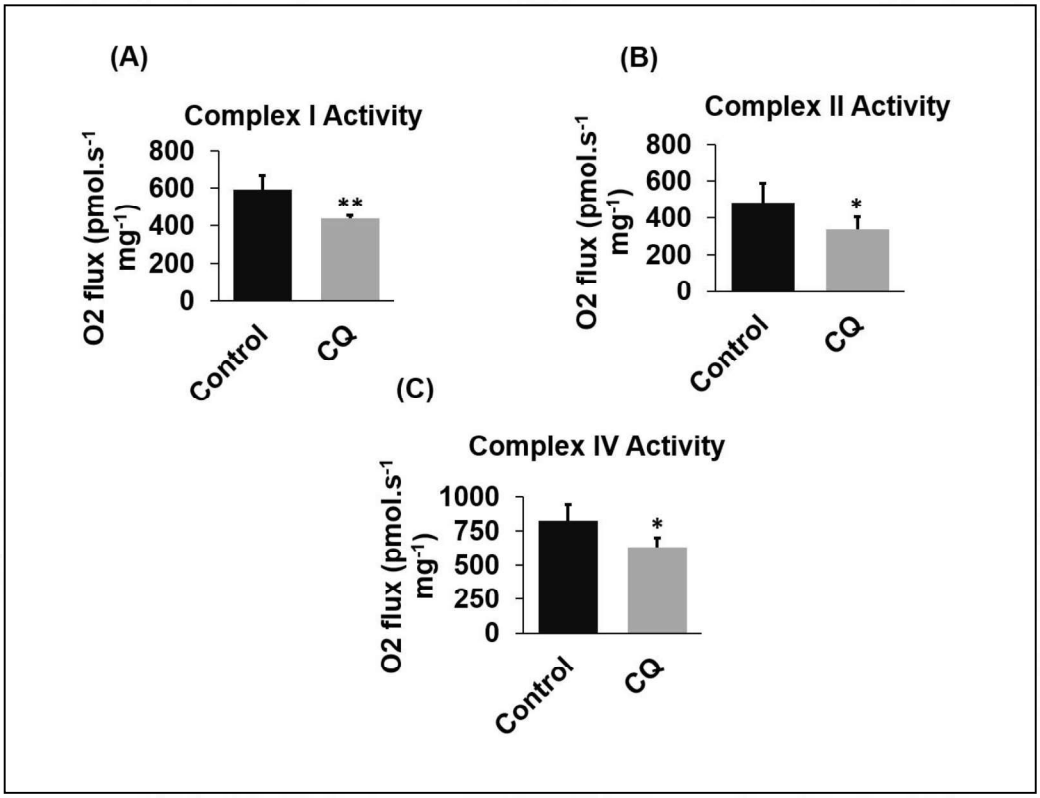

Figure IV. 5: **Substrate-linked respiration:** *The substrate-linked respiration following the addition of exogenous substrates showed that the CQ treatment reduced the capacity of mitochondrial complexes to utilize the substrates effectively.* ***A****- N-linked respiration following the addition of substrates that feed electrons to the N-junction (Pyruvate + Glutamate + Malate) followed by the addition of Rotenone* ***B****-*

Complex-II linked respiration, following the addition of Succinate followed by Malonate ***C*** *– Complex-IV linked respiration following the addition of TMPD + Ascorbate, followed by Azide.*

IV.A.1.5. Analysis of Mitochondrial copy number:

We performed a relative quantification of mitochondrial content by qPCR assay, where a mitochondrial gene (mitochondrial tRNA) was amplified and normalized to a nuclear gene (β2 Microglobin).

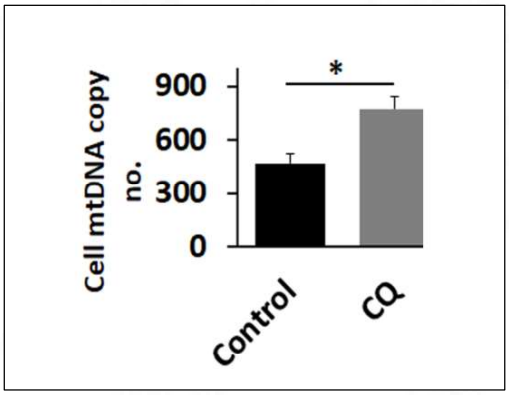

Figure IV. 6: Assay for Mitochondrial DNA copy number: *Mitochondrial content was determined through the quantification of mitochondrial DNA via qPCR and normalized to nuclear DNA showing CQ treatment caused accumulation of mitochondria thus increasing its total content. The bar graph represents change in the mitochondrial copy number in CQ treated cells with respect to the controls.*

It was observed that the CQ-treated cells had increased mitochondrial content compared to respective controls (Fig. 6).

IV.A.1.6. qPCR assay for Mitochondrial Biogenesis:

The mRNA expression of an array of transcription factors in the PGC1α axis, Nuclear Respiratory factor 1 (NRF1), NRF 2A, NRF 2B, Mitochondrial Transcription Factor B1 (TFB1), TFB2 and Transcription Factor A – Mitochondrial (TFAM), which regulates mitochondrial biogenesis under the control of peroxisome proliferator-activated receptor gamma co-activator 1 alpha (PGC1α) were assessed, and all these showed a significant enhancement after 12 h of CQ treatment (Fig. 7).

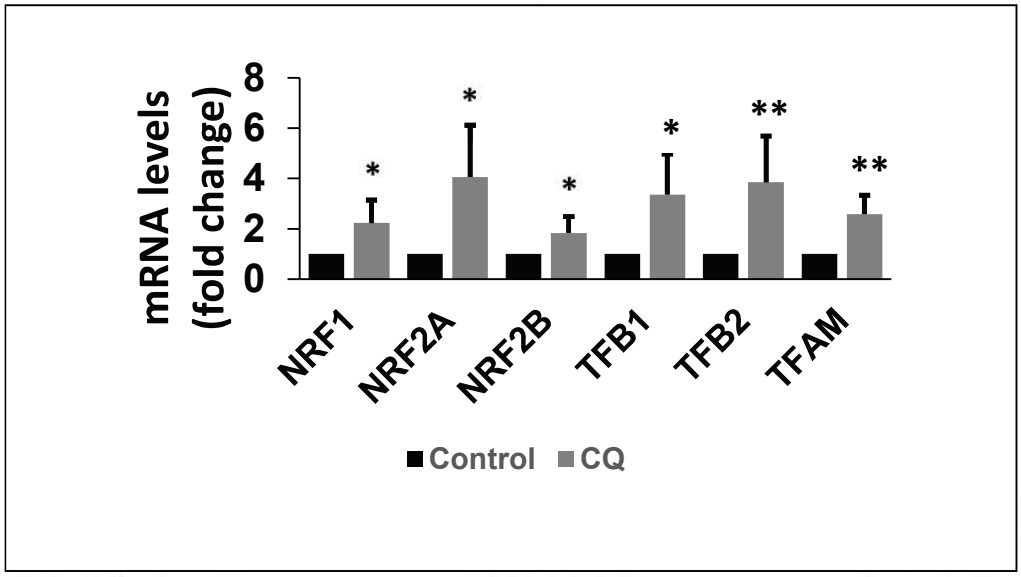

Figure IV. 7: qPCR analysis of the expression of transcription factors: *Expression pattern of the transcription factors shows a significant rise after 12 h of CQ treatment (50 µM). The bar graphs represent the fold change in the mRNA expression levels with respect to controls.*

IV.A.1.7. Assessment of mitochondrial membrane potential

Mitochondrial membrane potential (MMP) was measured by staining cells with TMRM, a cationic dye, that accumulates in to the mitochondria driven by their memmbrane potential. It was observed that the MMP in the cells treated with CQ for 24 h was significantly lower than that in the control condition (Fig. 8**A** & 8**B**).

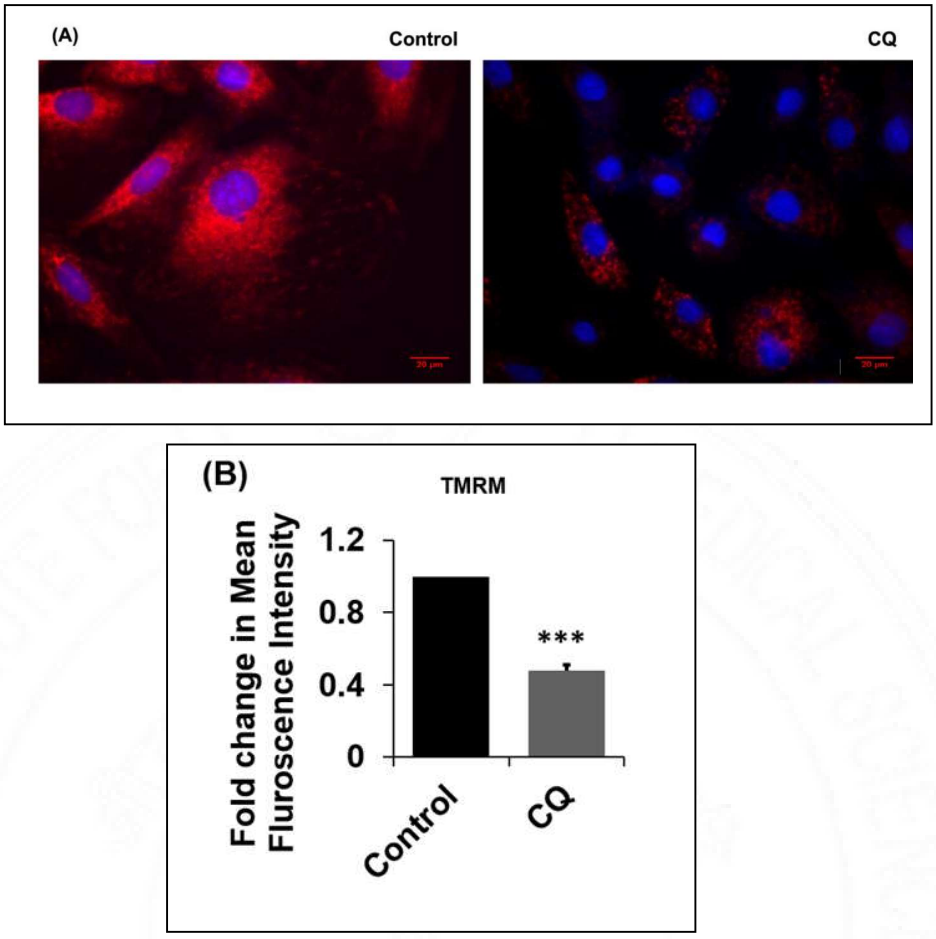

Figure IV. 8: TMRM staining for Mitochondrial membrane potential - *CQ affected the Membrane potential of Mitochondria shown by the TMRM fluorescence intensity Fig **A** represents the TMRM staining which shows the decline in the relative fluorescence intensity following CQ treatment. The bar graph, Fig **B**, represents the foldchange in the fluorescent intensity with respect to controls.*

IV.A.1.8. MitoSox staining to detect Mitochondrial Superoxide

Mitochondrial superoxide assessment was done through Mito Sox staining and subsequent FACS analysis which revealed an elevated mitochondrial superoxide production post CQ treatment. Representative histogram and bar diagram for MitoSox staining is shown in Figure (Fig. 9**A &**9**B**).

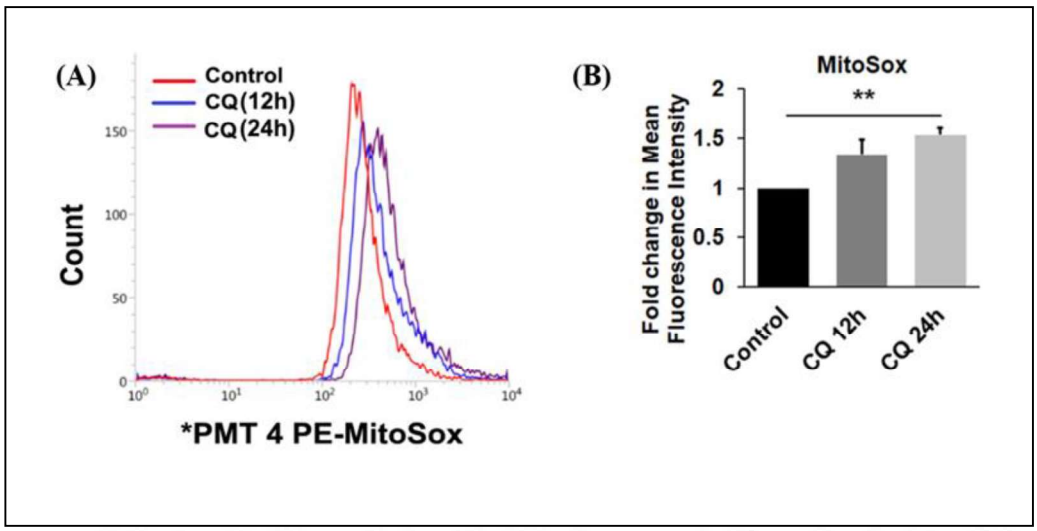

Figure IV. 9: Flow cytometry analysis of Mitochondrial ROS – *Mitochondrial Superoxide levels were estimated at 12 h and 24 h following CQ treatments with respective controls. The histogram represents the FACs result. The bar graph represents the fold change in the fluorescent intensity with respect to controls.*

IV.A.1.9. Assessment of mitochondrial morphology

Mitochondrial network was stained with Mitotracker Deep Red fluorescent stain that accumulates into metabolically active mitochondria regardless of the membrane potential. Following the CQ treatment, cells seeded on the chambered coverslips were incubated with the stain for 30 min and analysed by whole cell analysis with a custom designed macro for NIH ImageJ, developed by Dagda et al., 2009. This helped tracing the individual mitochondrial units in an unbiased way and estimate the indices of mitochondrial interconnectivity and mitochondrial elongation. CQ treatment of cardiomyoblasts resulted in decreased mitochondrial interconnectivity and elongation scores compared to control untreated cells (Fig. 10**A** and 10**B**,). Analysis of TOM20, an outer mitochondrial membrane protein through immunocytochemistry also confirms the fragmentation and dispersion of mitochondria (Fig. 10**C**)

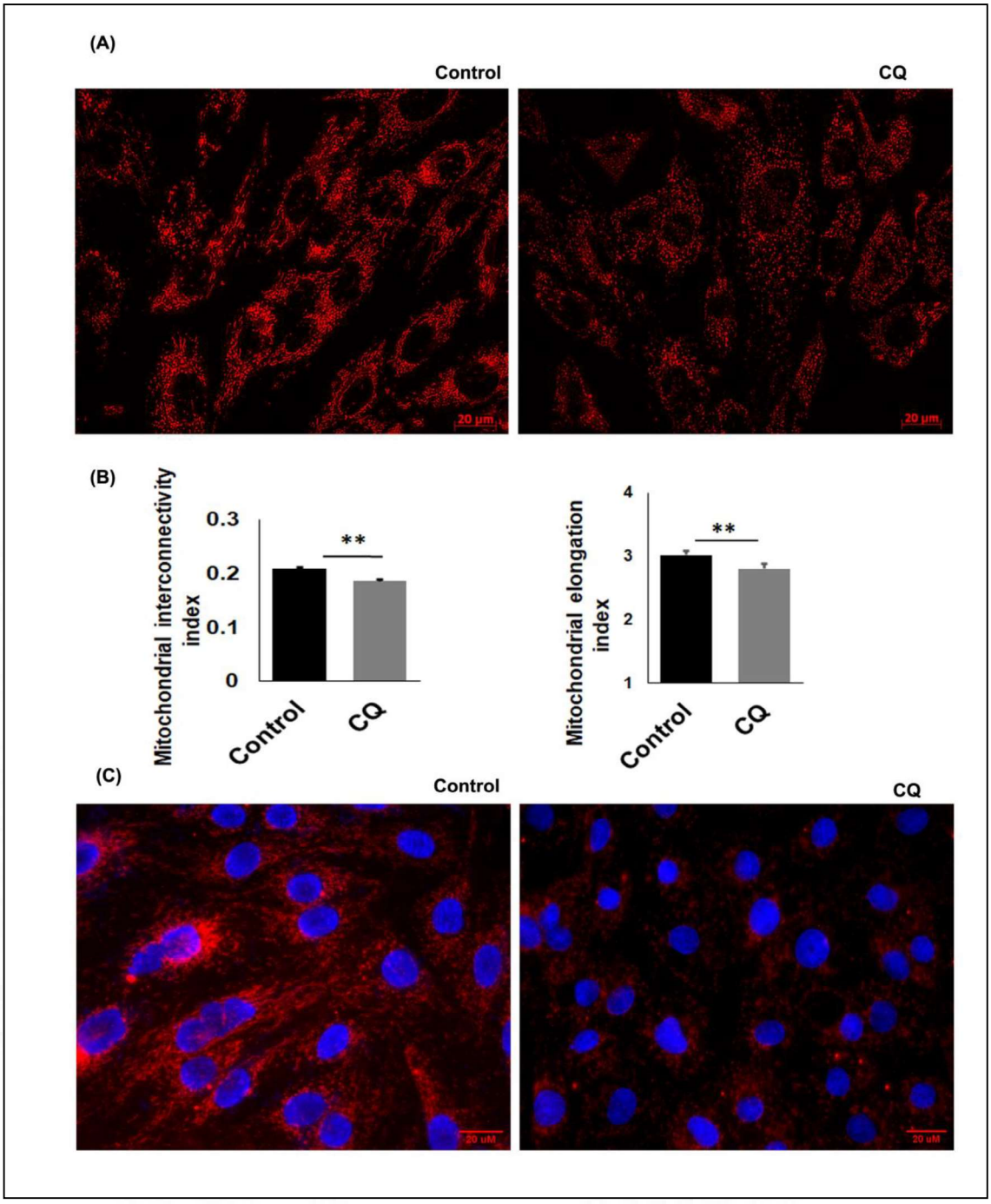

Figure IV. 10: Assessment of Mitochondrial morphology - *semi-quantitative analysis following the MitoTracker staining (Fig A) shows mitochondrial fragmentation and dispersion following CQ treatment. Fig B Shows the bar graph that represents the change in the mitochondrial interconnectivity and elongation with*

respect to controls. TOM20 Immunofluorescent analysis (Fig C) also indicates the same.

IV.A.1.10. Gene expression levels of OPA 1 and FIS 1

The gene expression pattern of OPA1, an inner membrane fusion protein, showed an increasing trend after 24 h of CQ treatment, although it was not statistically significant. While the gene expression of FIS1, a critical component of mitochondrial fission complex is significantly reduced post CQ treatment. (Fig.11)

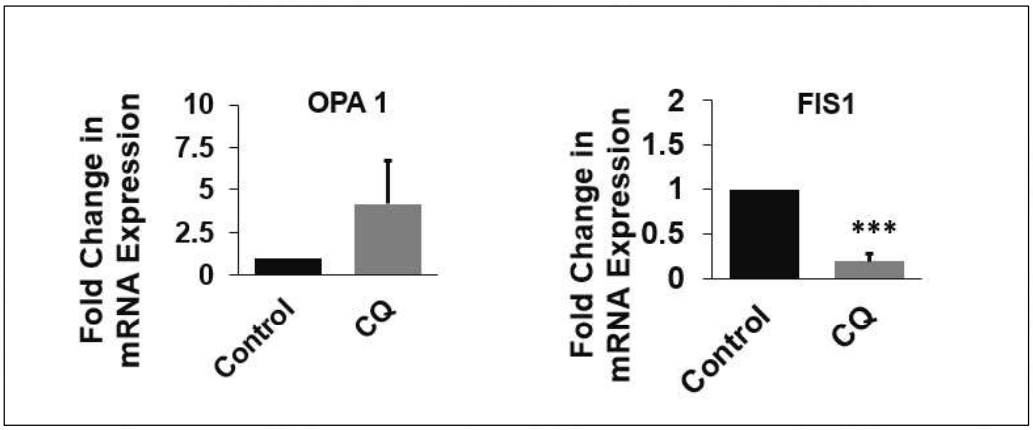

Figure IV. 11: Gene expression levels of OPA1 and FIS1- *mRNA expression levels of OPA-1 and FIS-1 were analysed post CQ treatment. The bar graph represents the foldchange in the mRNA expression levels with respect to respective controls.*

IV.A.1.11. OPA-1 (L- form) and DRP1 expression

OPA-1 is an inner mitochondrial membrane protein which aids the membrane fusion. The L- form or long form is the membrane associated form, while the soluble form is a proteolytic product of long form. Here, we observed that the OPA-1 (L form) is significantly reduced post CQ treatment (Fig 12A). While, the expression of DRP1,

an important protein involved in the orchestration of mitochondrial fission process, remains unaltered (Fig 12B).

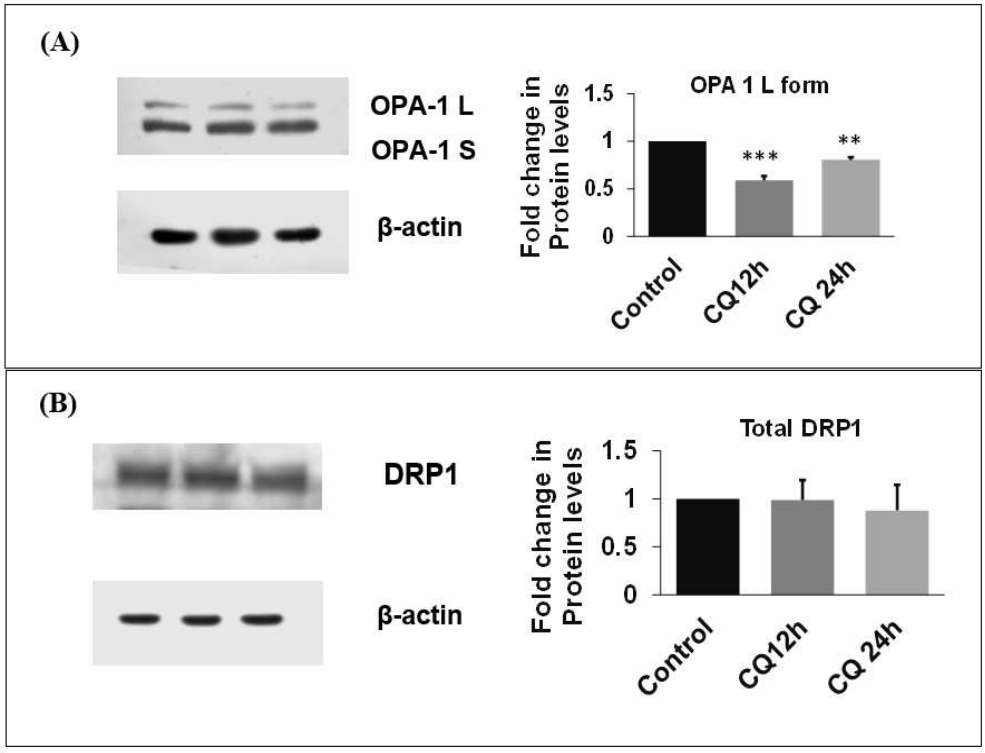

Figure IV. 12: OPA-1 (L form) and total DRP1 expression- *Fig. 12A shows the western blotting for OPA-1 with bar graph showing the fold change in the expression levels of OPA-1 L, While Fig. 12B shows the western blotting for Total DRP1 with the corresponding bar graph.*

IV.A.2. Effect of HCQ on mitochondrial in cardiac cells

Hydroxychloroquine (HCQ) is a hydroxylated derivative of CQ, and was demonstrated to possess much less (~40%) toxicity than that of CQ in animal models. Thus, we wanted to assess the mitotoxic effect of this derivative of CQ and it was done in cardiomyoblasts. The concentration of HCQ used was the same as that of CQ, 50 μM. Intact cell respiration parameters and the respiratory control ratios were assessed with standard coupling control protocol for intact cells after exposure to HCQ (50 μM) for 24 h. HCQ also induced a significant decline in cellular bioenergetics as evident from overall respiratory parameters, Routine (**R**), Maximal (**E**), ATP-linked (**R-L**) and

Spare capacity (**E-R**) of mitochondria (Fig. 13**A-D**), as well as the Respiratory Control Ratios (Fig. 14**A-**14**D)**.

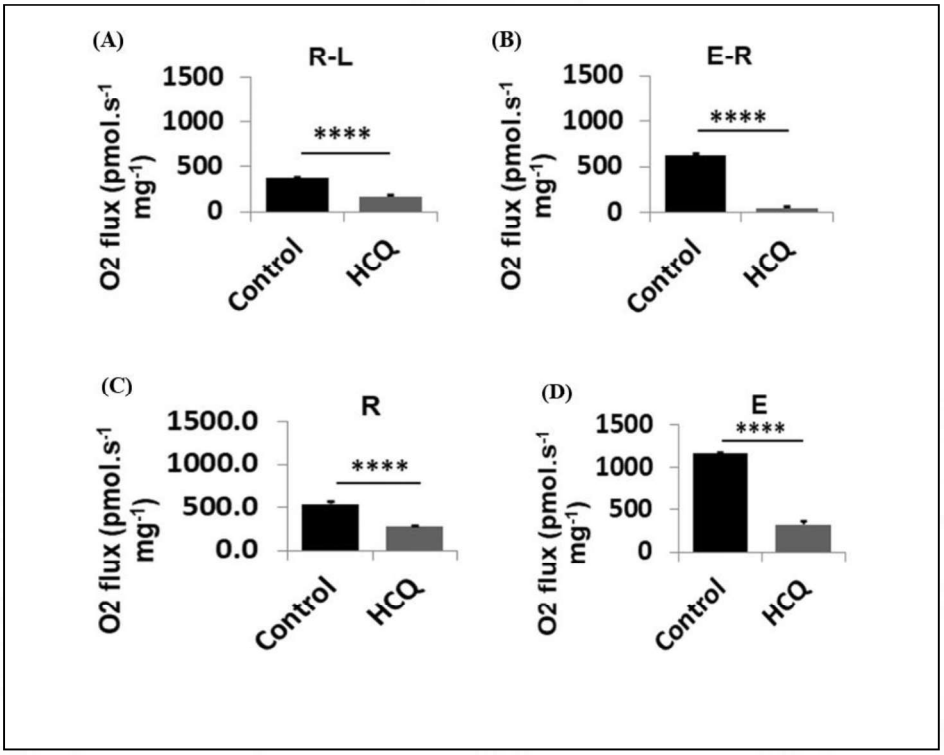

Figure IV. 13: HCQ and cellular bioenergetics. ***A –*** *Intact cell respiration of HCQ treated cells along with respective controls were measured following resuspension of cells in serum free DMEM in Oroboros Oxygraph. In accordance with Oroboros guidelines different respiratory parameters were recorded as Routine respiration (R)* ***B –*** *Maximal respiration (E) following uncoupling with CCCP* ***C –*** *ATP turnover (R-L)* ***D –*** *Spare respiratory capacity (E-R).*

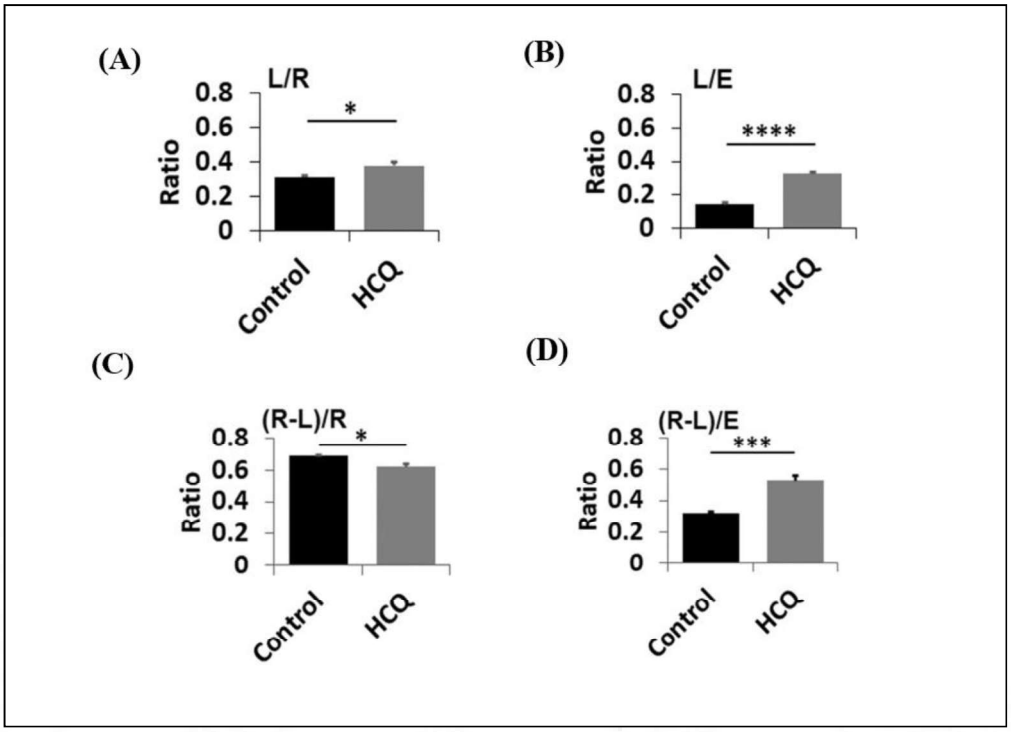

Figure 14: Respiratory control ratios with HCQ - *derived from the respiratory parameters measured in the intact cell respiration*. **A–** (L/R), **B –** (L/E), **C –** (R-L)/R, **D –** (R-L)/E

While HCQ is reported to have lesser toxicity compared to CQ, our data suggest that the mitotoxicity of HCQ in the in-vitro is comparable to that of CQ.

IV.A.3. Effects of BAF and 3MA on mitochondria

IV.A.3.1. Cytotoxicity and cell death analysis with BAF

Bafilomycin A1 (BAF) inhibits the process of autophagy in the last stage of lysosomal degradation as it is a V-type ATPase inhibitor that inhibits the proton pump in lysosomes thus contributing to lysosomal dysfunction. The optimal concentration of BAF for *in-vitro* studies was determined by assessing the cell viability as well as cytotoxicity in cardiomyoblasts exposed to different concentrations of BAF (1 nM-100 nM) for 24h.

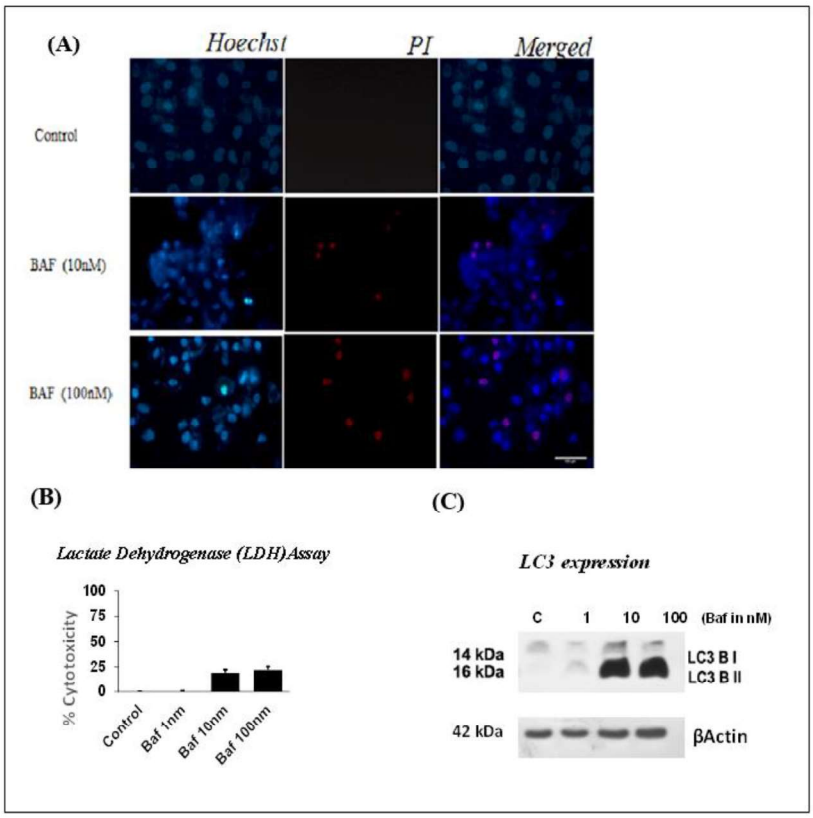

Figure IV. 15: Determination of BAF concentration for *in vitro* assays**: A-** *Hoechst Propidium Iodide imaging shows the cell viability at different Bafilomycin (1 nM- 100 nM) concentrations.* **B –** *Cytotoxicity assessment of different concentrations of Bafilomycin, which showed that unlike CQ, even at lower concentrations bafilomycin is highly cytotoxic.* **C –** *Western Blot analysis for assessment of LC3 II accumulation (which gives a measure of the autophagic arrest).*

The accumulation of autophagic vacuoles (with LC3II, as a readout for autophagosome accumulation) in cardiomyoblasts exposed to different concentrations of BAF (1 nM-100 nM) for 24h was also assessed (Fig 15 C).

It was observed that BAF treatment for 24 h had very high cytotoxic effects (as evident from the Fig. 15 **A&B**) even at a concentration as low as 10 nM. But, 10 nM BAF was chosen for further experiments as concentrations lower than that had negligible effects on the process of autophagy.

IV.A.3.2. Intact-cell bioenergetics with BAF treatment

Cellular respiration and mitochondrial efficiency assessed with standard coupling control protocol for intact cells shows that, exposure to BAF (10 nM) resulted in significant decline of overall respiratory parameters which includes Routine (**R**), Leak (**L**), Maximal (**E**), ATP-linked (**R-L**) and Spare capacity (**E-R**) of mitochondria, implying a decline in the cellular bioenergetics (Fig. 16**A-E**). The coupling control ratios, L/R and L/E (Fig. 17 **A&B**) shows an increase while, the Coupling efficiency (R-L)/R as well as the (R-L)/E (Fig. 17 **C&D**) shows a significant decline.

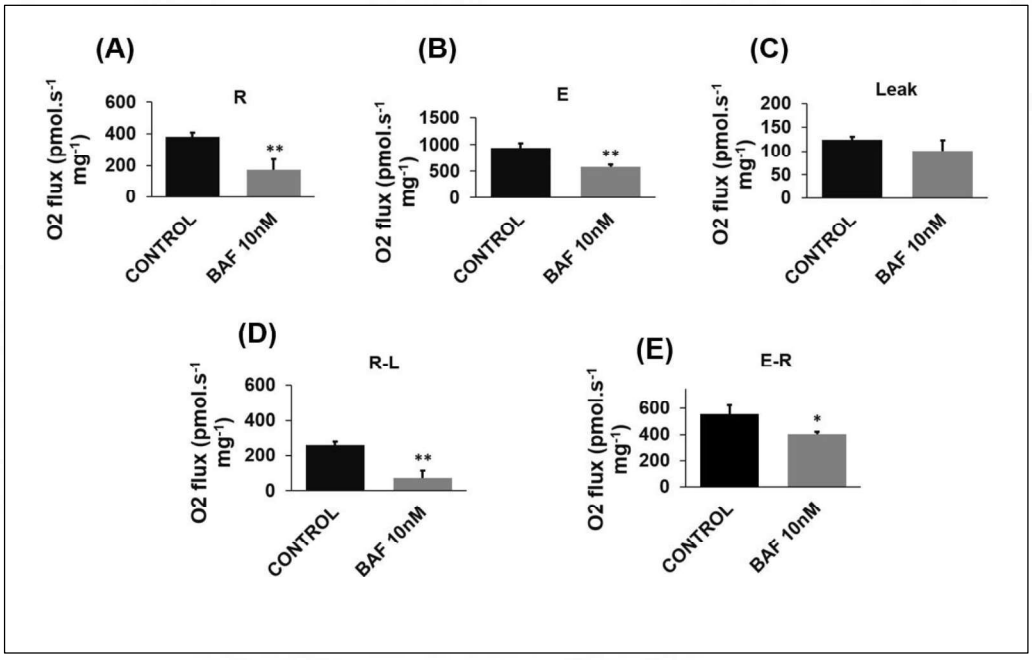

Figure IV. 16: **Intact cell bioenergetics with BAF treatment –** *the assessments were done in a similar way as that of CQ and different respiratory parameters were recorded with respect to control and represented in the image as* ***A*** *– Routine respiration (R),* ***B*** *– Maximal respiration (E),* ***C*** *– Leak (L),* ***D –*** *ATP turnover (R-L) and* ***E*** *– Spare respiratory capacity (E-R).*

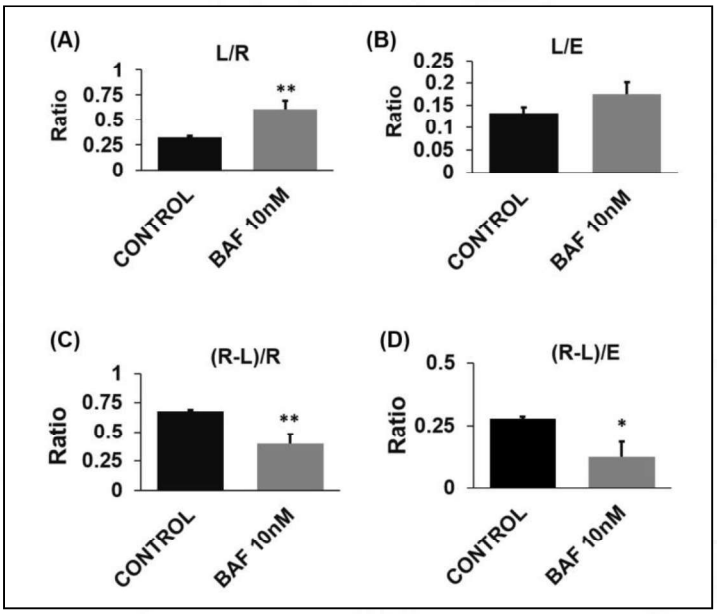

Figure IV. 17: Respiratory control ratios with BAF *derived from the respiratory parameters measured in the intact cell respiration post BAF treatment*. **A–** (L/R), **B –** (L/E), **C –** (R-L)/R, **D –** (R-L)/E

IV.A.3.3. Cytotoxicity and cell death analysis with 3MA

3-Methyladenine (3-MA) is reported to inhibit the process of autophagy in the initial stage and blocks the phagophore formation. 3methyladenine is a widely used autophagy inhibitor and the optimal concentration suggested to be used is 5 mM. Thus, the effect of 3methyladenine on the cell viability as well as cytotoxicity in cardiomyoblasts was assessed with two different concentrations of 3methyladenine (5 mM &10 mM) for 24 h. Both the concentrations of 3methyladenine had no significant impact on the viability of cardiomyoblasts when exposed for 24 h (Fig. 18**A**&**B**).

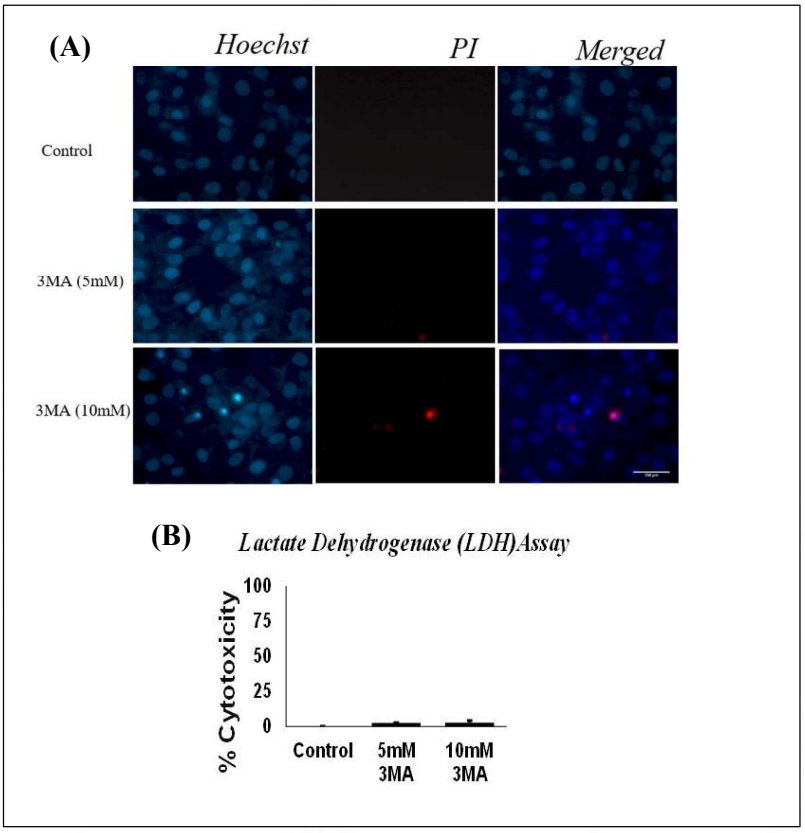

Figure IV. 18: Cytotoxicity assay for 3MA - *Hoechst Propidium Iodide imaging shows the cell viability at two different 3methyladenine (5 mM & 10 mM) concentrations.* **B –** *Cytotoxicity assessment with 3methyladenine, shows that unlike CQ or Bafilomycin, 3methyladenine induced negligible cell death.*

IV.A.3.4. Impact of 3MA on intact-cell bioenergetics

Cellular respiration measurements of intact cells showed that, overall respiratory parameters, except for Routine (**R**) respiration, showed a similar trend to that of control (Fig. 19). With 5mM 3methyladenine, the routine respiration showed a decline as was the Leak respiration (Fig 19**A** & 19**E**). The net routine as well as other respiratory parameters were unaffected. With 10mM 3methyladenine also Leak respiration showed a significant decline with other parameters remaining unchanged.

The coupling control ratios, L/R and L/E shows a significant decline with 5mM 3methyladenine (Fig. 20 **A**& 20**B**), while the Coupling efficiency, (R-L)/R (Fig 20 **C**),

showed a significant improvement with 5mM 3methyladenine. Other Coupling control ratios were unaffected.

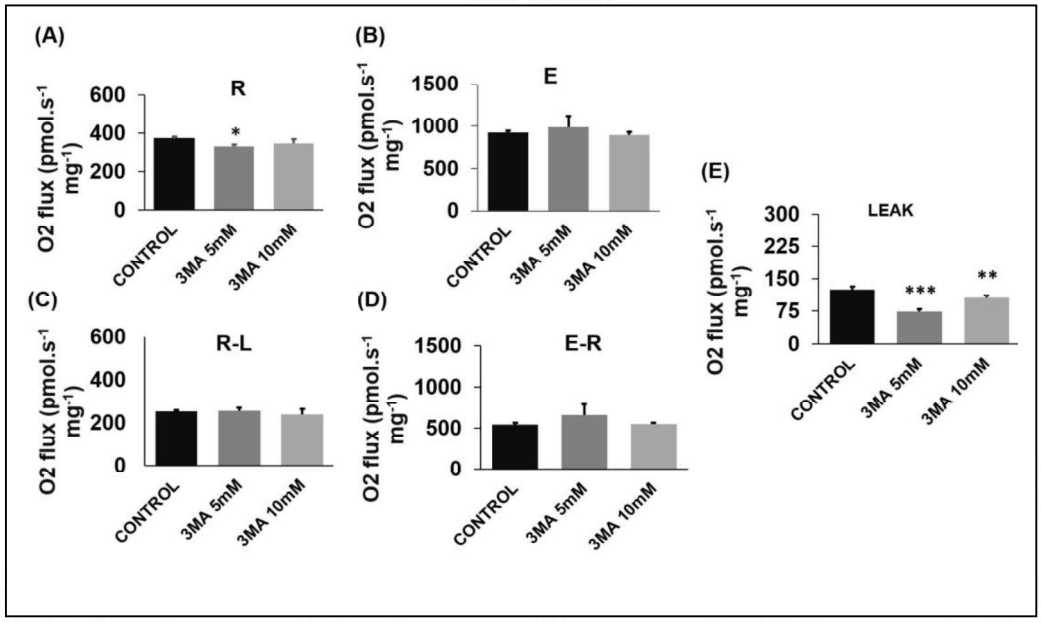

Figure IV. 19: 3MA & intact cell bioenergetics – *The bar graphs show various respiration measurements done on cardiomyoblasts subjected to 3methyladenine treatment.* ***A*** *- Routine respiration (R),* ***B*** *– Maximal respiration (E),* ***C*** *– ATP turnover (R-L),* ***D*** *– Spare respiratory capacity (E-R) and* ***E*** *– Leak respiration.*

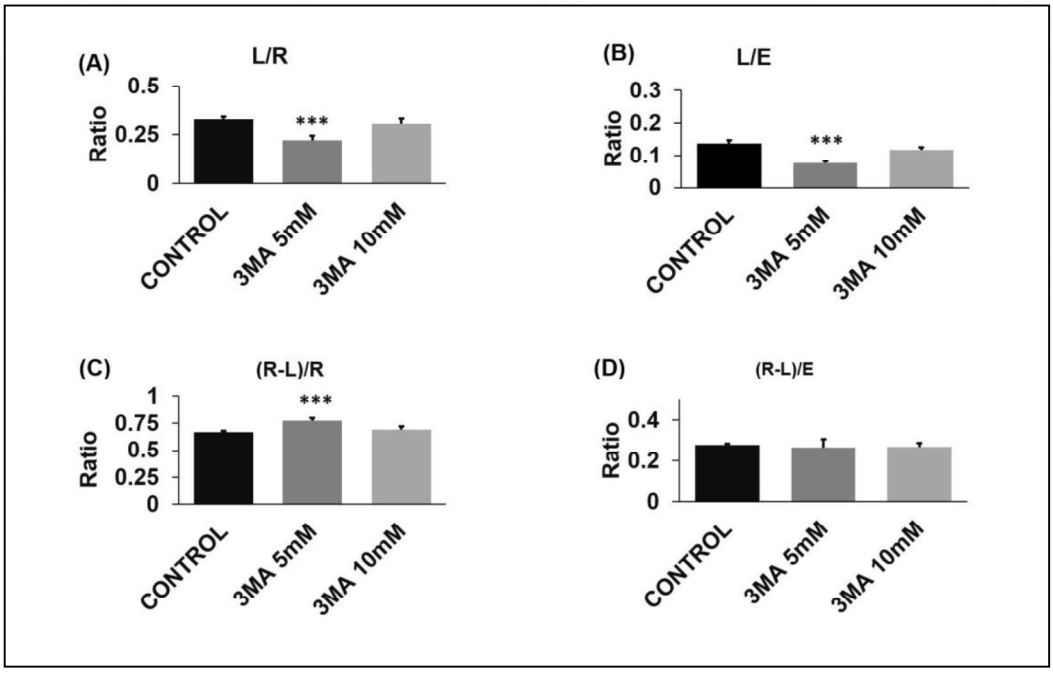

Figure IV. 20: Respiratory control ratios with 3MA- *The bar graphs show the coupling control ratios calculated from the respiratory parameters measured post 3methyladenine treatment.* **A–** (L/R), **B –** (L/E), **C –** (R-L)/R, **D –** (R-L)/E

IV.A.3.5. Assessment of mitochondrial membrane potential

As mentioned above, the mitochondrial efficiency is directly associated with the mitochondrial membrane potential. Thus, measurement of mitochondrial membrane potential is a good indicator of mitochondrial health. To understand the effect of BAF and 3MA, the mitochondrial network was stained with TMRM. It was observed that the BAF treatment resulted in a reduction of MMP compared to the control condition (Fig. 21). But there was no visible difference in the fluorescence intensity of cells treated with 3MA.

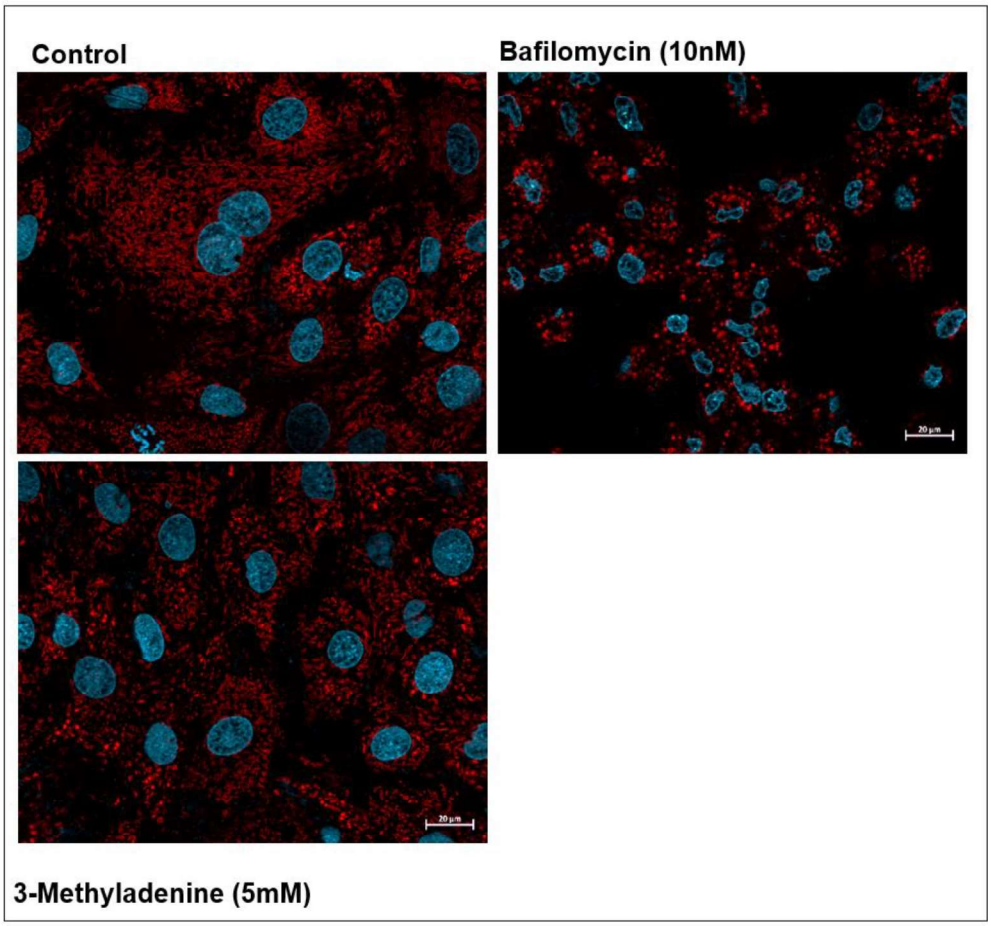

Figure IV. 21: TMRM staining for mitochondrial membrane potential **–** *BAF affected the Membrane potential of Mitochondria shown by the TMRM fluorescence intensity, while 3MA treated cells showed no visible difference in the fluorescent intensity.*

IV.A.3.6. Analysis of mitochondrial morphology

Mitochondrial network was stained with Mitotracker Deep Red fluorescent stain. Following the BAF treatment, the mitochondrial network within the cardiomyoblasts showed a high degree of fragmentation (Fig. 22).

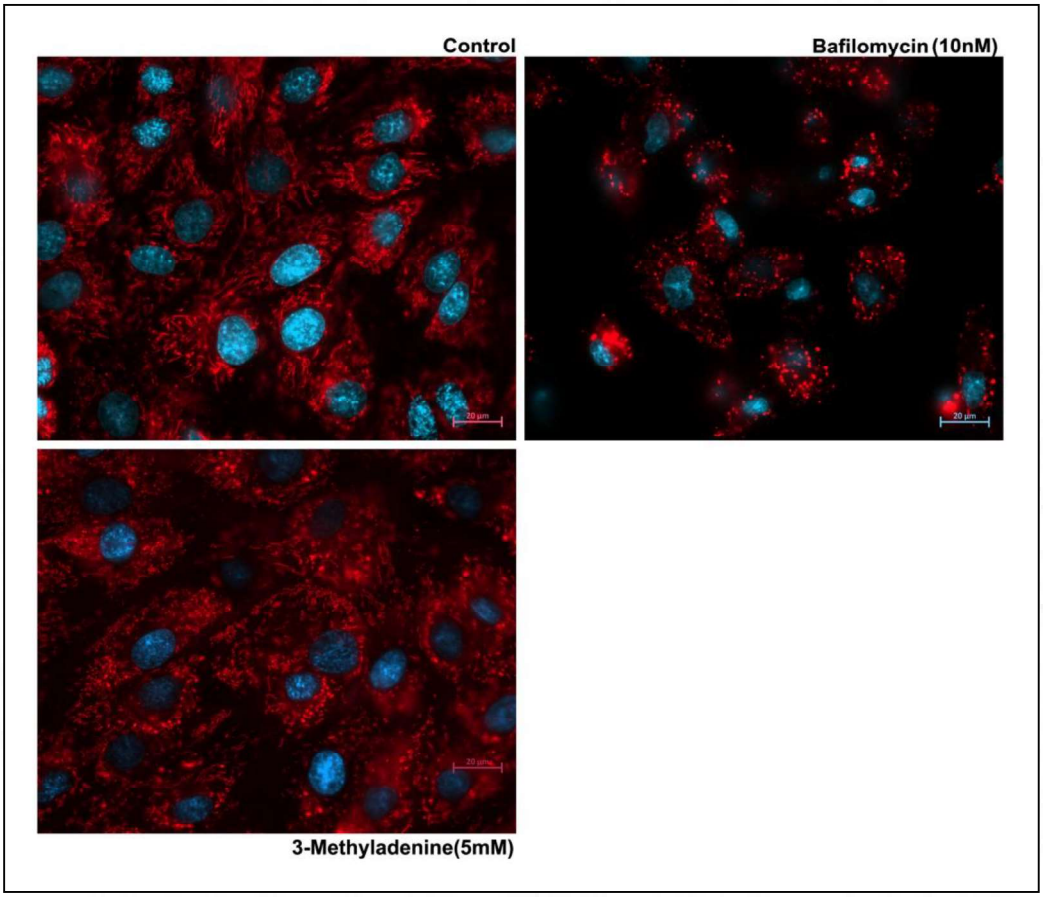

Figure IV. 22: Mitotracker Deep Red staining for mitochondrial morphology- *MitoTracker staining shows mitochondrial fragmentation and dispersion following BAF treatment. While, 3MA treatment group shows no visible difference in the mitochondrial architecture.*

IV.B. Autophagy activation

To study the effect of autophagy activators on cardiac cells, H9c2 cardiomyoblasts were treated with Resveratrol (RES) at different concentration (20, 50 and 100 µM) for 24 h. Resveratrol was the primary choice for autophagy activation study as it is a well-established autophagy activator, and a natural polyphenol found in ~70 plant species, especially in Grapes, Raspberries, etc.

IV.B.1. Effects of Resveratrol on mitochondria

IV.B.1.1. Impact of RES on Intact-cell bioenergetics

Intact cell respiration and the coupling control ratios assessed with resveratrol treated cells indicated that Res have a dose dependent effect on the cellular respiration.

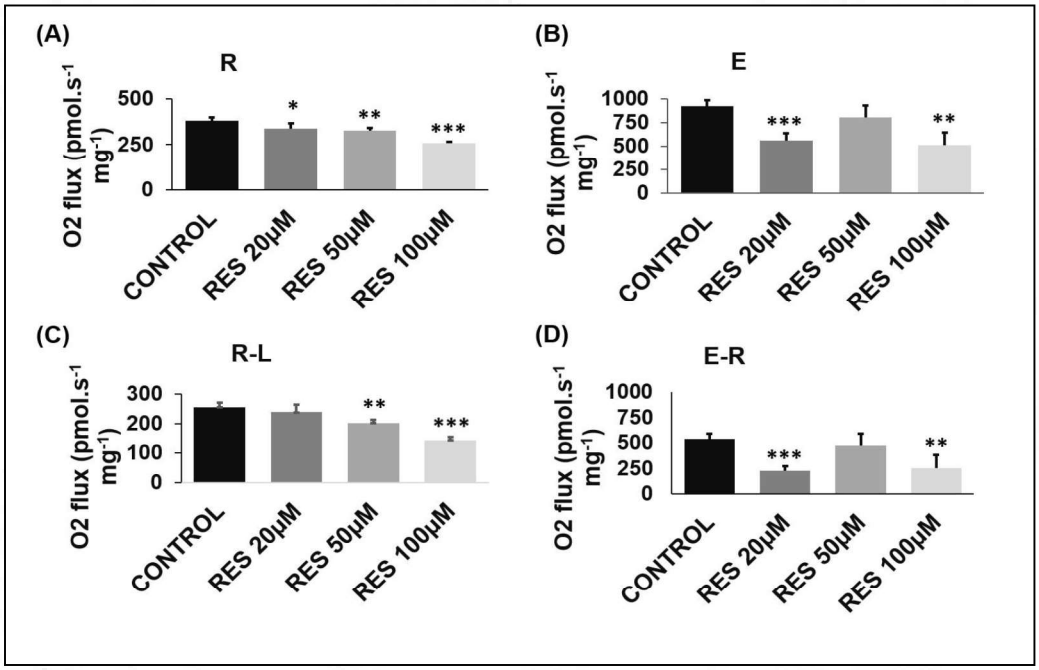

Figure IV. 23: Intact cell bioenergetics with RES treatment - *The bar graphs show the respiratory parameters recorded with respect to controls,* ***A*** *- Routine respiration (R),* ***B –*** *Maximal respiration (E),* ***C –*** *ATP turnover (R-L) and* ***D –*** *Spare respiratory capacity (E-R).*

The Routine respiration declined with Resveratrol treatment (Fig. 23 A) with regard to all the three concentrations of Resveratrol. Maximal respiration also declines in the 20 µM and 100 µM treatment group, but not with 50 µM of Resveratrol (Fig. 23B).

Leak respiration, as indicated by Fig. 24, falls significantly with 20 µM and 100 µM Resveratrol. The ATP linked respiration (R-L) (Fig. 23C) shows a significant decline in both 50 µM and 100 µM treatment groups, with no effect on 20 µM treatment groups, while the Spare capacity (E-R) (Fig. 23D) declines significantly with 20 µM and 100 µM but with 50 µM of Resveratrol, the spare capacity values remain unchanged and similar to that of Control.

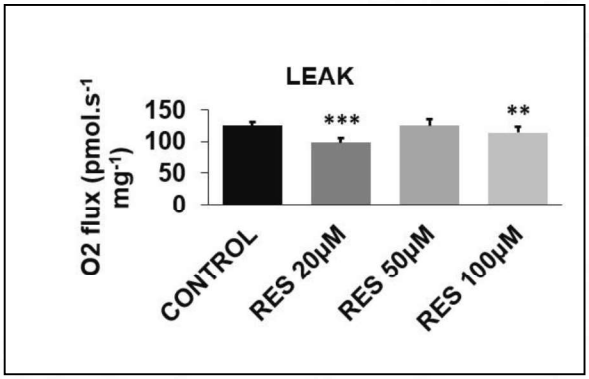

Figure IV. 24: Leak respiration with RES - *The bar graphs indicate the leak respiration of Resveratrol treated cardiomyoblasts with respect to Controls.*

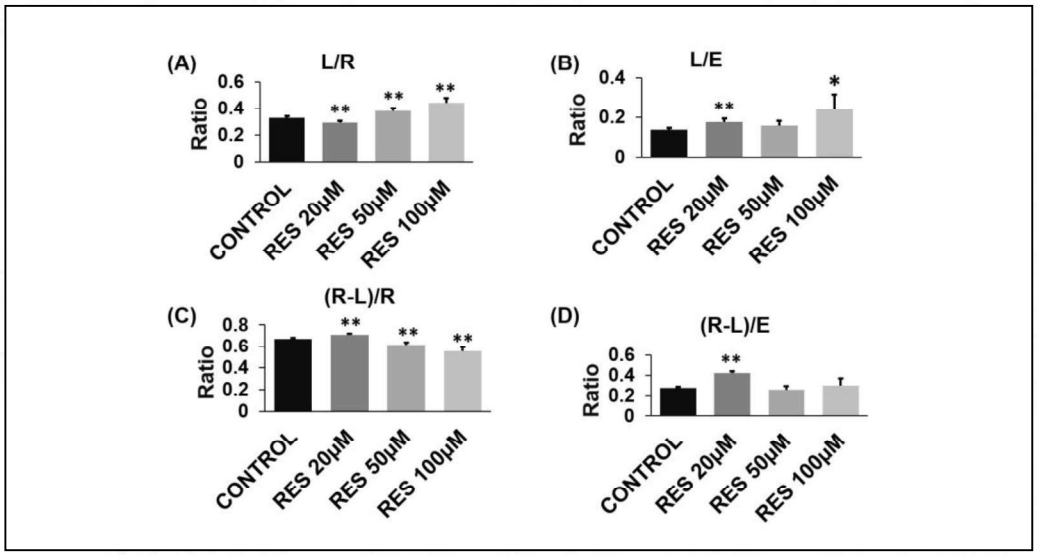

Figure IV. 25: Respiratory control ratios with RES - *The bar graphs show the coupling control ratios calculated from the respiratory parameters measured post Resveratrol treatment.* **A–** (L/R), **B –** (L/E), **C –** (R-L)/R, **D –** (R-L)/E.

The coupling control ratios also showed a dose dependent effect, as the Leak to Routine (L/R) ratio decreasing with 20 µM Resveratrol treatment, while significantly increasing with 50 µM and 100 µM Resveratrol treatment (Fig 25 **A**). The Leak to ETS

(L/E) ratio significant increase with 20 μM and 100 μM Resveratrol treatment while the 50 μM Resveratrol group showing no change (Fig 25 **B**). The Coupling efficiency, (R-L)/R, showed a significant improvement with the lower concentration, while 50 μM and 100 μM Resveratrol treatment results show a significant reduction (Fig25 **C**). The ratio of Net routine to ETS, (R-L)/E, showed a significant increase with 20 μM resveratrol with no difference observed in the 50 μM and 100 μM Resveratrol treatment, with respect to controls (Fig 25 **D**).

IV.B.1.2. Substrate linked respiration

Substrate-linked respiration of mitochondrial electron transport chain complexes like, Complex-I/N-linked respiration, Complex-II linked respiration and Complex-IV linked respiration were assessed in the presence of exogenously supplied substrates as well as inhibitors specific for each complex. RES treatment resulted in the improvement of the substrate-linked respiration of Complex-I (Fig. 26**A**), II (Fig. 26**B**) and IV. (Fig. 26**C**).

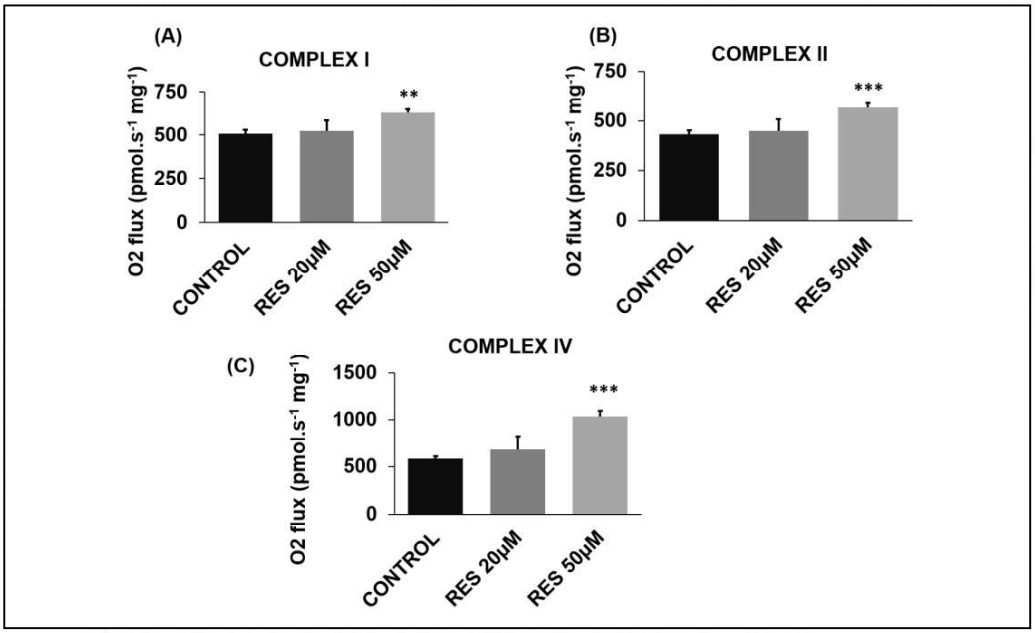

Figure IV. 26: **Substrate-linked respiration with RES -** The *substrate-linked respiration following the addition of exogenous substrates shows that the RES treatment improved the capacity of mitochondrial complexes to utilize the substrates effectively. **A**- N-linked respiration following the addition of substrates that feed*

electrons to the N-junction (Pyruvate + Glutamate + Malate) followed by the addition of Rotenone ***B****- Complex-II linked respiration, following the addition of Succinate followed by Malonate* ***C*** *– Complex-IV linked respiration following the addition of TMPD + Ascorbate, followed by Azide.*

IV.B.1.3. Gene expression levels of OPA 1 and FIS 1

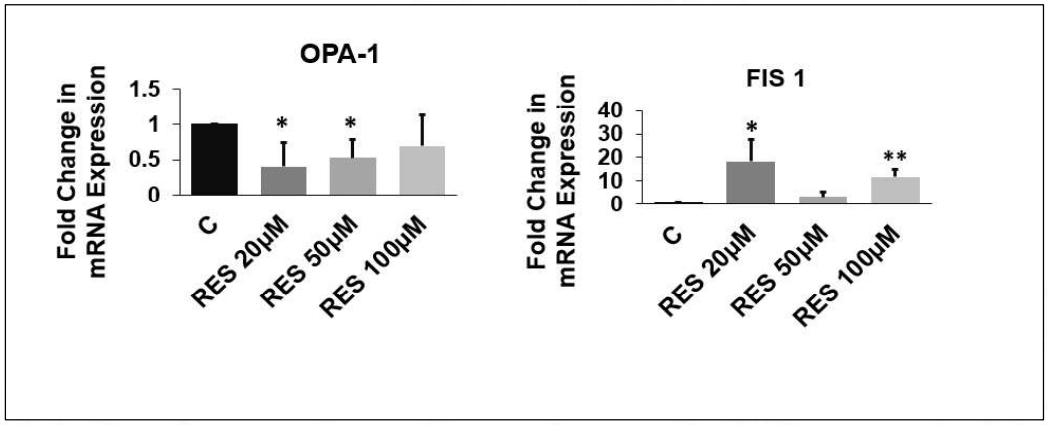

Figure IV. 27: Gene expression levels of OPA1 and FIS1- *mRNA expression levels of OPA-1 and FIS-1 were analysed post Resveratrol treatment for 24h. The bar graph represents the foldchange in the mRNA expression levels with respect to controls.*

The mRNA expression levels of OPA1, the inner membrane fusion protein, showed a significant decline after 24h of Resveratrol treatment in the 20 μM and 50 μM treatment groups, while in 100 μM treatment group, it showed a decline although not significant (Fig. 27). While the gene expression of FIS1, a critical component of mitochondrial fission complex is elevated post Resveratrol treatment with a significant increase in the 20 μM and 100 μM treatments (Fig. 27), while in 50 μM treatment group also showed an increment in the gene expression levels, although not significant.

IV.B.1.4. OPA-1 (L- form) and DRP1 Expression

We observed that the OPA-1 L form was significantly reduced with 100 μM Resveratrol treatment, but the decline was not statistically significant in both 20 μM and 50 μM Resveratrol treatment groups (Fig 28A). While, the expression of DRP1, an important protein involved in the orchestration of mitochondrial fission process showed a significant decline in all the three groups of Resveratrol treatment (Fig. 28 **B**)

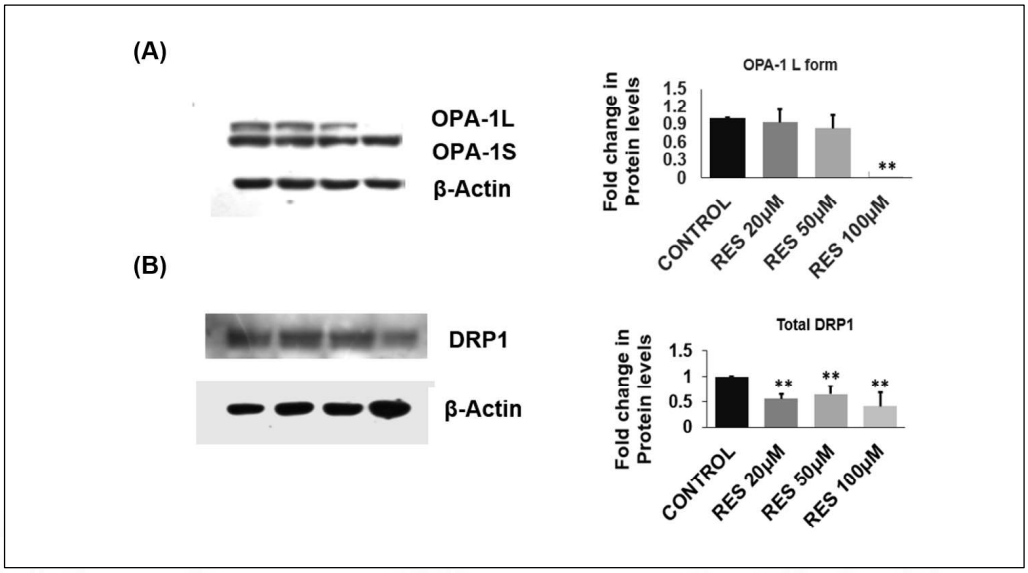

.

Figure IV. 28: OPA-1 (L form) and total DRP1 expression- *Fig. 28A shows the western blotting for OPA-1 with bar graph showing the fold change in the expression levels of OPA-1 L, While the Fig. 28B shows the western blotting for Total DRP1 with the corresponding bar graph.*

IV.B.1.5. Assessment of Mitochondrial membrane potential

To understand the effect of Resveratrol on mitochondrial membrane potential, the mitochondrial network was stained with TMRM post 24 h treatment. It was observed that there was a dose dependent increment in the fluorescence intensity of TMRM compared to the control (Fig. 29).

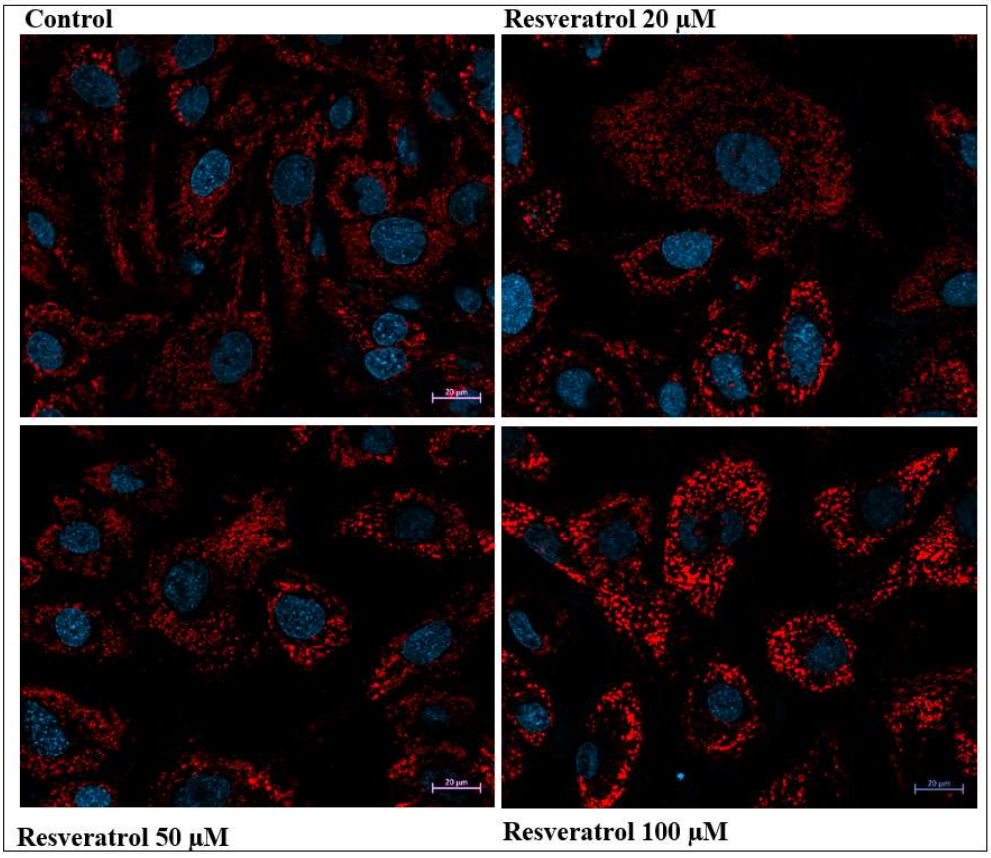

Figure IV. 29: TMRM staining for Mitochondrial membrane potential – *Resveratrol's dose dependent impact on the membrane potential of mitochondria shown by the TMRM fluorescence intensity. Here, there is a visible increment in the fluorescence intensity following resveratrol treatment compared to control.*

IV.B.1.6. MitoSox staining:

Mitochondrial superoxide assessment post Resveratrol treatment was done through Fluorescence staining with MitoSox followed by microscopic analysis. MitoSox staining revealed an elevation in the mitochondrial superoxide levels post Resveratrol treatment (Fig. 30).

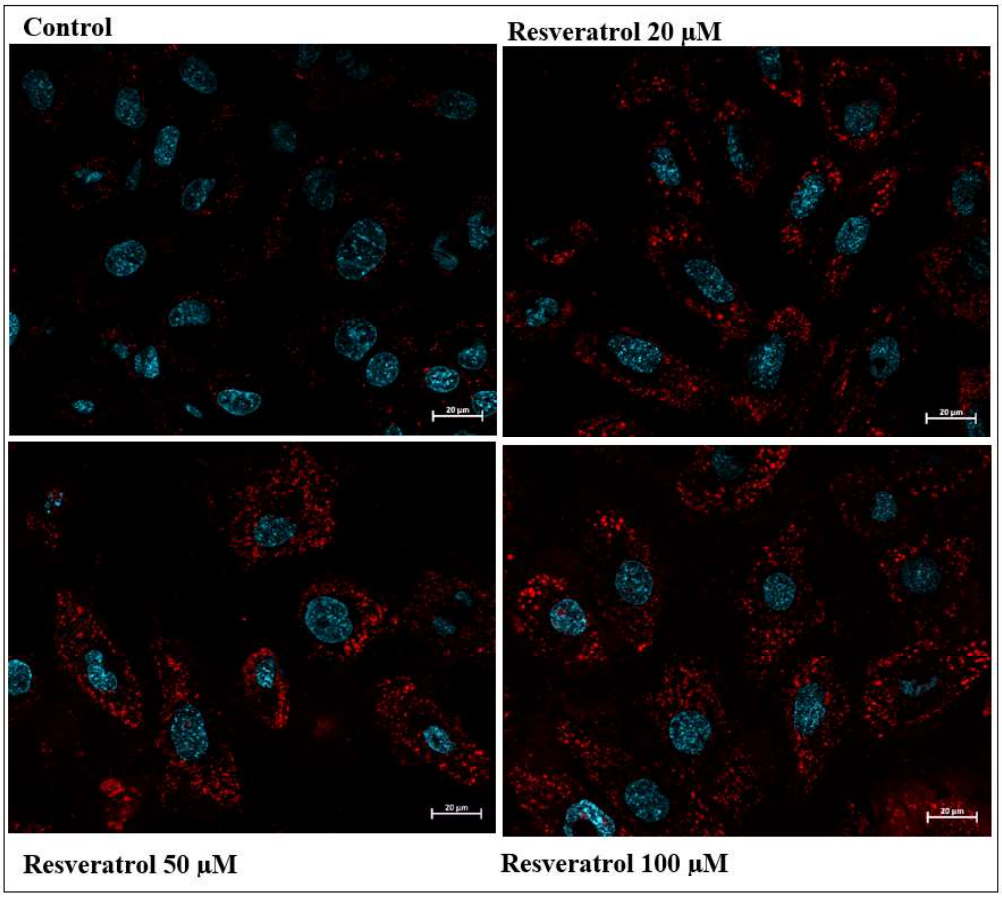

Figure IV. 30: MitoSox Red of Mitochondrial ROS – *Mitochondrial Superoxide levels were analysed 24h post Resveratrol treatment. There occurs a visible elevation in the Fluorescence signal post Resveratrol treatment with respect to controls.*

IV.B.1.7. Assessment of mitochondrial morphology

Mitochondrial network was stained with Mitotracker Deep Red and fluorescent signals were captured. The Fluorescence imaging revealed that Resveratrol treatment of cardiomyoblasts resulted in the fragmentation of mitochondria with respect to controls (Fig 31).

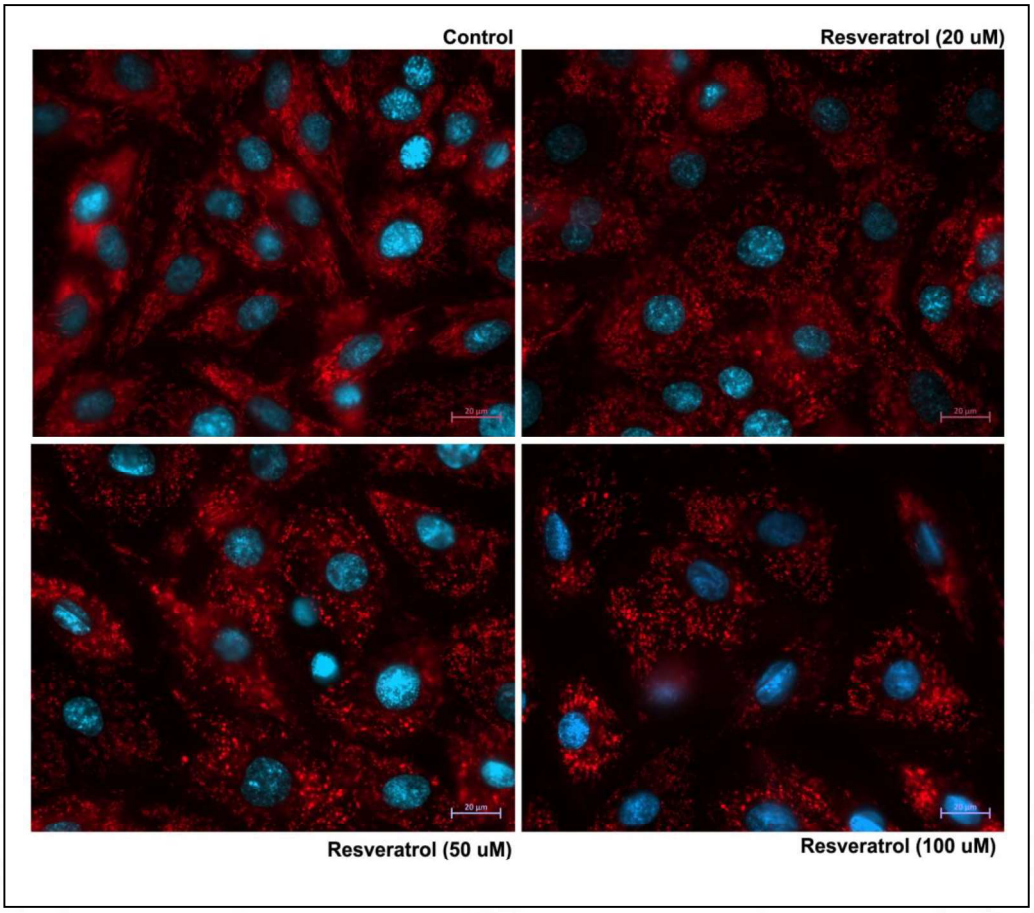

Figure IV. 31: Mitotracker Deep Red staining - *MitoTracker staining shows an increased mitochondrial fragmentation following Resveratrol treatment.*

IV.C. Analysis of cardiac mitochondrial respiration

In order to analyse the activity of cardiac mitochondrial electron transport chain complexes by regulating the process of autophagy in an *in-vivo system*, high-resolution respirometry was used for mitochondrial respiration from hearts.

For that 10 µl aliquot of the freshly isolated mitochondrial suspension (from the mouse whole heart, treated vs non-treated) was added to both the chambers of the Oroboros Oxygraph O_2K, which was followed by the sequential addition of substrates (palmitoyl L- carnitine, malate, ADP, pyruvate, glutamate, succinate) as a source of electrons to the Electron transport chain complexes, uncoupler (FCCP) and inhibitors (Rotenone, Oligomycin & Antimycin).The OCR was expressed in $pmol/s^{-1}mg^{-1}$ of mitochondrial protein and the values are ROX corrected. ROX represented the residual oxygen flux due to some oxidative side reactions in the electron transport pathway or the instrument background.

IV.C.1. Cardiac mitochondrial respiration of CQ treated group

To analyse the effect of chloroquine on cardiac mitochondrial function under physiological conditions in the mice heart, grouped as Mature adult/Group A and Elderly groups/Group B, the animals were treated with chloroquine (10 mg/kg) for 2 weeks. After the treatment period, the animals were sacrificed for the extraction of the whole heart and mitochondria was freshly isolated for the respiratory measurements.

There was a decline in the mitochondrial efficiency for substrate utilization following chloroquine treatment in both Group A as well as Group B. The fatty acid and fatty acid plus carbohydrate mediated respiration was significantly lowered in the Group B, while total OxPhos (respiration measurements done with Complex I, Complex II and ETF substrates together) and Uncoupled respiration measurements were significantly declined in both Group A and Group B.

Even though chloroquine treatment resulted in declined mitochondrial efficiency in both Mature adults as well as Elderly groups, the effect was more prominent in the Elderly animals, as their mitochondrial substrate utilization was already hindered,

probably because of the age associated factors (Fig 32).

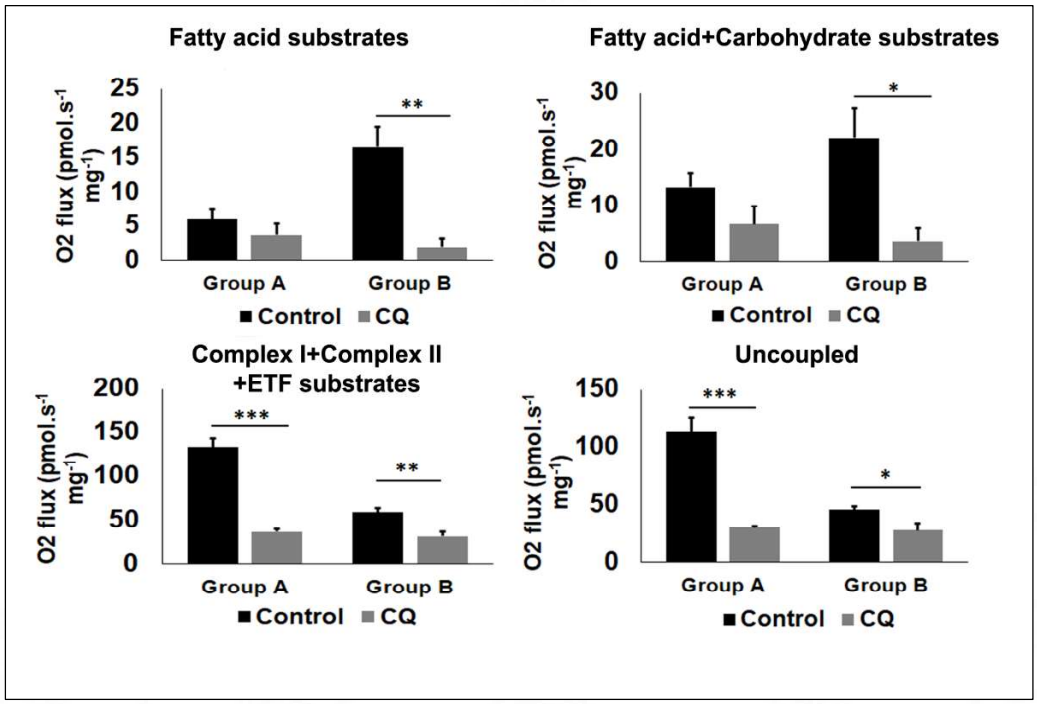

Figure IV. 32: Substrate-linked respiration with isolated mitochondria: *The substrate-linked respiration following the addition of exogenous substrates showed that the CQ treatment reduced the capacity of mitochondrial complexes to utilize the substrates effectively. The bar graph represents Fatty acid mediated respiration (following the addition of Palmitoyl carnitine + Malate), followed by the Fatty acid + Carbohydrate mediated respiration (Palmitoyl carnitine + Malate + Glutamate + pyruvate), Total OxPhos (with Complex I + Complex II + Electron transfer flavoprotein) substrates and Uncoupled respiration.*

IV.C.2. Cardiac mitochondrial respiration of RES treated group

To analyse the effect of Resveratrol treatment on cardiac mitochondrial function under physiological conditions in Mature adult as well as Elderly groups, the animals were treated with Resveratrol (5mg/kg) for 2 weeks. After the treatment period, the animals were sacrificed for the extraction of the whole heart and mitochondria was freshly isolated for the respiratory measurements.

Resveratrol treatment resulted in improvement of mitochondrial efficiency in both Mature adults as well as Elderly groups.

The fatty acid as well as fatty acid and carbohydrate substrates mediated respiration showed a significant improvement in the Group A, while it showed a decline in the Group B. But after the addition of Complex II substrate as well as uncoupler the rise in the respiration measurements were more prominent in the Elderly group, while Mature adult group showed a trend towards improvement (Fig 33).

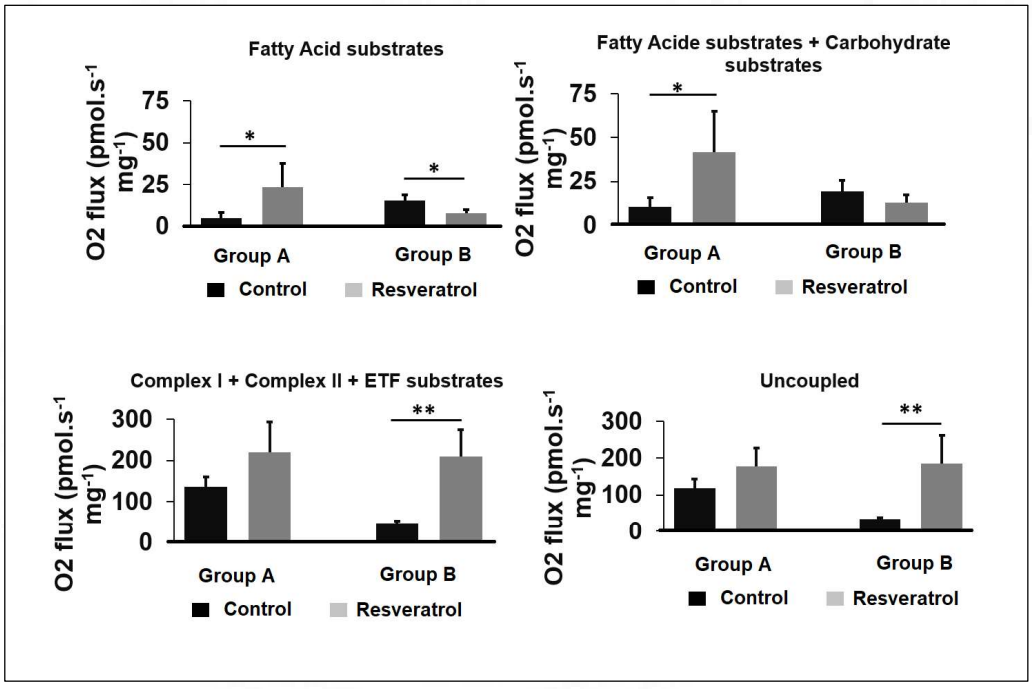

Figure IV. 33: Substrate-linked respiration with isolated mitochondria: *The substrate-linked respiration following the addition of exogenous substrates showed that the Resveratrol treatment improved the efficiency of mitochondrial complexes to*

utilize the substrates effectively. The bar graph represents Fatty acid mediated respiration (following the addition of Palmitoyl carnitine + Malate), followed by the Fatty acid + Carbohydrate mediated respiration (Palmitoyl carnitine + Malate + Glutamate + pyruvate), Total OxPhos (with Complex I + Complex II + Electron transfer flavoprotein) substrates and Uncoupled respiration.

V. Summary of Results

Autophagy inhibition and mitochondrial metabolism and network:

- The reduction in formazan crystal formation indicates reduced cellular metabolic activity due to Chloroquine treatment.
- Intact cell bioenergetics falls significantly with Chloroquine treatment with a significant decline in coupling efficiency pointing towards damaged mitochondria.
- Permeabilized cell oxygraph measurements done in the presence of exogenous substrates confirmed decreased mitochondrial efficiency.
- The other autophagy inhibitors showed similar results with mitochondrial function suggesting that the effects observed is due to the autophagy inhibition.
- qPCR data revealed increased mitochondrial content, which could be because of the reduction in mitophagy (mitochondrial degradation via Autophagy), due to Chloroquine treatment.
- TMRM staining shows decline in mitochondrial membrane potential while MitoSOX staining revealed increased mitoROS generation
- Thus although higher in content, the mitochondrial population shows damage and inefficiency.
- Increased vacuolation and accumulation of acidic compartments with Chloroquine treatment suggests an increase in the lysosomes within the cell, due to the decline in the cellular degradation.
- The mitochondrial network analysis with Mitotracker staining showed disruption of mitochondrial network and increased fragmentation of mitochondria.
- The in vivo experiments suggest that CQ had mitotoxic effects in the cardiac tissue.
- With the increase in the age of the animal, there is a decline in the basal autophagy and when CQ was administered in that condition, the mitotoxic effects were more pronounced.

Effect of Autophagy activation on mitochondrial metabolism and network:

- There was a decline in the intact cell respiration with Resveratrol treatment, this decline in the bioenergetics could be due to the changes in the cellular metabolite pool.
- The Permeabilized cell oxygraph measurements done in the presence of exogenous substrates showed an improvement of mitochondrial efficiency.
- TMRM staining shows significant improvement in mitochondrial membrane potential suggesting highly efficient mitochondrial population.
- Although mitoctracker imaging showed a decline in mitochondrial network, this did not reflect in the overall mitochondrial performance.
- But the dose of Resveratrol could have a critical impact on the observable benefits with only a narrow optimal range proving beneficial for mitochondrial efficiency.
- The in vivo studies showed that the autophagy induction in the young heart thorough resveratrol may not have much beneficial effects and the benefits become apparent only with the natural age associated decline in cardiac health.

VI. Discussion

Mitochondrial quality control is critical for the preservation of homeostasis in the myocardium. This task is achieved through the intricate harmonisation of various quality control pathways (Dutta et al., 2012b). Modulation of these quality control pathways, especially autophagy, thus can result in altered mitochondrial homeostasis and could contribute towards the generation of mitochondrial derived ROS in excess along with accumulation of dysfunctional proteins and organelles. All of these, could culminate in to the pathogenesis of chronic cardiovascular diseases.

Mitochondrial dynamics is acutely affected by the alterations in cellular processes resulting in the adjustment of mitochondrial morphologies to specific cellular needs. Autophagy is one such process that could decide the fate of mitochondrial architecture via orchestrating mitochondrial fission and fusion. Events that trigger the process of autophagy is reported to result in mitochondrial fusion in both in vitro and in vivo model systems (Gomes et al., 2011b; Rambold et al., 2011). Inhibition of autophagy is reported to be coupled with mitochondrial cristae as well as network remodelling with increased fragmentation which could culminate in to the unleashing of the apoptotic process (Corrado et al., 2016). Even though the influence of autophagic modulators on cellular as well as mitochondrial context is widely investigated, only a few studies were focused on the influence of autophagy modulators on cardiac metabolism (Riffelmacher et al., 2017; Sciarretta et al., 2018; Wu et al., 2019). This prompted us to look into the mechanistic basis of autophagic modulators on mitochondrial function under normal physiology, especially in the cardiac system which relies heavily on mitochondrial metabolism.

CQ was used as the primary choice for autophagy inhibition studies, while BAF and 3MA were also used. While, both CQ and BAF inhibits autophagy at the final stage, CQ inhibits the process by impairing autophagosome fusion with lysosomes, whereas BAF, a V- type ATPase inhibitor, affects the degradative activity of lysosomes (Bowman et al., 1988; Mauthe et al., 2018a). Both, CQ and BAF has been shown to induce mitochondrial dysfunction in primary neurons and this corroborated with our results on mitochondrial function which showed the diminishment of mitochondrial efficiency with CQ and BAF treatment (Redmann et al., 2017). To drive a more comprehensive analysis of mitochondrial efficiency from the respiratory parameters

measured, we further calculated coupling control ratios, Leak to Routine (L/R) and Leak to ETS capacity (L/E) gives an account of the leakiness of the mitochondria (i.e., as the value increases, the leakiness increases) while (R-L)/R represents the coupling-efficiency and (R-L)/E represents the limitation of respiratory capacity by impairment of components of the ETC complexes. The ratio of Leak to Routine (L/R) and Leak to ETS capacity (L/E) showed an increase in CQ and BAF treated groups compared to their respective controls, providing an estimation of the pathological uncoupling caused by the toxic effects of the compounds. The coupling efficiency, (R-L)/R, shows a significant decline with CQ and BAF treatment, indicating a deterioration in oxidative phosphorylation and a concomitant increase in the Leak, whereas the fraction of net Routine to ETS capacity i.e., (R-L)/E shows an increase owing to a decline of the Maximal respiration (ETS capacity) following CQ exposure, while (R-L)/E value decreases with BAF treatment. This could be attributed to the differences in the values of individual respiratory parameters, as with BAF treatment, the net routine (R-L) respiration values were too low, while ETS/Maximal respiration showed only ~50% reduction compared to respective controls.

Further, the decline in mitochondrial respiration as well as the efficiency of the electron transport chain complexes following CQ treatment was substantiated with Substrate-linked complex activity assessments, where Complex I, II and IV showed a significant decline in substrate utilization compared to their respective controls. Whether the decrease in the complex activity is concomitant with the decreased expression of OXPHOS proteins remains to be assessed and could reveal a wider range of CQ effect in controlling mitochondrial metabolism.

While, CQ and BAF is reported to inhibit autophagy at the final stage, i.e., autophagosome lysosome fusion, we used another inhibitor, 3MA, which is reported to inhibit autophagy in the initial stages (Petiot et al., 2000). Even though 3MA is reported to result in moderate accumulation of large (senescent-like), there are no reports which shows a decline in mitochondrial quality (Terman et al., 2004; Terman and Brunk, 2005). Thus, contrary to what we observed with CQ and BAF treatment, exposure of cardiomyoblasts to 3MA resulted in improved functional efficiency as evident from the decline in Leak respiration as well as the enhancement of Coupling

efficiency, (R-L)/R. The TMRM staining also revealed a diminished mitochondrial membrane potential with CQ as well as BAF treatment, while 3-Methyladenine had no visible impact on the TMRM fluorescence intensity.

While, this was a fascinating finding, as we observed contrasting results with 3MA compared to other autophagy inhibitors with different mode of action, we couldn't look in to the reason behind this phenomenon. Here, we speculate the involvement of mitochondrial derived vesicles which would be compensating for the loss of functional autophagy and help maintain a healthy mitochondrial pool (Towers et al., 2021). Or it could also be due to the dual role of 3MA (either inhibiting or activating) in autophagic process or by its action on PtdIns3k (Wu et al., 2010; Heckman BL et al., 2013)

Mauthe et al., 2018, revealed that CQ and HCQ affect the intracellular vesicular transport as well as induced disorganization of the Golgi and ER network *in-vitro* and *in-vivo* (Mauthe et al., 2018b). Our results with Live cell staining with MitoTracker Deep Red revealed that the CQ induced mitochondrial fragmentation and resulted in the loss of interconnectivity. TOM20 immunocytochemistry analysis corroborated the Mitotracker staining. The mitochondrial morphology is a critical determinant of mitochondrial behaviour and performance, as it is intimately associated with the fate of the organelle. While, the process of mitochondrial fusion is regarded as a gateway for the exchange of metabolites as well as mitochondrial genome, fission is shown to aid the renewal of the organelle. Thus, a healthy mitochondrial pool is maintained by constant fission fusion cycle (Barsoum et al., 2006; Gomes and Scorrano, 2008; Malena et al., 2009). Mitochondria with diminished membrane potential are targeted for degradation as they are less likely to be involved in the fission- fusion cycle. Autophagy arrest is reported to cause the accumulation of mitochondria with low membrane potential and reduced OPA1 levels (Twig et al., 2008b; Westermann, 2010). CQ treatment also resulted in the accumulation of mitochondria with lower membrane potential as evidenced from the qPCR targeting mitochondrial content as well as TMRM staining. The expression levels of the mitochondrial fusion protein, OPA-1 (long form) reported to be the active form of OPA-1, declines with CQ treatment for 24 h, even though its mRNA expression levels showed an increasing trend. Albeit the unaltered expression of DRP1, a critical regulator of mitochondrial

fission, the gene expression levels of mitochondrial fission protein, FIS1 is significantly reduced. These changes in the mRNA levels of OPA-1, which increased and FIS-1 which showed a significant decline at 24 h time point could be attributed to the compensatory mechanisms involved in the cell survival and whether these changes would be reflected in the protein levels would determine the overall effect. Our results on BAF treatment and mitochondrial architecture were also falling in line with that of CQ, while 3MA had no visible impact on the mitochondrial network. Thus, CQ treatment invariably causes dysfunctional mitochondria to accumulate in cells, an event that could seriously compromise the overall functional ability, particularly in tissues that depend on OXPHOS for energy production.

Dysfunctional mitochondria can serve as a source of ROS, which could further aggravate the damage (Leadsham et al., 2013; Murphy et al., 2019; Murphy, 2013). CQ treatment augmented mitochondrial superoxide production as evidenced from MitoSox staining to detect mitochondria derived superoxides. The elevation in the mRNA levels of transcription factors related to mitochondrial biogenesis suggest the induction of mitochondrial biogenesis with CQ treatment, contributing towards the accumulation of dysfunctional/damaged mitochondria. Although we could not empirically verify, this accumulation can cause deleterious effects to the cell by leaching out calcium, opening of the membrane permeability transition pores, and apoptosis. This could be a potential cause of cardiotoxicity associated with CQ/HCQ.

In concordance to our results that show an abnormal mitochondrial architecture and deterioration in function, CQ and HCQ treatments have been reported to induce pathologic features at the cellular level together with the ultrastructural changes, like the formation of myeloid and curvilinear inclusion bodies, that are shared between cardiopathy and neuropathy (Khosa et al., 2018; Siddiqui et al., 2007; Stein et al., 2000). Even though HCQ was reported to have a better safety profile compared to CQ, our *in-vitro* analysis shows a comparable mitotoxic nature of HCQ to that of CQ. CQ/HCQ treatments are shown to have ill effects on cardiac rhythm and electrophysiology leading to conditions like bradycardia, tachycardia, prolongation of the QT interval, and various forms of conduction abnormalities (Keating et al., 2005; Roos et al., 2002; Yilmazer et al., 2015). Chronic treatment with CQ/HCQ has also

been shown to result in myocardial remodelling that is characterized by thickening of the wall and other microscopic structural changes which would further aggravate underlying pathological conditions, if any, affecting the heart (Baguet et al., 1999a). The very long biological half-life of these drugs, as long as 30–60 days, also contributes towards their toxicity as there is a possibility for retention in tissues with repeated administration even in small doses (Derendorf, 2020; Ducharme and Farinotti, 1996; Krishna and White, 1996).

The inefficiency of mitochondrial complexes by autophagy inhibition with CQ was further substantiated by mitochondrial functional assessment using *in-vivo* experiments. Following CQ treatment there was a significant decline in the respiratory parameters measured, while the effect was more pronounced in the Elderly mice group compared to the young adult mice. Although, the cardiotoxicity of CQ/HCQ is widely studied (Baguet et al., 1999b; Chaanine et al., 2015; Essien and Ette, 1986; Mubagwa, 2020), the mitochondrial dysfunction associated with CQ treatment in normal physiological condition was unexplored. Thus, it is the first report which focuses, the influence of CQ on substrate utilization by the mitochondrial complexes in the cardiac tissue and it could partly provide a mechanistic basis for the documented detrimental effects of CQ.

Resveratrol (Res) was used as the autophagic activator in our study. This polyphenolic compound, often designated to have promising therapeutic capability, especially in metabolic diseases, with the health benefits mainly attributed to its ability to induce autophagy as well as ameliorate oxidative stress, is reported to improve cardiac function as well as mitochondrial biogenesis (Csiszar et al., 2009; Gu et al., 2014; Zhou et al., 2021).

While, the cardioprotective effects of RES is widely studied in the context of various pathologies especially LV dysfunction, cardiac I/R injury, pharmacologically induced cardiotoxicity, obesity, and diabetes, this particular study focuses to investigate the role of RES on mitochondrial dynamics and function in cardiac cells under normal physiological context. RES has been shown to negatively impact mitochondrial respiration in cancer cells, whereas noncancerous cells were shown to have no effect

with regard to mitochondrial respiration (Öztürk et al., 2019; Saunier et al., 2017). HRR measurements of cardiomyoblasts exposed to different concentrations of RES for 24 h revealed a significant decline in respiratory parameters. But the coupling control ratios derived from these respiratory parameters revealed that the mitochondrial coupling efficiency, (R-L)/R, showed a significant improvement with 20 µM RES for 24 h, while the other two concentrations, 50 µM, and 100 µM of RES treatment resulted in a significant decline in the Coupling efficiency. This result point towards a concentration dependent effect of RES on mitochondrial function; as RES is shown to elicit hormetic dose responses with lower doses having cytoprotective effects (Calabrese et al., 2010; Mizuguchi et al., 2017; Shaito et al., 2020). However, the substrate-linked respiration measurements showed an improvement in substrate utilization with 50 µM RES having a statistically significant enhancement on Complex-I, II & IV linked respiration. TMRM staining also showed a concentration dependent increase in the fluorescent intensity suggesting an increase in the MMP. This indicates the maintenance of a healthy pool of mitochondrial population, even when the cells are exposed to higher concentrations of RES. But, assessment of mitochondrial superoxide levels shows that RES treatment results in the elevation of mtROS generation. Elevated levels of mtROS could be a by-product of increase in mitochondrial metabolism or could be explained by the pro-oxidant nature of RES which would cause an increase in mitochondrial membrane potential and mtROS has been explained by Madrigal-Perez et al., 2016. RES with reported inhibitory effect on complex I as well as complex V/F_1F_0-ATPase could cause disengagement of the ETC with an increase in mitochondrial membrane potential, ROS generation, as well as a decrease in ATP production. And this elevated ROS generation could be a reason for the fragmentation of mitochondrial network as evident from the live cell staining using Mitotracker DEEP Red. The gene expression analysis showed that the OPA-1 mRNA levels declined with all the three concentrations of RES for 24 h, While FIS-1 mRNA levels increased with 20 µM, and 100 µM RES treated group showing statistical significance. The protein expression analysis shows a decline in OPA-1 (L form) with 100 µM RES treatment for 24 h while DRP1 levels declined significantly with all the three concentrations of RES.

As discussed earlier, the biological responses of RES can either be as an antioxidant, that induces mitochondrial biogenesis and protects against ROS induced damage, usually associated with lower concentrations of RES, or promote mitochondrial dysfunction as well as elicit pro-oxidant activity usually associated with exposure to higher concentrations of RES. Thus, the dose of RES could have a critical impact on the beneficial effects exerted and a narrow optimal dose must be determined before employing for any therapeutic targets.

Even though, RES is proven to have beneficial effects on cardiac health and mitochondrial function under Ischemia/reperfusion injury, obesity and diabetic models, there is no evidence available regarding the influence of resveratrol on cardiac mitochondrial function under physiological context (Beaudoin et al., 2014; Dong et al., 2015; Lu et al., 2019). Here, the beneficial effects of RES treatment on the substrate utilization by mitochondrial complexes was assessed using isolated mitochondria in HRR. RES improved mitochondrial efficiency in both mature adults as well as elderly groups under normal physiological conditions. Even though RES treatment resulted in an improved mitochondrial efficiency in both the groups, the effect on Complex II mediated as well as uncoupled respiration measurements was more pronounced in the Elderly group, suggesting that RES treatment could have greater significance as a Phyto-therapy under cardiovascular challenges which would render the mitochondrial network susceptible to more damage.

VII. Conclusion

- CQ affects mitochondrial architecture and functional efficiency with the accumulation of unhealthy mitochondria in the cardiac cells; our results point towards a clear deterioration of metabolic function in the cardiac tissue with CQ and its derivatives.
- 3-Methyladenine showed an improvement of mitochondrial coupling efficiency and it thus warrant more investigation so as to elucidate the alternate mitochondrial clearance mechanism, if any.
- The decline in mitochondrial functional efficiency could aggravate the pre-existing disproportion in metabolic demand and cardiac output, as observed in conditions like cancer chemotherapeutics induced heart ailments, rheumatic heart disease, etc. with accompanying cardiopulmonary derangement. This warrants the need of investigations in more detail in the *in-vivo* systems to unravel the cardiotoxicity of CQ and its derivatives.
- The autophagy induction by resveratrol had beneficial effects on cardiac mitochondrial efficiency,
- The dose of Resveratrol could have critical impact on the beneficial effects and a narrow optimal dose must be determined before employing for any therapeutic targets.

VIII. Limitations of the study

- Mitophagy markers and its expression levels were not assessed.
- Genetic manipulation of autophagy to study its impact on mitochondrial function was not included.
- Even though the cardiac mitochondrial functional assessments were done *in-vivo*, the analysis of mitochondrial dynamics related protein expression could not be done.
- Cardiac functional analysis like ECG, Echo was not done in mice model.
- Reason behind the contrasting results obtained with 3MA was not explored.

IX. References

Al-Bari, M.A.A., 2017. Targeting endosomal acidification by chloroquine analogs as a promising strategy for the treatment of emerging viral diseases. Pharmacol Res Perspect 5, e00293. https://doi.org/10.1002/prp2.293

Baguet, J.-P., Tremel, F., Fabre, M., 1999a. Chloroquine cardiomyopathy with conduction disorders. Heart 81, 221–223. https://doi.org/10.1136/hrt.81.2.221

Baguet, J.-P., Tremel, F., Fabre, M., 1999b. Chloroquine cardiomyopathy with conduction disorders. Heart 81, 221–223. https://doi.org/10.1136/hrt.81.2.221

Barger, J.L., Kayo, T., Vann, J.M., Arias, E.B., Wang, J., Hacker, T.A., Wang, Y., Raederstorff, D., Morrow, J.D., Leeuwenburgh, C., Allison, D.B., Saupe, K.W., Cartee, G.D., Weindruch, R., Prolla, T.A., 2008. A low dose of dietary resveratrol partially mimics caloric restriction and retards aging parameters in mice. PLoS One 3, e2264. https://doi.org/10.1371/journal.pone.0002264

Barsoum, M.J., Yuan, H., Gerencser, A.A., Liot, G., Kushnareva, Y., Gräber, S., Kovacs, I., Lee, W.D., Waggoner, J., Cui, J., White, A.D., Bossy, B., Martinou, J.-C., Youle, R.J., Lipton, S.A., Ellisman, M.H., Perkins, G.A., Bossy-Wetzel, E., 2006. Nitric oxide-induced mitochondrial fission is regulated by dynamin-related GTPases in neurons. EMBO J 25, 3900–3911. https://doi.org/10.1038/sj.emboj.7601253

Beaudoin, M.-S., Perry, C.G.R., Arkell, A.M., Chabowski, A., Simpson, J.A., Wright, D.C., Holloway, G.P., 2014. Impairments in mitochondrial palmitoyl-CoA respiratory kinetics that precede development of diabetic cardiomyopathy are prevented by resveratrol in ZDF rats. J Physiol 592, 2519–2533. https://doi.org/10.1113/jphysiol.2013.270538

Bereiter-Hahn, J., 1990. Behavior of mitochondria in the living cell. Int Rev Cytol 122, 1–63. https://doi.org/10.1016/s0074-7696(08)61205-x

Blignaut, M., Espach, Y., van Vuuren, M., Dhanabalan, K., Huisamen, B., 2019. Revisiting the Cardiotoxic Effect of Chloroquine. Cardiovasc Drugs Ther 33, 1–11. https://doi.org/10.1007/s10557-018-06847-9

Bowman, E.J., Siebers, A., Altendorf, K., 1988. Bafilomycins: a class of inhibitors of membrane ATPases from microorganisms, animal cells, and plant cells. Proc Natl Acad Sci U S A 85, 7972–7976. https://doi.org/10.1073/pnas.85.21.7972

Boya, P., Reggiori, F., Codogno, P., 2013. Emerging regulation and functions of autophagy. Nat Cell Biol 15, 713–720. https://doi.org/10.1038/ncb2788

Calabrese, E.J., Mattson, M.P., Calabrese, V., 2010. Resveratrol commonly displays hormesis: occurrence and biomedical significance. Hum Exp Toxicol 29, 980–1015. https://doi.org/10.1177/0960327110383625

Camont, L., Collin, F., Couturier, M., Thérond, P., Jore, D., Gardès-Albert, M., Bonnefont-Rousselot, D., 2012. Radical-induced oxidation of trans-resveratrol. Biochimie 94, 741–747. https://doi.org/10.1016/j.biochi.2011.11.005

Cao, D.J., Gillette, T.G., Hill, J.A., 2009. Cardiomyocyte Autophagy: Remodeling, Repairing, and Reconstructing the Heart. Curr Hypertens Rep 11, 406–411.

Cecconi, F., Levine, B., 2008. The Role of Autophagy in Mammalian Development: Cell Makeover Rather than Cell Death. Developmental Cell 15, 344–357. https://doi.org/10.1016/j.devcel.2008.08.012

Chaanine, A.H., Gordon, R.E., Nonnenmacher, M., Kohlbrenner, E., Benard, L., Hajjar, R.J., 2015. High-dose chloroquine is metabolically cardiotoxic by inducing lysosomes and mitochondria dysfunction in a rat model of pressure overload hypertrophy. Physiol Rep 3, e12413. https://doi.org/10.14814/phy2.12413

Chatre, C., Roubille, F., Vernhet, H., Jorgensen, C., Pers, Y.-M., 2018. Cardiac Complications Attributed to Chloroquine and Hydroxychloroquine: A Systematic Review of the Literature. Drug Saf 41, 919–931. https://doi.org/10.1007/s40264-018-0689-4

Corrado, M., Mariotti, F.R., Trapani, L., Taraborrelli, L., Nazio, F., Cianfanelli, V., Soriano, M.E., Schrepfer, E., Cecconi, F., Scorrano, L., Campello, S., 2016. Macroautophagy inhibition maintains fragmented mitochondria to foster T cell receptor-dependent apoptosis. EMBO J 35, 1793–1809. https://doi.org/10.15252/embj.201593727

Csiszar, A., Labinskyy, N., Pinto, J.T., Ballabh, P., Zhang, H., Losonczy, G., Pearson, K., de Cabo, R., Pacher, P., Zhang, C., Ungvari, Z., 2009. Resveratrol induces mitochondrial biogenesis in endothelial cells. American Journal of Physiology-Heart and Circulatory Physiology 297, H13–H20. https://doi.org/10.1152/ajpheart.00368.2009

de Duve, C., Pressman, B.C., Gianetto, R., Wattiaux, R., Appelmans, F., 1955. Tissue fractionation studies. 6. Intracellular distribution patterns of enzymes in rat-liver tissue*. Biochemical Journal 60, 604–617. https://doi.org/10.1042/bj0600604

Derendorf, H., 2020. Excessive lysosomal ion-trapping of hydroxychloroquine and azithromycin. International Journal of Antimicrobial Agents 55, 106007. https://doi.org/10.1016/j.ijantimicag.2020.106007

Dikic, I., Elazar, Z., 2018. Mechanism and medical implications of mammalian autophagy. Nat Rev Mol Cell Biol 19, 349–364. https://doi.org/10.1038/s41580-018-0003-4

Dong, W., Yang, R., Yang, Jian, Yang, Jun, Ding, J., Wu, H., Zhang, J., 2015. Resveratrol pretreatment protects rat hearts from ischemia/reperfusion injury partly via a NALP3 inflammasome pathway. Int J Clin Exp Pathol 8, 8731–8741.

Druzhyna, N.M., Wilson, G.L., LeDoux, S.P., 2008. Mitochondrial DNA repair in aging and disease. Mech Ageing Dev 129, 383–390. https://doi.org/10.1016/j.mad.2008.03.002

Ducharme, J., Farinotti, R., 1996. Clinical Pharmacokinetics and Metabolism of Chloroquine. Clin-Pharmacokinet 31, 257–274. https://doi.org/10.2165/00003088-199631040-00003

Dutta, D., Calvani, R., Bernabei, R., Leeuwenburgh, C., Marzetti, E., 2012a. Contribution of impaired mitochondrial autophagy to cardiac aging: mechanisms and therapeutic opportunities. Circ Res 110, 1125–1138. https://doi.org/10.1161/CIRCRESAHA.111.246108

Dutta, D., Calvani, R., Bernabei, R., Leeuwenburgh, C., Marzetti, E., 2012b. Contribution of impaired mitochondrial autophagy to cardiac aging: mechanisms and therapeutic opportunities. Circ Res 110, 1125–1138. https://doi.org/10.1161/CIRCRESAHA.111.246108

Essien, E.E., Ette, E.I., 1986. Effects of chloroquine and didesethylchloroquine on rabbit myocardium and mitochondria. J Pharm Pharmacol 38, 543–546. https://doi.org/10.1111/j.2042-7158.1986.tb04635.x

Glancy, B., Hartnell, L.M., Combs, C.A., Femnou, A., Sun, J., Murphy, E., Subramaniam, S., Balaban, R.S., 2017. Power Grid Protection of the Muscle Mitochondrial Reticulum. Cell Rep 19, 487–496. https://doi.org/10.1016/j.celrep.2017.03.063

Glick, D., Barth, S., Macleod, K.F., 2010. Autophagy: cellular and molecular mechanisms. The Journal of Pathology 221, 3–12. https://doi.org/10.1002/path.2697

Gnaiger, E., 2009. Capacity of oxidative phosphorylation in human skeletal muscle: New perspectives of mitochondrial physiology. The International Journal of Biochemistry

& Cell Biology, Mitochondrial Dynamics and Function in Biology and Medicine 41, 1837–1845. https://doi.org/10.1016/j.biocel.2009.03.013
Gomes, L.C., Benedetto, G.D., Scorrano, L., 2011a. During autophagy mitochondria elongate, are spared from degradation and sustain cell viability. Nat Cell Biol 13, 589–598. https://doi.org/10.1038/ncb2220
Gomes, L.C., Di Benedetto, G., Scorrano, L., 2011b. During autophagy mitochondria elongate, are spared from degradation and sustain cell viability. Nat Cell Biol 13, 589–598. https://doi.org/10.1038/ncb2220
Gomes, L.C., Scorrano, L., 2008. High levels of Fis1, a pro-fission mitochondrial protein, trigger autophagy. Biochim Biophys Acta 1777, 860–866. https://doi.org/10.1016/j.bbabio.2008.05.442
Goswami, S.K., Das, D.K., 2006. Autophagy in the myocardium: Dying for survival? Exp Clin Cardiol 11, 183–188.
Gu, X.S., Wang, Z.B., Ye, Z., Lei, J.P., Li, L., Su, D.F., Zheng, X., 2014. Resveratrol, an activator of SIRT1, upregulates AMPK and improves cardiac function in heart failure. Genet Mol Res 13, 323–335. https://doi.org/10.4238/2014.January.17.17
Hansen, M., Chandra, A., Mitic, L.L., Onken, B., Driscoll, M., Kenyon, C., 2008. A Role for Autophagy in the Extension of Lifespan by Dietary Restriction in C. elegans. PLOS Genetics 4, e24. https://doi.org/10.1371/journal.pgen.0040024
Hom, J., Sheu, S.-S., 2009. Morphological Dynamics of Mitochondria – A Special Emphasis on Cardiac Muscle Cells. J Mol Cell Cardiol 46, 811–820. https://doi.org/10.1016/j.yjmcc.2009.02.023
Hoppel, C.L., Tandler, B., Fujioka, H., Riva, A., 2009. Dynamic organization of mitochondria in human heart and in myocardial disease. Int J Biochem Cell Biol 41, 1949–1956. https://doi.org/10.1016/j.biocel.2009.05.004
Huang, J.-P., Huang, S.-S., Deng, J.-Y., Chang, C.-C., Day, Y.-J., Hung, L.-M., 2010. Insulin and resveratrol act synergistically, preventing cardiac dysfunction in diabetes, but the advantage of resveratrol in diabetics with acute heart attack is antagonized by insulin. Free Radical Biology and Medicine 49, 1710–1721. https://doi.org/10.1016/j.freeradbiomed.2010.08.032
Ichishita, R., Tanaka, K., Sugiura, Y., Sayano, T., Mihara, K., Oka, T., 2008. An RNAi screen for mitochondrial proteins required to maintain the morphology of the organelle in Caenorhabditis elegans. J Biochem 143, 449–454. https://doi.org/10.1093/jb/mvm245
Ingerman, E., Perkins, E.M., Marino, M., Mears, J.A., McCaffery, J.M., Hinshaw, J.E., Nunnari, J., 2005. Dnm1 forms spirals that are structurally tailored to fit mitochondria. J Cell Biol 170, 1021–1027. https://doi.org/10.1083/jcb.200506078
Jia, K., Chen, D., Riddle, D.L., 2004. The TOR pathway interacts with the insulin signaling pathway to regulate C. elegans larval development, metabolism and life span. Development 131, 3897–3906. https://doi.org/10.1242/dev.01255
Keating, R.J., Bhatia, S., Amin, S., Williams, A., Sinak, L.J., Edwards, W.D., 2005. Hydroxychloroquine-induced Cardiotoxicity in a 39-year-old Woman with Systemic Lupus Erythematosus and Systolic Dysfunction. Journal of the American Society of Echocardiography 18, 981.e1-981.e5. https://doi.org/10.1016/j.echo.2005.01.012
Khosa, S., Khanlou, N., Khosa, G.S., Mishra, S.K., 2018. Hydroxychloroquine-induced autophagic vacuolar myopathy with mitochondrial abnormalities. Neuropathology 38, 646–652. https://doi.org/10.1111/neup.12520

Kifle, Z.D., Ayele, A.G., Enyew, E.F., 2021. Drug Repurposing Approach, Potential Drugs, and Novel Drug Targets for COVID-19 Treatment. J Environ Public Health 2021, 6631721. https://doi.org/10.1155/2021/6631721

Krishna, S., White, N.J., 1996. Pharmacokinetics of Quinine, Chloroquine and Amodiaquine. Clin-Pharmacokinet 30, 263–299. https://doi.org/10.2165/00003088-199630040-00002

Kuma, A., Hatano, M., Matsui, M., Yamamoto, A., Nakaya, H., Yoshimori, T., Ohsumi, Y., Tokuhisa, T., Mizushima, N., 2004. The role of autophagy during the early neonatal starvation period. Nature 432, 1032–1036. https://doi.org/10.1038/nature03029

Kuroyanagi, H., Yan, J., Seki, N., Yamanouchi, Y., Suzuki, Y., Takano, T., Muramatsu, M., Shirasawa, T., 1998. Human ULK1, a novel serine/threonine kinase related to UNC-51 kinase of Caenorhabditis elegans: cDNA cloning, expression, and chromosomal assignment. Genomics 51, 76–85. https://doi.org/10.1006/geno.1998.5340

Leadsham, J.E., Sanders, G., Giannaki, S., Bastow, E.L., Hutton, R., Naeimi, W.R., Breitenbach, M., Gourlay, C.W., 2013. Loss of cytochrome c oxidase promotes RAS-dependent ROS production from the ER resident NADPH oxidase, Yno1p, in yeast. Cell Metab 18, 279–286. https://doi.org/10.1016/j.cmet.2013.07.005

Li, P., Hao, L., Guo, Y.-Y., Yang, G.-L., Mei, H., Li, X.-H., Zhai, Q.-X., 2018. Chloroquine inhibits autophagy and deteriorates the mitochondrial dysfunction and apoptosis in hypoxic rat neurons. Life Sci 202, 70–77. https://doi.org/10.1016/j.lfs.2018.01.011

Liu, L., Han, C., Yu, H., Zhu, W., Cui, H., Zheng, L., Zhang, C., Yue, L., 2018. Chloroquine inhibits cell growth in human A549 lung cancer cells by blocking autophagy and inducing mitochondrial-mediated apoptosis. Oncology Reports 39, 2807–2816. https://doi.org/10.3892/or.2018.6363

Lu, Y., Lu, X., Wang, L., Yang, W., 2019. Resveratrol attenuates high fat diet-induced mouse cardiomyopathy through upregulation of estrogen related receptor-α. Eur J Pharmacol 843, 88–95. https://doi.org/10.1016/j.ejphar.2018.10.018

Ma, K., Chen, G., Li, W., Kepp, O., Zhu, Y., Chen, Q., 2020. Mitophagy, Mitochondrial Homeostasis, and Cell Fate. Frontiers in Cell and Developmental Biology 8, 467. https://doi.org/10.3389/fcell.2020.00467

Madrigal-Perez, L.A., Ramos-Gomez, M., 2016. Resveratrol Inhibition of Cellular Respiration: New Paradigm for an Old Mechanism. Int J Mol Sci 17, 368. https://doi.org/10.3390/ijms17030368

Malena, A., Loro, E., Di Re, M., Holt, I.J., Vergani, L., 2009. Inhibition of mitochondrial fission favours mutant over wild-type mitochondrial DNA. Hum Mol Genet 18, 3407–3416. https://doi.org/10.1093/hmg/ddp281

Mauthe, M., Orhon, I., Rocchi, C., Zhou, X., Luhr, M., Hijlkema, K.-J., Coppes, R.P., Engedal, N., Mari, M., Reggiori, F., 2018a. Chloroquine inhibits autophagic flux by decreasing autophagosome-lysosome fusion. Autophagy 14, 1435–1455. https://doi.org/10.1080/15548627.2018.1474314

Mauthe, M., Orhon, I., Rocchi, C., Zhou, X., Luhr, M., Hijlkema, K.-J., Coppes, R.P., Engedal, N., Mari, M., Reggiori, F., 2018b. Chloroquine inhibits autophagic flux by decreasing autophagosome-lysosome fusion. Autophagy 14, 1435–1455. https://doi.org/10.1080/15548627.2018.1474314

Mayorga, M., Bahi, N., Ballester, M., Comella, J.X., Sanchis, D., 2004. Bcl-2 Is a Key Factor for Cardiac Fibroblast Resistance to Programmed Cell Death*. Journal of Biological Chemistry 279, 34882–34889. https://doi.org/10.1074/jbc.M404616200

MiPNet08.09 CellRespiration - Bioblast [WWW Document], n.d. URL https://wiki.oroboros.at/index.php/MiPNet08.09_CellRespiration (accessed 2.19.21).
Mizuguchi, Y., Hatakeyama, H., Sueoka, K., Tanaka, M., Goto, Y., 2017. Low dose resveratrol ameliorates mitochondrial respiratory dysfunction and enhances cellular reprogramming. Mitochondrion 34, 43–48. https://doi.org/10.1016/j.mito.2016.12.006
Mohiuddin, A.K., 20190122. A Comprehensive Review of Clinical Pharmacists in Chronic Care Management. International Journal of Hospital Pharmacy 5. https://doi.org/10.28933/ijhp-2019-10-1805
Mubagwa, K., 2020. Cardiac effects and toxicity of chloroquine: a short update. International Journal of Antimicrobial Agents 56, 106057. https://doi.org/10.1016/j.ijantimicag.2020.106057
Murphy, K.R., Baggett, B., Cooper, L.L., Lu, Y., O-Uchi, J., Sedivy, J.M., Terentyev, D., Koren, G., 2019. Enhancing Autophagy Diminishes Aberrant Ca2+ Homeostasis and Arrhythmogenesis in Aging Rabbit Hearts. Frontiers in Physiology 10, 1277. https://doi.org/10.3389/fphys.2019.01277
Murphy, M.P., 2013. Mitochondrial dysfunction indirectly elevates ROS production by the endoplasmic reticulum. Cell Metab 18, 145–146. https://doi.org/10.1016/j.cmet.2013.07.006
Nakai, A., Yamaguchi, O., Takeda, T., Higuchi, Y., Hikoso, S., Taniike, M., Omiya, S., Mizote, I., Matsumura, Y., Asahi, M., Nishida, K., Hori, M., Mizushima, N., Otsu, K., 2007. The role of autophagy in cardiomyocytes in the basal state and in response to hemodynamic stress. Nat Med 13, 619–624. https://doi.org/10.1038/nm1574
Nakatogawa, H., Suzuki, K., Kamada, Y., Ohsumi, Y., 2009. Dynamics and diversity in autophagy mechanisms: lessons from yeast. Nat Rev Mol Cell Biol 10, 458–467. https://doi.org/10.1038/nrm2708
Nakou, E.S., Parthenakis, F.I., Kallergis, E.M., Marketou, M.E., Nakos, K.S., Vardas, P.E., 2016. Healthy aging and myocardium: A complicated process with various effects in cardiac structure and physiology. Int J Cardiol 209, 167–175. https://doi.org/10.1016/j.ijcard.2016.02.039
Nishida, K., Kyoi, S., Yamaguchi, O., Sadoshima, J., Otsu, K., 2009. The role of autophagy in the heart. Cell Death Differ 16, 31–38. https://doi.org/10.1038/cdd.2008.163
Nishino, I., Fu, J., Tanji, K., Yamada, T., Shimojo, S., Koori, T., Mora, M., Riggs, J.E., Oh, S.J., Koga, Y., Sue, C.M., Yamamoto, A., Murakami, N., Shanske, S., Byrne, E., Bonilla, E., Nonaka, I., DiMauro, S., Hirano, M., 2000. Primary LAMP-2 deficiency causes X-linked vacuolar cardiomyopathy and myopathy (Danon disease). Nature 406, 906–910. https://doi.org/10.1038/35022604
Öztürk, Y., Günaydın, C., Yalçın, F., Nazıroğlu, M., Braidy, N., 2019. Resveratrol Enhances Apoptotic and Oxidant Effects of Paclitaxel through TRPM2 Channel Activation in DBTRG Glioblastoma Cells. Oxidative Medicine and Cellular Longevity 2019, e4619865. https://doi.org/10.1155/2019/4619865
Parzych, K.R., Klionsky, D.J., 2014. An Overview of Autophagy: Morphology, Mechanism, and Regulation. Antioxid Redox Signal 20, 460–473. https://doi.org/10.1089/ars.2013.5371
Pesta, D., Gnaiger, E., 2012. High-resolution respirometry: OXPHOS protocols for human cells and permeabilized fibers from small biopsies of human muscle. Methods Mol Biol 810, 25–58. https://doi.org/10.1007/978-1-61779-382-0_3

Petiot, A., Ogier-Denis, E., Blommaart, E.F.C., Meijer, A.J., Codogno, P., 2000. Distinct Classes of Phosphatidylinositol 3'-Kinases Are Involved in Signaling Pathways That Control Macroautophagy in HT-29 Cells*. Journal of Biological Chemistry 275, 992–998. https://doi.org/10.1074/jbc.275.2.992

Pfaffl, M.W., 2001. A new mathematical model for relative quantification in real-time RT–PCR. Nucleic Acids Res 29, e45.

Qu, X., Sheng, J., Shen, L., Su, J., Xu, Y., Xie, Q., Wu, Y., Zhang, X., Sun, L., 2017. Autophagy inhibitor chloroquine increases sensitivity to cisplatin in QBC939 cholangiocarcinoma cells by mitochondrial ROS. PLOS ONE 12, e0173712. https://doi.org/10.1371/journal.pone.0173712

Rambold, A.S., Kostelecky, B., Elia, N., Lippincott-Schwartz, J., 2011. Tubular network formation protects mitochondria from autophagosomal degradation during nutrient starvation. Proc Natl Acad Sci U S A 108, 10190–10195. https://doi.org/10.1073/pnas.1107402108

Redmann, M., Benavides, G.A., Berryhill, T.F., Wani, W.Y., Ouyang, X., Johnson, M.S., Ravi, S., Barnes, S., Darley-Usmar, V.M., Zhang, J., 2017. Inhibition of autophagy with bafilomycin and chloroquine decreases mitochondrial quality and bioenergetic function in primary neurons. Redox Biology 11, 73–81. https://doi.org/10.1016/j.redox.2016.11.004

Ren, S.Y., Xu, X., 2015. Role of autophagy in metabolic syndrome-associated heart disease. Biochim Biophys Acta 1852, 225–231. https://doi.org/10.1016/j.bbadis.2014.04.029

Renaud, S., de Lorgeril, M., 1992. Wine, alcohol, platelets, and the French paradox for coronary heart disease. Lancet 339, 1523–1526. https://doi.org/10.1016/0140-6736(92)91277-f

Riffelmacher, T., Richter, F.C., Simon, A.K., 2017. Autophagy dictates metabolism and differentiation of inflammatory immune cells. Autophagy 14, 199–206. https://doi.org/10.1080/15548627.2017.1362525

Rifki, O.F., Hill, J.A., 2012. Cardiac Autophagy: Good with the Bad. J Cardiovasc Pharmacol 60, 248–252. https://doi.org/10.1097/FJC.0b013e3182646cb1

Roos, J.M., Aubry, M.-C., Edwards, W.D., 2002. Chloroquine cardiotoxicity: Clinicopathologic features in three patients and comparison with three patients with Fabry disease. Cardiovascular Pathology 11, 277–283. https://doi.org/10.1016/S1054-8807(02)00118-7

Rubinsztein, D.C., Mariño, G., Kroemer, G., 2011. Autophagy and Aging. Cell 146, 682–695. https://doi.org/10.1016/j.cell.2011.07.030

Ruijter, J.M., Ramakers, C., Hoogaars, W.M.H., Karlen, Y., Bakker, O., van den Hoff, M.J.B., Moorman, A.F.M., 2009. Amplification efficiency: linking baseline and bias in the analysis of quantitative PCR data. Nucleic Acids Res 37, e45. https://doi.org/10.1093/nar/gkp045

Saunier, E., Antonio, S., Regazzetti, A., Auzeil, N., Laprévote, O., Shay, J.W., Coumoul, X., Barouki, R., Benelli, C., Huc, L., Bortoli, S., 2017. Resveratrol reverses the Warburg effect by targeting the pyruvate dehydrogenase complex in colon cancer cells. Sci Rep 7, 6945. https://doi.org/10.1038/s41598-017-07006-0

Sciarretta, S., Boppana, V.S., Umapathi, M., Frati, G., Sadoshima, J., 2015. Boosting autophagy in the diabetic heart: a translational perspective. Cardiovasc Diagn Ther 5, 394–402. https://doi.org/10.3978/j.issn.2223-3652.2015.07.02

Sciarretta, S., Hariharan, N., Monden, Y., Zablocki, D., Sadoshima, J., 2011. Is Autophagy in Response to Ischemia and Reperfusion Protective or Detrimental for the Heart? Pediatr Cardiol 32, 275–281. https://doi.org/10.1007/s00246-010-9855-x

Sciarretta, S., Yee, D., Nagarajan, N., Bianchi, F., Saito, T., Valenti, V., Tong, M., Del Re, D.P., Vecchione, C., Schirone, L., Forte, M., Rubattu, S., Shirakabe, A., Boppana, V.S., Volpe, M., Frati, G., Zhai, P., Sadoshima, J., 2018. Trehalose-Induced Activation of Autophagy Improves Cardiac Remodeling After Myocardial Infarction. Journal of the American College of Cardiology 71, 1999–2010. https://doi.org/10.1016/j.jacc.2018.02.066

Seo, A.Y., Joseph, A.-M., Dutta, D., Hwang, J.C.Y., Aris, J.P., Leeuwenburgh, C., 2010. New insights into the role of mitochondria in aging: mitochondrial dynamics and more. Journal of Cell Science 123, 2533–2542. https://doi.org/10.1242/jcs.070490

Shaito, A., Posadino, A.M., Younes, N., Hasan, H., Halabi, S., Alhababi, D., Al-Mohannadi, A., Abdel-Rahman, W.M., Eid, A.H., Nasrallah, G.K., Pintus, G., 2020. Potential Adverse Effects of Resveratrol: A Literature Review. Int J Mol Sci 21, E2084. https://doi.org/10.3390/ijms21062084

Shiea, J., Huang, M.-Z., Hsu, H.-J., Lee, C.-Y., Yuan, C.-H., Beech, I., Sunner, J., 2005. Electrospray-assisted laser desorption/ionization mass spectrometry for direct ambient analysis of solids. Rapid Commun Mass Spectrom 19, 3701–3704. https://doi.org/10.1002/rcm.2243

Shirakabe, A., Zhai, P., Ikeda, Y., Saito, T., Maejima, Y., Hsu, C.-P., Nomura, M., Egashira, K., Levine, B., Sadoshima, J., 2016. Drp1-Dependent Mitochondrial Autophagy Plays a Protective Role Against Pressure Overload-Induced Mitochondrial Dysfunction and Heart Failure. Circulation 133, 1249–1263. https://doi.org/10.1161/CIRCULATIONAHA.115.020502

Siddiqui, A.K., Huberfeld, S.I., Weidenheim, K.M., Einberg, K.R., Efferen, L.S., 2007. Hydroxychloroquine-Induced Toxic Myopathy Causing Respiratory Failure. CHEST 131, 588–590. https://doi.org/10.1378/chest.06-1146

Singh, R., Cuervo, A.M., 2011. Autophagy in the Cellular Energetic Balance. Cell Metabolism 13, 495–504. https://doi.org/10.1016/j.cmet.2011.04.004

Sivasailam, A., Ganjoo, M., Panicker, V.T., Pillai, V., Gopala, S., 2019. The Evolving Concept of Mitochondrial Dynamics in Heart: Interventional Opportunities. Modulation of Oxidative Stress in Heart Disease. https://doi.org/10.1007/978-981-13-8946-7_25

Song, S., Tan, J., Miao, Y., Li, M., Zhang, Q., 2017. Crosstalk of autophagy and apoptosis: Involvement of the dual role of autophagy under ER stress. J Cell Physiol 232, 2977–2984. https://doi.org/10.1002/jcp.25785

Soubannier, V., McBride, H.M., 2009. Positioning mitochondrial plasticity within cellular signaling cascades. Biochim Biophys Acta 1793, 154–170. https://doi.org/10.1016/j.bbamcr.2008.07.008

Stein, M., Bell, M.J., Ang, L.C., 2000. Hydroxychloroquine neuromyotoxicity. J Rheumatol 27, 2927–2931.

Strauss, M., Hofhaus, G., Schröder, R.R., Kühlbrandt, W., 2008. Dimer ribbons of ATP synthase shape the inner mitochondrial membrane. EMBO J 27, 1154–1160. https://doi.org/10.1038/emboj.2008.35

Terman, A., Brunk, U.T., 2005. Autophagy in cardiac myocyte homeostasis, aging, and pathology. Cardiovascular Research 68, 355–365. https://doi.org/10.1016/j.cardiores.2005.08.014

Terman, A., Dalen, H., Eaton, J.W., Neuzil, J., Brunk, U.T., 2004. Aging of Cardiac Myocytes in Culture: Oxidative Stress, Lipofuscin Accumulation, and Mitochondrial Turnover. Annals of the New York Academy of Sciences 1019, 70–77. https://doi.org/10.1196/annals.1297.015

The Mouse in Biomedical Research - 2nd Edition [WWW Document], n.d. URL https://www.elsevier.com/books/the-mouse-in-biomedical-research/fox/978-0-12-369454-6 (accessed 2.18.21).

Thomas, R.L., Roberts, D.J., Kubli, D.A., Lee, Y., Quinsay, M.N., Owens, J.B., Fischer, K.M., Sussman, M.A., Miyamoto, S., Gustafsson, Å.B., 2013. Loss of MCL-1 leads to impaired autophagy and rapid development of heart failure. Genes Dev. 27, 1365–1377. https://doi.org/10.1101/gad.215871.113

Towers, C.G., Wodetzki, D.K., Thorburn, J., Smith, K.R., Caino, M.C., Thorburn, A., 2021. Mitochondrial-derived vesicles compensate for loss of LC3-mediated mitophagy. Developmental Cell 56, 2029-2042.e5. https://doi.org/10.1016/j.devcel.2021.06.003

Troncoso, R., Vicencio, J.M., Parra, V., Nemchenko, A., Kawashima, Y., del Campo, A., Toro, B., Battiprolu, P.K., Aranguiz, P., Chiong, M., Yakar, S., Gillette, T.G., Hill, J.A., Abel, E.D., LeRoith, D., Lavandero, S., 2012. Energy-preserving effects of IGF-1 antagonize starvation-induced cardiac autophagy. Cardiovasc Res 93, 320–329. https://doi.org/10.1093/cvr/cvr321

Twig, G., Elorza, A., Molina, A.J.A., Mohamed, H., Wikstrom, J.D., Walzer, G., Stiles, L., Haigh, S.E., Katz, S., Las, G., Alroy, J., Wu, M., Py, B.F., Yuan, J., Deeney, J.T., Corkey, B.E., Shirihai, O.S., 2008a. Fission and selective fusion govern mitochondrial segregation and elimination by autophagy. EMBO J 27, 433–446. https://doi.org/10.1038/sj.emboj.7601963

Twig, G., Elorza, A., Molina, A.J.A., Mohamed, H., Wikstrom, J.D., Walzer, G., Stiles, L., Haigh, S.E., Katz, S., Las, G., Alroy, J., Wu, M., Py, B.F., Yuan, J., Deeney, J.T., Corkey, B.E., Shirihai, O.S., 2008b. Fission and selective fusion govern mitochondrial segregation and elimination by autophagy. EMBO J 27, 433–446. https://doi.org/10.1038/sj.emboj.7601963

Wang, Y., Li, Y., He, C., Gou, B., Song, M., 2019. Mitochondrial regulation of cardiac aging. Biochimica et Biophysica Acta (BBA) - Molecular Basis of Disease, Genetic and epigenetic regulation of aging and longevity 1865, 1853–1864. https://doi.org/10.1016/j.bbadis.2018.12.008

Westermann, B., 2012. Bioenergetic role of mitochondrial fusion and fission. Biochimica et Biophysica Acta (BBA) - Bioenergetics, 17th European Bioenergetics Conference 1817, 1833–1838. https://doi.org/10.1016/j.bbabio.2012.02.033

Westermann, B., 2010. Mitochondrial fusion and fission in cell life and death. Nat Rev Mol Cell Biol 11, 872–884. https://doi.org/10.1038/nrm3013

Wu, D., Zhang, K., Hu, P., 2019. The Role of Autophagy in Acute Myocardial Infarction. Frontiers in Pharmacology 10, 551. https://doi.org/10.3389/fphar.2019.00551

Xu, Xihui, Hua, Y., Nair, S., Sreejayan, N., Zhang, Y., Ren, J., 2013. Akt2 knockout preserves cardiac function in high-fat diet-induced obesity by rescuing cardiac autophagosome maturation. J Mol Cell Biol 5, 61–63. https://doi.org/10.1093/jmcb/mjs055

Xu, Xianmin, Kobayashi, S., Chen, K., Timm, D., Volden, P., Huang, Y., Gulick, J., Yue, Z., Robbins, J., Epstein, P.N., Liang, Q., 2013. Diminished autophagy limits cardiac

injury in mouse models of type 1 diabetes. J Biol Chem 288, 18077–18092. https://doi.org/10.1074/jbc.M113.474650
Yilmazer, B., Sali, M., Cosan, F., Cefle, A., 2015. Sinus node dysfunction in adult systemic lupus erythematosus flare: A case report. Modern Rheumatology 25, 472–475. https://doi.org/10.3109/14397595.2013.843744
Youle, R.J., van der Bliek, A.M., 2012. Mitochondrial fission, fusion, and stress. Science 337, 1062–1065. https://doi.org/10.1126/science.1219855
Zemirli, N., Morel, E., Molino, D., 2018. Mitochondrial Dynamics in Basal and Stressful Conditions. International Journal of Molecular Sciences 19, 564. https://doi.org/10.3390/ijms19020564
Zhang, H., Morgan, B., Potter, B.J., Ma, L., Dellsperger, K.C., Ungvari, Z., Zhang, C., 2010. Resveratrol improves left ventricular diastolic relaxation in type 2 diabetes by inhibiting oxidative/nitrative stress: in vivo demonstration with magnetic resonance imaging. Am J Physiol Heart Circ Physiol 299, H985–H994. https://doi.org/10.1152/ajpheart.00489.2010
Zhou, J., Yang, Z., Shen, R., Zhong, W., Zheng, H., Chen, Z., Tang, J., Zhu, J., 2021. Resveratrol Improves Mitochondrial Biogenesis Function and Activates PGC-1α Pathway in a Preclinical Model of Early Brain Injury Following Subarachnoid Hemorrhage. Frontiers in Molecular Biosciences 8, 223. https://doi.org/10.3389/fmolb.2021.620683